NTNU
Norwegian University of
Science and Technology

Concepts for Large Scale Hydrogen Production

Daniel Jakobsen
Vegar Åtland

Master of Science in Mechanical Engineering
Submission date: June 2016
Supervisor: Petter Nekså, EPT
Co-supervisor: David Berstad, SINTEF Energy Research
Øivind Wilhelmsen, SINTEF Energy Research

Norwegian University of Science and Technology
Department of Energy and Process Engineering

NTNU

Norwegian University
of Science and Technology

Department of Energy
and Process Engineering

EPT-M-2016-63 and EPT-M-2016-158

MASTER THESIS

for

Students Daniel Jakobsen and Vegar Åtland

Spring 2016

Concepts for large scale hydrogen production

Konsepter for storskala hydrogenproduksjon

Background and objective

There is an increasing concern related to climate change. This has led to the interest in using hydrogen as energy carrier and fuel for transportation and potentially other applications.

Norway has vast amounts of energy resources in form of natural gas (NG) and electricity from hydro- and wind power. A valorization of these resources by large scale hydrogen production for export may be of great interest.

Use of hydrogen as energy carrier can reduce or eliminate CO_2 emissions from various applications. There is however several aspects related to technical and economical implementation that needs further investigations.

The candidates evaluated different value chains for hydrogen in their project thesis. Several aspects where identified for possible further evaluation.

The aim of this Master work is to explore some technical and market related aspects of large-scale hydrogen production and export in more detail.

The following tasks are to be considered:

1. Perform a literature survey on the topics:
    a. Different concepts for large scale hydrogen production from NG with CCS
    b. Potential hydrogen markets in Norway, scenarios for market build-up and alternative ways to decarbonize these applications
2. Evaluate and compare different concepts for hydrogen production from NG with CCS from a technical and economic perspective
    a. As baseline, steam methane reforming (SMR) with CO_2 capture from syngas using conventional/mature technology
    b. SMR with minimised CO_2 emissions
    c. Auto thermal reforming (ATR)
        i. ATR based on air separation
        ii. ATR utilising O_2 as a by-product from electrolysis
    d. Membrane concepts for separation of H_2 and CO_2
    e. Other concepts and combinations

3. Evaluate co-production from NG and electrolysis based on renewable wind- or hydro power from a technical and economical perspective.
    a. Stationary, constant ratio between NG and electrolysis
    b. Fluctuating, e.g. due to wind power transients
4. Propose a plan for further work

-- ” --

Within 14 days of receiving the written text on the master thesis, the candidate shall submit a research plan for his project to the department.

When the thesis is evaluated, emphasis is put on processing of the results, and that they are presented in tabular and/or graphic form in a clear manner, and that they are analyzed carefully.

The thesis should be formulated as a research report with summary both in English and Norwegian, conclusion, literature references, table of contents etc. During the preparation of the text, the candidate should make an effort to produce a well-structured and easily readable report. In order to ease the evaluation of the thesis, it is important that the cross-references are correct. In the making of the report, strong emphasis should be placed on both a thorough discussion of the results and an orderly presentation.

The candidate is requested to initiate and keep close contact with his/her academic supervisor(s) throughout the working period. The candidate must follow the rules and regulations of NTNU as well as passive directions given by the Department of Energy and Process Engineering.

Risk assessment of the candidate's work shall be carried out according to the department's procedures. The risk assessment must be documented and included as part of the final report. Events related to the candidate's work adversely affecting the health, safety or security, must be documented and included as part of the final report. If the documentation on risk assessment represents a large number of pages, the full version is to be submitted electronically to the supervisor and an excerpt is included in the report.

Pursuant to “Regulations concerning the supplementary provisions to the technology study program/Master of Science” at NTNU §20, the Department reserves the permission to utilize all the results and data for teaching and research purposes as well as in future publications.

The final report is to be submitted digitally in DAIM. An executive summary of the thesis including title, student’s name, supervisor's name, year, department name, and NTNU's logo and name, shall be submitted to the department as a separate pdf file. Based on an agreement with the supervisor, the final report and other material and documents may be given to the supervisor in digital format.

☐ Work to be done in lab (Water power lab, Fluids engineering lab, Thermal engineering lab)
☐ Field work

Department of Energy and Process Engineering, 25. January 2016

Olav Bolland	Petter Nekså
Department Head	Academic Supervisor

Research Advisor:

David Berstad,	SINTEF Energy Research
Øyvind Wilhelmsen,	SINTEF Energy Research

Abstract

The objective of this thesis is to perform a techno-economic analysis of large-scale, carbon-lean hydrogen production in Norway, in order to evaluate various production methods and estimate a breakeven price level. Norway possesses vast energy resources and the export of oil and gas is vital to the country's economy. The results of this thesis indicate that hydrogen represents a viable, carbon-lean opportunity to utilize these resources, which can prove key in the future of Norwegian energy exports.

This thesis evaluates six different systems for hydrogen production; Steam methane reforming (SMR), SMR using hydrogen as fuel in the furnace (SMR+), autothermal reforming (ATR), partial oxidation (POX), water electrolysis and a system combining electrolysis and ATR. Aspen HYSYS simulation tool is used to analyse the mentioned production systems. The simulations show that SMR and ATR produce hydrogen with the highest energy efficiency of 0.82. Although the efficiencies are similar, producing hydrogen with ATR reduces the emissions with 70% compared with SMR. SMR captures 3047 tonnes of CO_2/day and emits 1198 tonnes/day, while producing 500 tonnes of hydrogen/day.

With a hydrogen production rate of 500 tonnes/day, SMR proves to be most cost-efficient, with a breakeven price of 1.51 €/kgH_2. In this method, CCS accounts for 0.32 €/kgH_2 of the total price. ATR produce hydrogen at 1.59 €/kgH_2, although with a smaller carbon footprint. A natural gas price of 0.17 €/Sm^3 and an electricity price of 20.03 €/MWh is applied in the analysis[1]. Given the same feedstock prices, electrolysis proves to be the most cost-efficient production system at capacities up to around 150 tonnes/day. When producing 100 tonnes of hydrogen/day, the breakeven price of electrolysis is 1.87 €/kgH_2 while SMR produces the hydrogen at 1.94 €/kgH_2. Based on early market predictions and given assumed development in distribution technology, hydrogen produced from all systems fully evaluated in this thesis can be cost-competitive in export scenarios.

A case study of hydrogen production combining ATR and electrolysis in Mid-Norway is performed to test the viability of utilizing excess wind power to reduce production cost. The results indicate that, given the boundary conditions in this thesis, a combined electrolysis and reforming system utilizing excess wind power is not likely to be cost-competitive with either stationary CRE powered by the grid or traditional reforming.

---

[1] Based on the internal gas price of Statoil and Nasdaq Norwegian EL-commodities, respectively

Sammendrag

Målet med denne avhandlingen er å gjennomføre en tekno-økonomisk analyse av storskala hydrogenproduksjon med redusert CO_2-utlipp i Norge, for å kartlegge ulike produksjonsmetoder og estimere et prisnivå. Norge innehar enorme energiressurser og eksporten av olje og gass er sentral for landets økonomi. Resultatene i denne avhandlingen indikerer at hydrogen med reduserte utslipp representerer en levedyktig, alternativ utnyttelse av disse ressursene, noe som kan vise seg viktig for fremtiden til norsk energieksport.

Avhandlingen undersøker seks ulike hydrogenproduksjonssystemer; Dampreformering (SMR), dampreformering hvor hydrogen erstatter naturgass i forbrenningskammeret (SMR+), Delvis forbrenning (POX), Autotermisk reformering (ATR), elektrolyse (EL) og et kombinasjonssystem med ATR og EL. Karbonfangst og lagring (CCS) er forutsatt i alle produksjonsanleggene. De nevnte systemene er simulert med prosessverktøyet Aspen HYSYS, og simuleringene viser at SMR og ATR produserer hydrogen med høyest energieffektivitet, 0.82. Til tross for lik virkningsgrad, opererer ATR med 70% mindre CO_2-utslipp sammenlignet med SMR. Produksjon av 500 tonn hydrogen/dag med SMR medfører fangst av 3047 tonn CO_2/dag og utslipp av 1198 tonn CO_2/dag.

Gitt en produksjonskapasitet på 500 tonn hydrogen/dag viser SMR seg å være det mest kostnadseffektive alternativet, med en nullpunktspris på 1.51 €/kgH_2. Med denne metoden står CCS for 0.32 €/kgH_2 av den totale prisen. ATR er beregnet til 1.59 €/kgH_2, dog med et betydelig mindre karbonfotavtrykk. En naturgasspris på 0.17€/Sm^3 og en elektrisitetspris på 20.03 €/MWh er benyttet i analysen[2]. Gitt de samme råvarekostnadene, fremstår EL som det mest kostnadseffektive alternativet for anlegg opp til rundt 150 tonn hydrogen/dag. Gitt en produksjonskapasitet på 100 tonn hydrogen om dagen, ender EL og SMR med en nullpunktspris på henholdsvis 1.87 €/kgH_2 og 1.94 €/kgH_2. Basert på tilgjengelige markedsanalyser og gitt antatt teknologiutvikling, kan hydrogen produsert fra alle de evaluerte systemene i denne avhandlingen være konkurransedyktige i eksportscenarioer.

Et studie av kombinasjonsanlegget med ATR og EL ble gjennomført i Midt-Norge, for å teste hvordan utnyttelsen av overskuddsstrøm fra vindkraft kan redusere den totale produksjonskostnaden. Resultatene viser at utnyttelsen av overskuddsstrøm sannsynligvis ikke vil gi bedre lønnsomhet enn stasjonær produksjon fra enten nett eller tradisjonell reformering, gitt grensebetingelsene i denne avhandlingen.

---

[2] Basert på henholdsvis Statoils interne gasspris og Nasdaqs strøm-objekter ENOYR 17-19.

Preface

The present thesis was carried out at the Department of Energy and Process Engineering at the Norwegian University of Science and Technology (NTNU) from January to June 2016. Our supervisors were Professor II Petter Nekså (NTNU and SINTEF Energy Research), David Berstad (SINTEF Energy Research) and Øivind Wilhelmsen (SINTEF Energy Research).

Acknowledgements

This thesis has been realized with help from several knowledgeable people, both internally at NTNU and externally. We would especially like to thank our supervisors David Berstad, Øivind Wilhelmsen and Professor Petter Nekså. We are grateful for the time they spent and for their insights and valuable contributions throughout the project period.

We would also like to thank Professor Magnus Korpås for his assistance within renewable power systems and energy storage.

Table of Contents

List of Figures

List of Tables

List of Abbreviations:

ATR – Autothermal Reforming

CAPEX – Capital expenditures

CCGT - Combined Cycle Gas Turbines

CCS – Carbon Capture and Storage

CRE – Combined Reforming and Electrolysis

EJ - Exajoule

EL – Electrolysis

FCV – Fuel Cell Vehicles

GHR – Gas Heated Reformer

HHV – Higher Heating Value

HTS – High Temperature Shift

IEA – International Energy Agency

LHV – Lower Heating Value

LNG – Liquid Natural Gas

LTS – Low Temperature Shift

MDEA - Methyl Diethanolamine

MEA – Monoethanolamine

NG – Natural Gas

O/F – Oxygen-to-Fuel

OPEX – Operational Expenditures

PEMFC – Proton Exchange Membrane Fuel Cell

POX – Partial Oxidation

PR – Peng-Robinson

PSA – Pressure swing Adsorption

S/C – Steam-to-Carbon

SMR – Steam Methane Reforming

WGS – Water-gas Shift

1 Introduction:

The global energy system is experiencing a change of scenery. Unstable energy markets and an increasing focus on climate change and sustainable development is forcing businesses to pursue new solutions in order to ensure future economic growth. This has led to the interest in using hydrogen as an energy carrier in transportation and industrial applications.

As an energy carrier, hydrogen is accessible and holds a high gravimetric energy density. Abundant in hydrocarbons, hydrogen can play an important role in the shift towards low-emission fossil value chains. By combining hydrogen production by natural gas reforming with carbon capture and storage, the overall CO_2 emissions are significantly reduced. In addition, the flexibility of hydrogen as an energy storage medium makes it applicable as a stabilizer in the renewable energy mix. The recent development in hydrogen fuel cells is also raising the expectations for a hydrogen powered transportation sector.

Hydrogen value chains exist to a large extent in the industry today. The global hydrogen consumption was approximately 50 million tonnes (7.2 EJ) in 2013, where refineries, ammonia and methanol production and metal processing were main consumers [1]. Natural gas reforming produced 48% of this hydrogen, but without carbon capture and storage (CCS) [1]. The total emissions from the production reached 500 million tonnes of CO_2, hence alternative production methods with lower emissions will be necessary in future value chains.

With the potential of being a sustainable solution to both the fossil industry and transportation, hydrogen inarguably has great benefits. This also benefits Norway. With one of Europe’s largest natural gas reserves, capacious and available reservoirs for carbon storage and some of the best accessible wind conditions in the world, Norway has the opportunity to be in the forefront of the development of future hydrogen value chains. The export of oil and gas is vital to the country’s economy and new carbon-lean methods of utilizing these resources could prove key in the future of Norwegian exports.

The aim of this thesis is to evaluate the technical and economic potential of large-scale production of carbon-lean hydrogen in Norway. First is a literature survey, explaining the main steps in hydrogen production from natural gas, followed by future hydrogen market considerations, both of domestic and international demand. Further is a detailed techno-economic analysis of carbon-lean hydrogen production, evaluating strengths and weaknesses of the individual processes in the context of Norwegian hydrogen production for export. The last part consists of different case studies, evaluating specific process designs combining the utilization of stranded natural gas and excess wind power in Mid-Norway.

What differentiates this thesis from other studies on large-scale hydrogen production is mainly two factors: The presence of Norwegian energy resources and CCS opportunities, as well as a focus on reduced CO_2 emissions. The breakeven price of hydrogen produced in Norway, with the current cost of electricity and natural gas may prove exceptional compared with countries like Germany, U.K. or Japan. The opportunities hydrogen represents in the future economy provides the motivation for a more extensive study of the techno-economic conditions for Norwegian, large-scale hydrogen production.

1.1 Scope of the Thesis:

In order to conduct an analysis to this extent, a defined scope is necessary. Listed are the main boundary conditions and technical assumptions in the thesis.

1. Desulfurized natural gas and electricity are the only energy inputs used in this thesis. Hydrogen can be produced from a large selection of feedstock like coal or biogas, but that is not included. Biogas may be a viable alternative in the future, but coal is irrelevant in a Norwegian hydrogen production chain.
2. Only mature, commercially available technologies for large-scale hydrogen production are considered.
3. Carbon capture is a prerequisite in the reforming processes and only pre-combustion CCS is evaluated. Carbon capture from flue gas with low partial pressures is not included in this thesis, due to lack of commercial availability. Carbon capture at high partial pressures are currently in operation at both the Sleipner oilfield and at Melkøya [2] [3].
4. Carbon transport and storage technology is out of scope. The cost of the entire CCS chain is included, but no technical analysis is done on either transport or storage alternatives.
5. The scale of the hydrogen production evaluated in this report is motivated by export scenarios.

2 Concepts for Large-Scale Hydrogen Production from Natural Gas

This chapter will provide a walk-through of large-scale hydrogen production from natural gas. The main steps of natural gas reforming will be discussed as well as the separate technologies available to fulfil these steps. Figure 1 shows the five steps this thesis has defined as the main groups of processes in a hydrogen production facility: natural gas pre-treatment, natural gas reforming, water gas shift, carbon capture and hydrogen purification. Of these five, natural gas reforming is the focus of this thesis. As the scope of the thesis assumes desulphurized natural gas, step number one is less important.

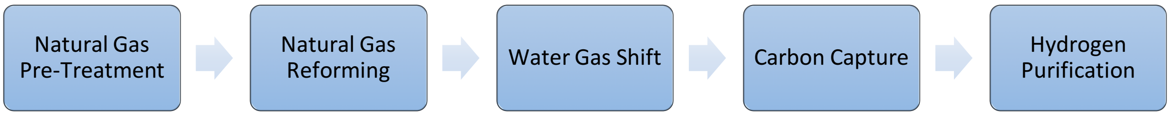

Figure 1 - Main steps of hydrogen production from natural gas. Natural gas reforming will be the main focus of this thesis

2.1 Natural gas Pre-treatment

For natural gas, the only pre-treatment required is desulphurization [4]. Natural gas reforming is usually a catalytic operation, and the catalysts are poisoned by even small amounts of sulphur. Catalyst poisoning is in this case when sulphur is adsorbed onto the catalyst surface reducing the catalytic activity significantly [5]. This results in a reduction of the total plant efficiency. Sulphur poisoning may be permanent and pre-treatment through desulphurization is therefore crucial for successful production of hydrogen from natural gas [5]. When pre-treating NG, the feed is first sent through a flash drum, removing all the liquids. The organic sulphur in the NG is then blown with recycled hydrogen and hydrogenated, releasing the sulphur as H_2S. The H_2S is adsorbed in a zinc oxide bed and reacts to form zinc sulphide, which is removed as a solid waste [6]. The desulphurisation operating temperature is between 260-430°C and the pressure is up to 50 bar. As the scope of the thesis assumes desulphurized natural gas feed, this step is not discussed any further.

2.2 Reforming Processes

Although hydrogen is in an early stage as a fuel within the transportation sector, it has been a major commodity in industry for decades. As mentioned in the introduction, the global hydrogen demand was 7.2 exajoules (EJ) in 2014, equivalent to 50 million tonnes [1]. 48% of this hydrogen is produced from the reforming of natural gas. This section will explain the main reforming principles and technologies available.

2.2.1 Pre-Reformer:

The principle of the pre-reformer is to convert heavier hydrocarbons to methane prior to the main reforming reactor. The pre-reforming reactor usually contains a nickel catalyst bed and is basically a low temperature adiabatic steam reforming unit. The temperature is normally in the range from 350 – 550 °C [4]. There are several benefits to pre-reforming, but most important is the enabling of process optimization of methane reforming. This results in lower feed consumption and hence a smaller reactor size.

2.2.1.1 Gas Heated Reformer

One example of a sophisticated pre-reformer is the gas heated reformer (GHR), also referred to as a convective reformer. What differentiates it from the traditional steam methane reforming (SMR) is the temperature range and the method of heat transfer. Where the SMR reactors are heated by external combustion of natural gas in a system of reactor tubes and burners, the GHR works as a heat exchanger, absorbing energy by convective heat transfer with another gas [7]. Figure 2 shows the basic principles of the GHR. In an integrated system, the GHR can be used as both a pre-reformer and a heat exchanger cooling the syngas prior to the water gas shift reactors.

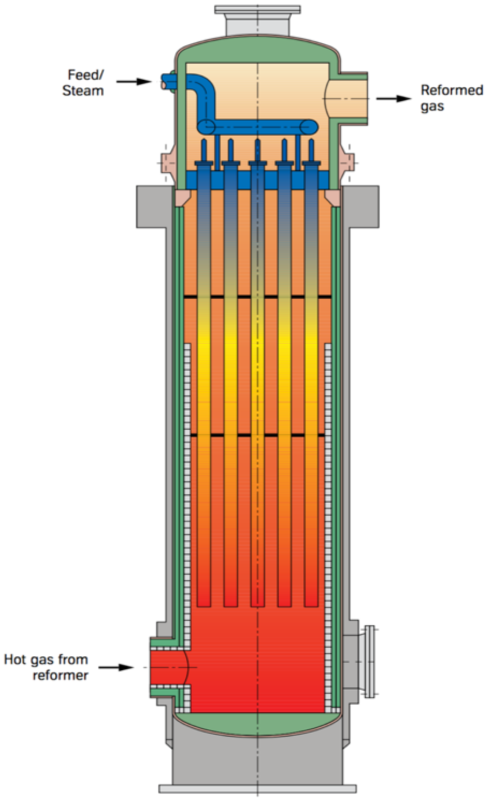

Figure 2 - Gas Heated Reformer. Illustration by ThyssenKrupp Industrial Solutions [7]

2.2.2 Steam Methane Reforming (SMR)

A widely used method to produce hydrogen from natural gas (NG) is by the use of steam methane reforming (SMR) [4]. The reaction is endothermic and converts steam and methane into H_2 and CO as shown in equation 2.1.

$$CH_4 + H_2O \rightleftharpoons CO + 3H_2 \tag{2.1}$$

The activation energy needed is 206 kJ/mol. The reaction is a catalytic reaction supported by nickel-based catalysts. Nickel-based catalysts are cost efficient and have sufficient activity. When more activity is needed, a more noble catalyst can be used. Nobel catalysts provides higher activities and faster reactions but are very expensive [4]. The reactor consists of several reactor tubes filled with reforming catalysts and kept in a furnace that provides the necessary heat for the reaction to happen. The design is illustrated in Figure 3.

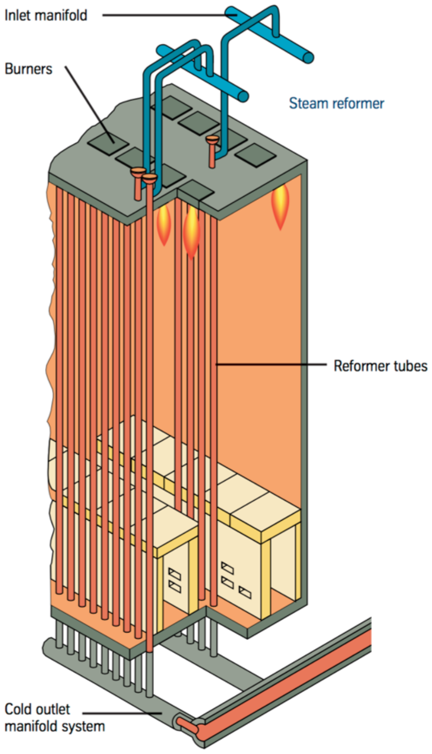

Figure 3 - Steam Methane Reformer Reactor. Illustration by TyssenKrupp Industrial Solutions [7].

The reaction is normally carried out at pressures above 20 bar, steam-to-carbon (S/C) ratio of 3-4[3] on a molar basis and temperatures between 500-900°C [8]. A higher S/C ratio is partially to reduce the risk of carbon deposition on the catalyst surface [4]. High conversion is thermodynamically favoured by low pressures, high S/C ratio and high temperatures. From an energy efficiency and economic point of view, low S/C ratio is preferred and modern SMR-plants have been design to withstand higher temperatures. The upper temperature limit is due to material limitations. SMR usually operates at an energy efficiency up to 80-85% and generally produces more hydrogen per carbon than both POX and ATR [9]. H_2/CO ratio is typically between 3.5 and 5.5 in the reformed product [10].

2.2.3 Partial Oxidation (POX)

A fundamentally different method of producing hydrogen from natural gas is by the use of partial oxidation (POX). The reaction is exothermic, in contrast to the highly endothermic SMR reaction. By burning the natural gas with a limited oxygen supply, the products are H_2 and CO, as shown in equation (2.2). This method can in theory be applied to any hydrocarbon, hence it is a method for a variety of feedstock.

$$\mathrm{C_mH_n} + \frac{\mathrm{m}}{2}\mathrm{O_2} \rightleftharpoons \mathrm{mCO} + \frac{\mathrm{n}}{2}\mathrm{H_2} \tag{2.2}$$

As can be seen by the reaction (eq. 2.2), a POX reactor has a hydrocarbon and an oxygen input. Most large-scale systems include an air separation plant in order to supply clean oxygen. This does not only reduce the necessary size of the reactor, but also increase the purity of the output [4]. The cases where air-blown reactors are used, nitrogen is favourable in the product, as is the case for ammonia production. The energy efficiency of POX is around 70 - 80% with the reactors usually operating at temperatures between 1150 - 1500 °C [4].

2.2.3.1 Air separation units

Since this thesis is focusing on fuel cell-grade hydrogen production, close to pure oxygen is needed in the partial oxidation. Many different systems for air separation is available, but if the oxygen purity is expected at >99.99% only cryogenic air separation is a viable option in a large-scale facility. The most available technologies used for air separation are listed in Table 1.

---

[3] Interview with SINTEF Research Scientist Rahoul Anantharaman

Table 1 - List of viable air separation technologies [11].

Process	Status	Production size (tonnes/day)	By-product capability	Purity Limit (vol. %)	Start-up time
Adsorption:	Semi-mature	< 136	Poor	95	Minutes
Cryogenic:	Mature	> 18	Excellent	99+	Hours
Membrane:	Semi-mature	< 18	Poor	~ 40	minutes

2.2.4 Autothermal Reforming (ATR)

Autothermal reforming (ATR) is the combination of POX and SMR in one reactor. NG is partially oxidised in a combustion zone, while steam is injected in a SMR zone. Hence, both the POX and the SMR reactions are active simultaneously. This concept also need pure oxygen input as well as a catalyst bed in the steam reforming section of the reactor. The core benefits of this system is that the heat generated by the POX reaction is consumed by the endothermic SMR reaction. This enables a closed system, insulated from external heat supply. In addition, since the oxidation occurs within the reaction chamber, flue gas is not produced, resulting in the potential of no local emissions.

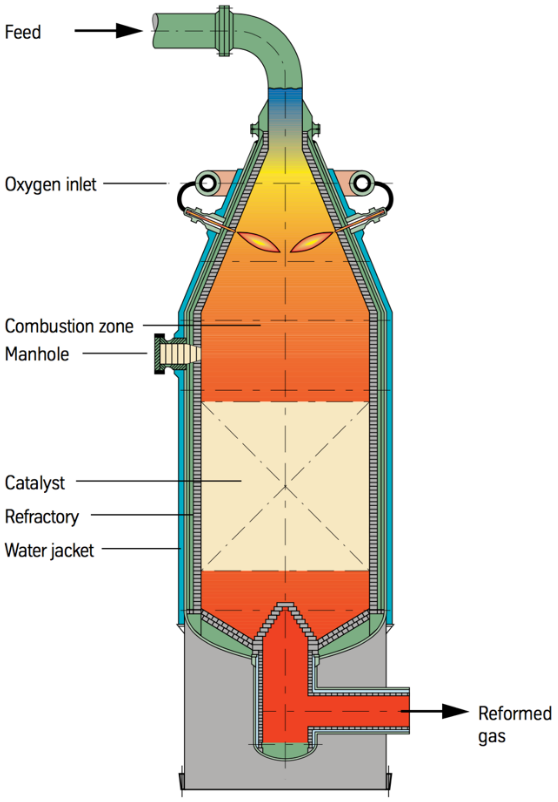

Figure 4 - Autothermal Reforming Reactor. Illustration by TyssenKrupp Industrial Solutions [7]

The ATR reactors usually operate at temperatures between 900-1150 °C, with pressure levels in the range 1 to 80 bar existing today [4]. Figure 4 shows the principles of the ATR reactor, with the different inputs and reaction zones. No specific range was found for the typical energy efficiency of ATR, but it should operate with lower energy efficiency than SMR [12].

2.2.5 Other reforming processes

The paper by Mari Voldsund, Kristin Jordal and Rahul Anantharaman, "Hydrogen Production with CO_2 Capture" is used actively when looking at other reforming processes [8].

2.2.5.1 Membrane Reactors

When producing hydrogen in membrane reactors, a chemical reaction like the ones in SMR, POX or ATR, mentioned in section 2.2.2 to 2.2.4, take place inside a reactor where either H_2 or CO_2 are selectively removed by a membrane [8]. This shifts the equilibrium of the reactions, which results in higher conversion, and/or allows reforming of hydrogen at milder thermal conditions [8]. H_2-selective reactors have a higher effect on the reaction conversion rate compared to CO_2-selective reactors, therefore far more research is done on the H_2-selective reactors [8]. These membrane reactors are currently in a developing phase and are not commercially available.

2.2.5.2 Sorption-enhanced hydrogen production

Sorption-enhanced hydrogen production is to use adsorbents in the reactor to selectively remove one or more of the products reformed. This will, similar to membrane reactors, shift the equilibrium of the reactions, resulting in higher conversion and/or the possibility to reform hydrogen at milder thermal conditions [8]. Sorption-enhanced hydrogen production is in principle combining traditional hydrogen production (SMR, POX and ATR) with hydrogen purification (PSA). This technology is also currently in a developing phase and is not commercially available [8].

2.3 Water Gas Shift (WGS)

After the reforming process, the syngas undergoes a water gas shift, where the CO is reacted with water, over a catalyst, to produce additional hydrogen as well as CO_2. The process is slightly exothermic and is controlled by equilibrium [4]. It follows the reaction equation 2.3.

$$\mathrm{CO} + \mathrm{H_2O} \rightleftharpoons \mathrm{CO_2} + \mathrm{H_2} \tag{2.3}$$

The equilibrium constant is a function of temperature, meaning the reaction is favourable at low temperatures. On the other hand, the reaction rates diminish at low temperatures. Because of this the process is usually done in two steps, a high temperature shift (HTS) and a low temperature shift (LTS). In the HTS, the mole fraction of CO is reduced from typically 10-13% to 2-3%, with an inlet temperature between 350-550°C. In the LTS, the CO concentration is further reduced to 0.2-0.4% at temperatures of 190-250 [4]. The lower limit is set due to the water dew point of the gas. Condensation could damage the catalysts in the WGS chamber [4].

2.4 Concepts for CO_2 Separation

After the WGS, hydrogen and CO_2 are produced and have to be separated and purified. Concepts for CO_2 separation are presented in this section, while different concepts for hydrogen purification are presented in Section 2.5.

2.4.1 Pressure Swing Adsorption (PSA)

Adsorption can be used to purify CO_2 form the syngas. This is usually done between the reforming and the hydrogen purification, and is done with CO_2-selective adsorbents. The process consists of two steps; first, wet CO_2 is removed in CO_2-selective adsorbent beds. Second, CH_4, CO, remaining CO_2 and other impurities are removed from the hydrogen [8]. As much as 90% of the CO_2 can be captured with a purity of 97% using this technology.

2.4.2 Absorption

CO_2 absorption is a commercially mature technology and is commonly used to remove CO_2 from NG [8]. The liquid solvent can be divided into two groups, chemical and physical solvents. Chemical solvents react with CO_2 and require heat to activate the reaction. Chemical solvents offer fast reaction rates which results in smaller plant size. MDEA, MEA, TEA and potassium carbonate are examples of chemical solvents used for CO_2 capture. Physical solvents do not react but dissolve CO_2 and require less heat than chemical solvents. Rectisol®, Selexol™, and Purisol® are all examples of technologies using physical absorption [8]. Chemical solvents have relatively high capacity at low pressure compared to physical solvents and are therefore preferred at low CO_2 partial pressures. The chemical solvents will begin to saturate with increasing CO_2 partial pressures and physical solvents are therefore preferred at high CO_2 partial pressures. The CO_2 recovery and purity will depend on the syngas composition and various solvents may be optimal for CO_2 separation. Studies have shown that MDEA can capture as much as 95% of the CO_2 with a purity of above 99% [8].

2.4.3 Membrane Separation

There are great challenges separating CO_2 from a hydrogen rich gas with membrane due to hydrogen molecules been significantly smaller than CO_2. Current CO_2-selective membranes are based on solution-diffusion mechanism or facilitated transport mechanism [8]. An example of such membrane is polymeric CO_2-selective membranes. There exist other CO_2-selective membranes as well such as mixed matrix membranes and porous inorganic membranes. The current, commercial, CO_2-selective membranes have low selectivity and operate at low temperatures [8]. More research on CO_2-selective membranes is needed to develop an efficient membrane with high CO_2 selectivity.

2.4.4 Cryogenic Separation

Cryogenic, or low-temperature separation, is the process where gas is cooled down and the difference in boiling point is used to separate the gas components. The gas is separated using a separator column. When separating CO_2 from syngas, the syngas is first compressed to 90-115 bar and then cooled down and condensed at temperatures around -55°C [8]. CO_2 purities of 99.7-99.9% with a recovery of 85-90% can be obtained [13]. An advantage with low-temperature separation of CO_2 is that the CO_2 in a liquid state, cost efficiently can be pressurized and transported. Cryogenic separation can also be used to separate hydrogen, but produces hydrogen with a low purity.

2.5 Hydrogen Purification Processes

To liquefy hydrogen and to use it in a fuel cell, a purity of above 99% is required [8]. There are currently only two hydrogen purification processes with the ability to produce hydrogen with a purity of above 99% and only these will be covered in this section.

2.5.1 Pressure Swing Adsorption (PSA):

Over 85% of current global hydrogen production units use PSA technology for hydrogen purification and is the most used hydrogen purification technology today [4]. When PSA is used to purify hydrogen, the syngas is sent through an adsorption column at high pressures letting through hydrogen while adsorbing CO_2 and other impurities. The pressure inside the column is then lowered near atmospheric pressure desorbing impurities from the adsorption material. There are usually several columns operating simultaneous making the hydrogen purification process semi-continuous. Columns with multiple adsorbents are normally used when purifying hydrogen. Typical adsorbents are silica gel, alumina, activated carbon and zeolite [8]. Operating temperature in PSA units is typically ambient temperature receiving the feed syngas at a pressure between 20-60 bar. Hydrogen is purified with a pressure drop between 1-2 bar. The off-gas exits the unit with pressures between 1-2 bar. The PSA unit produces hydrogen with a purity up to 99.9999% and with a hydrogen recovery between 60-95% [8]. The hydrogen recovery decreases with an increase in the hydrogen purity demand. Where methane, CO_2 and CO are easily adsorbed, oxygen, argon and nitrogen are more difficult to adsorb and may reduce the purity of the produced hydrogen.

2.5.2 Membrane Separation

Membranes are ideal for separation purposes as they are selective barriers and only let through certain components. The essential characteristics for membranes are high selectivity, high flux, low cost, high mechanical stability, high chemical stability [8]. The transported fluid over the membrane is driven by the difference in pressure. The currently most mature membranes for hydrogen separation are polymeric membranes. These membranes have an operating temperature of 100°C and are relatively inexpensive, however polymeric membranes have low hydrogen selectivity and hydrogen flux. Polymeric membranes can therefore not produce hydrogen with hydrogen purity of 99%. There are many high-temperature membranes currently under development. Such as metallic membranes (300-700°C), microporous ceramic membranes (200-600°C), porous carbon membranes (500-900°C) and dense ceramic membranes (600-900°C). These high-temperature membranes have possibilities to offer higher hydrogen flux and selectivity. The most studied membrane for hydrogen purification is metallic membranes, most often made of palladium. Palladium membranes have an infinite selectivity and can produce hydrogen with a purity of 99.999%. The challenges with the palladium membranes is the mechanical strength and chemical stability. There are palladium membranes on the market today, but these are expensive and to dense (Low flux). Reinertsen AS are currently developing a less dense palladium membrane and states that this membrane will become cost efficient, deliver high purity of hydrogen, have high hydrogen recovery and have a lifetime of 10 years. The membrane Reinertsen AS are developing will be sold in modules and can easily be scaled up for a large-scale hydrogen production plant[4].

---

[4] Interview with Frode Roness, Reinertsen AS

Table 2 - Summary of performance for different options for hydrogen and CO_2 separation from syngas [8].

	Unit	Adsorption – H_2 PSA	Adsorption – CO_2 PSA	Absorption – MDEA	Absorption – Physical	Membrane – Pd-based	Low temperature CO_2 capture
H_2 purity:	mol%	98 – 99.9999+	Low (<91)	Low(58)	Low(83-86)	99-99.995	Low(81-83)
H_2 recovery:	%	70-95	High	High	High	n/a	High
CO_2 purity:	mol%	Low(39-57)	>97	99.9	95-99.7	Low	99.7-99.9
CO_2 recovery:	%	High	>90	95	90-97	High	85-90
Syngas in source:		SMR	SMR	Air-blown ATR	Gasified Coal	SMR	Gasified Coal

3 Norwegian Hydrogen Markets, and the Potential for Large-scale Production

In Norway, CO_2 emissions are distributed evenly between transportation, oil and gas industry and general industry. Producing hydrogen from renewable energy can facilitate a completely carbon free value chain. In addition, environmental friendly solutions for reforming of fossil resources can provide cost competitive alternatives in a market penetration period for green hydrogen. Carbon capture and storage (CCS) enables large reductions in the oil and gas sector. This technology is already utilized at the Sleipner field and in Hammerfest, accounting for an annual storage of 1.7 million tonnes of CO_2 [14]. Producing hydrogen from natural gas enables a brilliant solution for the industry and transportation sector to benefit from CCS as well. The National transport plan, released in February 2016 highlights hydrogen as an important part of a low-emission transportation system. In addition, the company Greenstat signed a letter of intent to deliver a large-scale hydrogen production facility to Tizir in Tyssedal, redesigning the smelting oven from a coal-based to hydrogen-based reduction.

This section will provide an overview of the developments in the hydrogen demand of the transportation and industry sector as well as discussing the potential for hydrogen export.

3.1 Transportation Sector

The transportation sector accounts for approximately 36 % of the annual CO_2 emissions in Norway, close to 17.2 million tonnes of CO_2 equivalents [15]. In this thesis, the transportation sector includes all road traffic, as well as domestic air and marine traffic. The need for low- emission solutions across the entire range of utilities is urgent. As an energy carrier, hydrogen compliments the batteries in the more energy demanding and time consuming tasks, with longer range and short refuelling time. Therefore, hydrogen can prove to be the favourable carbon-lean solution for heavy transport, busses, trains, ferries, and eventually airplanes. In a recent study done by SINTEF, different scenarios for market introduction of hydrogen within the Norwegian transportation sector is presented [16]. The total hydrogen demand in the transportation sector ranges from 9 500 – 61 000 tonnes per year in 2030, mostly depending on policies and implementation in public transportation and fleet vehicles like busses and taxis.

A master's thesis performed at the Norwegian School of Economics evaluates the potential of using hydrogen fuel in ferries along the Norwegian coastline [17]. The project concludes that hydrogen that with further cost compression, hydrogen can potentially be an economically viable fuel for the ferry sector. In order to quantify the potential marked, assume all routes exceeding 10 kilometres and 30 minutes of travel time are fuelled by hydrogen. With a fuel cell efficiency of 50% the total hydrogen demand would be approximately 15 000 tonnes annually, or 41 tonnes per day.

3.2 Industry Sector

The global industrial hydrogen demand is mainly within the chemical and refining industries [9]. In Norway, the information regarding industrial demand for hydrogen is limited, but in general, the metal and chemical industries consume substantial amounts of hydrogen in various silicon and ammonia production processes. A significant growth in demand can be achieved if policy requirements enforce a switch to hydrogen consuming processes in order to reduce emissions. As mentioned earlier, an example of this is the letter of intent signed by Tizir and Greenstat in the fall of 2015 [18]. The project is a feasibility study regarding the replacement of coal with hydrogen in the reduction process in the ferrosilicon production facility. Pre-studies show that hydrogen will reduce production costs as well as eliminating 23 000 tonnes of CO_2 emissions annually from the smelting oven. The total hydrogen demand of this facility is expected to be 30 tonnes per day, equal to 11 000 tonnes annually. Compared to the marked estimations of hydrogen in the transportation sector this facility alone exceeds the low-case demand. This shows why industry, both domestic and international, is most likely to be the target for centralized large-scale hydrogen production facilities. A feasibility study, similar to Tizir, is conducted in Sweden by Vättenfall among others [19]. Here, the aim is to produce steel using hydrogen in a process called direct reduction.

3.3 Is There a Potential for Centralized Hydrogen Production in Norway?

Based only on the overview of the transportation market in Norway, a centralized production of more than 100 tonnes per day will be sufficient to supply more than 50% of even optimistic market estimations. If a Scandinavian distribution system is developed, large-scale hydrogen production for industrial use holds a more viable potential. The feasibility study by Tizir will be a crucial next step for Norwegian, industrial hydrogen. With this in mind, a large-scale hydrogen production facility with a capacity in the scale of above 100 tonnes per day will be more suited for export in a carbon-lean energy trade.

The international demand for carbon-lean hydrogen is estimated to increase rapidly in the coming years [20]. In Western Europe, dominated by UK and Germany, the demand for hydrogen is expected to reach more than 9 million tonnes per day in 2030, with carbon-lean hydrogen representing 15% in a CO_2 policy driven scenario [21]. In Japan, concrete plans for hydrogen import is on the table. Already in 2012, Kawasaki released a strategy related to importing hydrogen based on brown coal gasification in Australia, 770 tonnes per day [22].

This thesis uses a production capacity of 500 tonnes of hydrogen/day as a large-scale base scenario. In an export scenario, this production size can supply around 10% of the estimated carbon-lean hydrogen market in Europe in 2030 [20].

3.4 What to do with 500 Tonnes of Hydrogen?

Even though hydrogen is a familiar compound in industry, the general understanding of it as an energy carrier is limited. 500 tonnes of hydrogen hold 19.7 GWh of energy. 347 days of production adds up to a total of 6.8 TWh, equal to 0.2% of the energy consumption within road transportation in EU [23]. In comparison, the total electricity production in Norway in 2014 was 142.3 TWh [24]. Kawasaki are developing liquid hydrogen carriers for large-scale import. The assumed tank volume is 160 000 m^3, able to hold 11 328 tonnes of hydrogen[5] [25]. This equals 22 days of production in a plant with 500 tonnes per day capacity.

Based on the specification of Toyota Mirai, a fuel cell electric vehicle (FCEV) runs approximately 100 km per kg of hydrogen [26]. With an average travel distance of personal vehicles in Norway of 12 289 km annually, 500 tonnes of hydrogen per day can power 1.4 million cars [27]. On a higher heating value basis, 1 kg of hydrogen equals approximately the same amount of energy as 4 litres of petrol.

---

[5] Liquid hydrogen density of 70.8 kg/m^3

4 Technical Analysis of Large-scale Hydrogen Production

4.1 Introduction:

This chapter will provide a technical analysis of the different systems converting natural gas to hydrogen. The systems will be defined and modelled, and the results will be presented in order to do a comparative analysis. The scope of the project limits the hydrogen production to be based on natural gas with CCS, as well as it compares the results to non-fossil hydrogen production by electrolysis of water. The following hydrogen production systems will be evaluated in this thesis:

1. **Steam Methane Reforming – SMR**
2. **Steam Methane Reforming, with reduced emissions – SMR+**
3. **Partial Oxidation – POX**
4. **Autothermal Reforming – ATR**
5. **Electrolysis – EL**
6. **Combined Autothermal Reforming and Electrolysis – CRE**

Each system is designed and optimized based on a steady state, chemical process model, simulated in the software Aspen HYSYS. The systems are designed for a production capacity of 500 tonnes of pure, carbon-lean hydrogen every day.

Throughout this chapter, emphasis will be put on the following parameters: Energy efficiency and CO_2 emissions. With increasing power consumption, the efficiency of energy systems requires attention although it is often related to increased investment costs. With a fixed hydrogen production capacity, a high energy efficiency can be key to reduce operational expenditures, as well as CO_2 emissions.

4.2 Case Presentations

This section presents the different systems defined in this thesis, in order to get an overview of the individual designs. Each system will be explained in detail in Section 4.3.

4.2.1 System 1: Stream methane reforming – SMR

System number one is traditional steam methane reforming (SMR), described in Section 2.2.2, with carbon capture from the syngas stream. The heat required in the reactor is delivered by a furnace, burning the process tail gas as well as additional natural gas if needed. A system flowchart is presented in Figure 5.

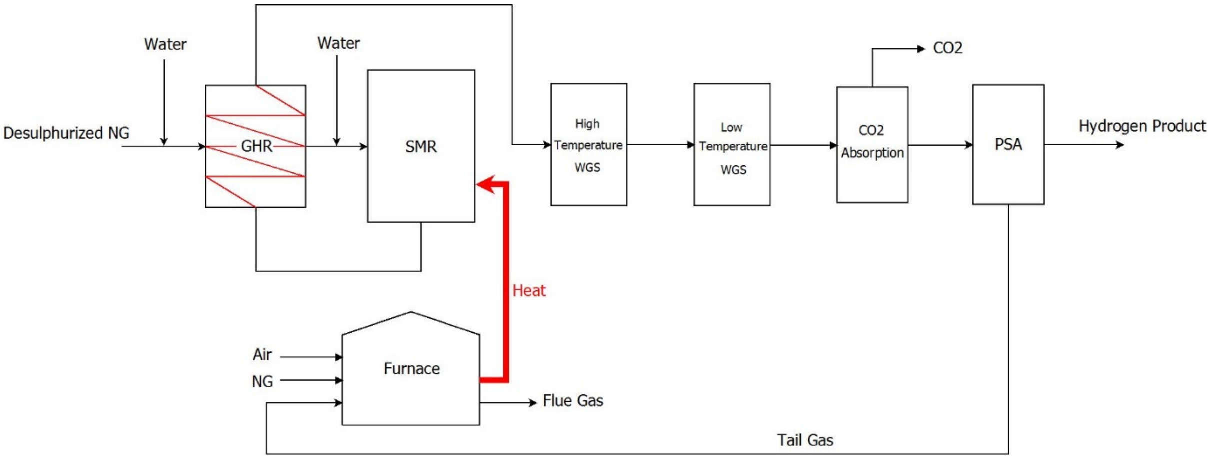

Figure 5 - SMR flowchart

4.2.2 System 2: Steam Methane Reforming with Reduced CO_2 Emissions – SMR+

Because of the external combustion, CCS is limited to approximately 70% of the CO_2 produced in SMR, disregarding carbon capture from the flue gas. Therefore, a new SMR design, replacing the natural gas feed in the furnace with hydrogen, is defined in order to reach close to 90% carbon capture. The system is named SMR+ and presented in Figure 6.

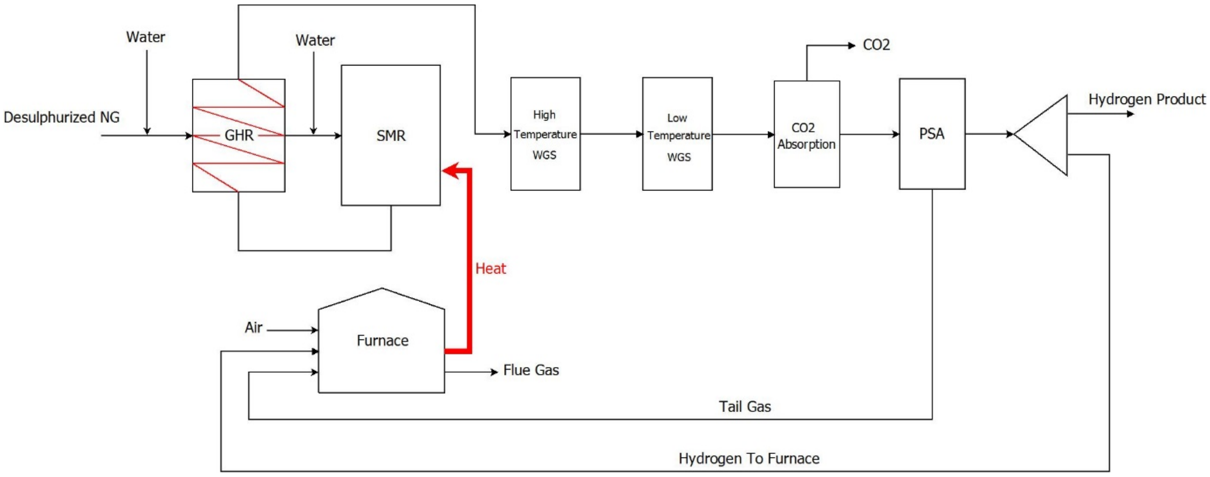

Figure 6 - SMR+ flowchart

4.2.3 System 3: Partial Oxidation – POX

The third system analysed in this thesis is partial oxidation (POX), described in Section 2.2.3. POX differs from SMR by utilizing the exothermic combustion of natural gas with limited oxygen supply, producing hydrogen and CO, instead of water and CO_2. Figure 7 shows the system layout.

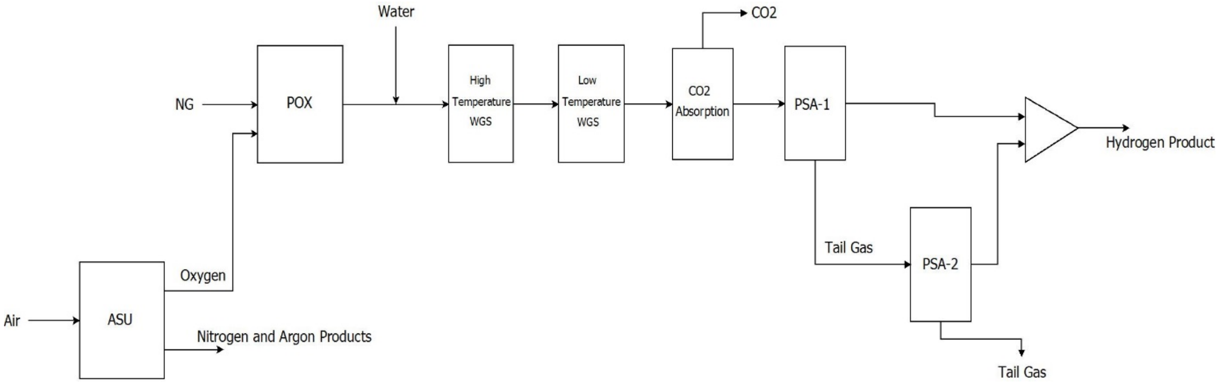

Figure 7 - POX flowchart

4.2.4 System 4: Autothermal Reforming – ATR

ATR, described in Section 2.2.4, utilize the heat produced from the exothermic POX to fuel the endothermic SMR, resulting in an efficient system with internal combustion. This design allows for extensive CCS, without compromising on efficient operation. The flowchart of ATR is presented in Figure 8.

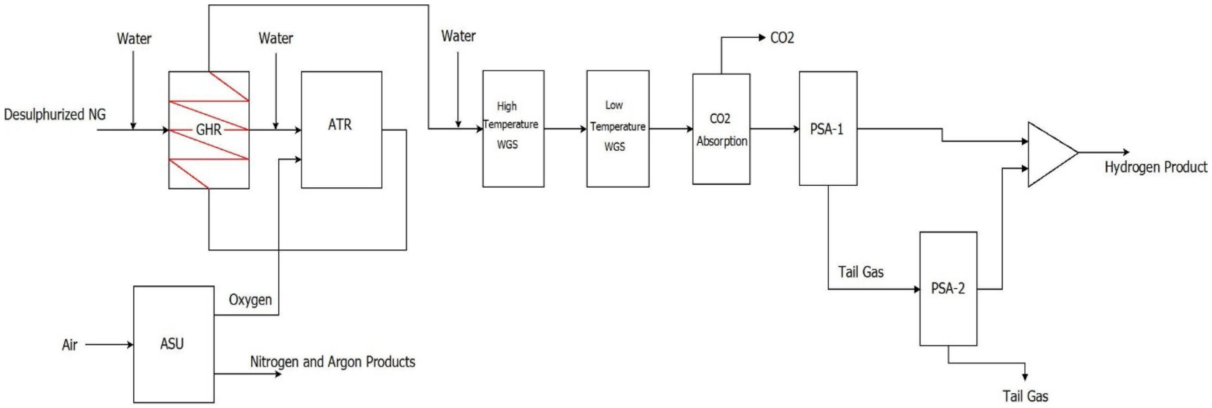

Figure 8 - ATR flowchart

4.2.5 System 5: Electrolysis – EL

Fundamentally different from natural gas reforming is electrolysis of water. By supplying a significant amount of electricity, EL splits water into hydrogen and oxygen. A completely carbon-free process. No simulation of EL has been conducted, but the technical and financial specifications are included in the thesis for comparison.

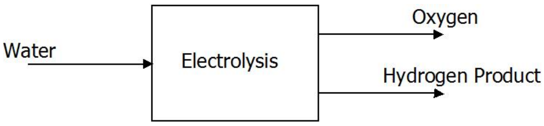

Figure 9 - Electrolysis flowchart

4.2.6 System 6: Combined Reforming and Electrolysis – CRE

As electrolysis of water produce oxygen as a by-product, a system of ATR utilizing this oxygen has been analysed. Replacing the air separation unit with electrolysers produces the required amount of oxygen to the ATR as well as additional hydrogen. The CRE system layout is shown in Figure 10.

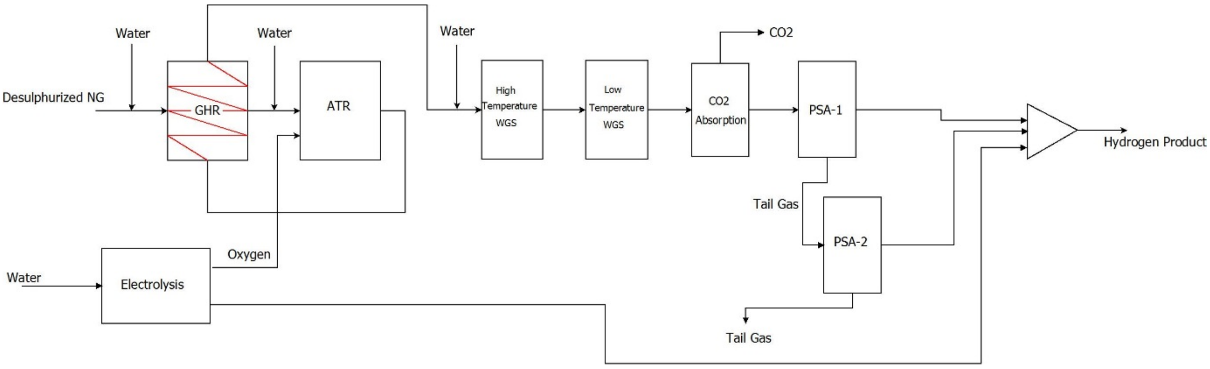

Figure 10 - CRE flowchart

4.3 Methodology and Simulation of Large-scale Hydrogen Production

Chapter 4 provides an overview of the different systems available for hydrogen production from natural gas. This specific section will design and model the main systems suitable for large-scale production, based on existing technology. More specifically, they are different methods for producing synthesis gas, also known as syngas, a gas mix consisting mainly of hydrogen, carbon monoxide and CO_2. The individual processes produce syngas with different properties and composition, specialized for their purpose. In the industry today, SMR is a widely used method for hydrogen production [4]. However, as the scope of this thesis highlights, carbon capture and storage (CCS) is a prerequisite for a broad acceptance of fossil-based hydrogen in a sustainable industry. Given a goal of an energy efficient hydrogen production process, which at the same time minimizes the CO_2 emissions, the boundary conditions are changed, hence SMR might not be the preferable method. This section will describe the six hydrogen production systems evaluated in this thesis and how they are modelled and optimized in Aspen HYSYS.

4.3.1 General Design Basis and Simulation Methodology.

This section will provide the design basis for the production systems and the methodology used in the simulations.

4.3.1.1 Design conditions

As mentioned in Chapter 3, a production of 500 tonnes of hydrogen/day has been defined as the large-scale scenario analysed in this thesis. The feedstock used in the hydrogen production system is natural gas (NG) of the composition available at Tjeldbergodden industrial complex. The NG properties can be seen in Appendix B. The properties of the hydrogen produced in all the production systems is set to 25°C and 20 bar.

4.3.1.2 CO_2 Separation and hydrogen purification

The CO_2 separation and the hydrogen purification processes are, in all systems presented in Section 4.2, modelled as component splitters, as seen in Appendix B. The only input parameters are the product purity and recovery rate. MDEA absorption for CO_2 separation and PSA for H_2 purification is chosen based on the technical data in Table 2 and the maturity of the technologies available. Although, given the same input parameters, any technology would provide the same technical results in these simulations.

4.3.1.3 System Heat Integration

All the systems presented in Section 4.2 are designed to be fully heat integrated. The system heat integration is further elaborated in Appendix B, where the heat integration data is presented.

4.3.1.4 Energy efficiency

In order to evaluate the system performance and optimize the hydrogen production, defining energy efficiencies is important. The two main efficiencies used in this thesis are plant energy efficiency and thermal efficiency, defined in equation 3.1 and 3.2, respectively. The plant energy efficiency represents the overall performance of the system, including the power consumption of components like oxygen compressors and process water pumps. The specific power consumption of the CO_2 compression related to storage is not included in the energy efficiencies defined, considering the CCS system is out of scope in this thesis. Expenditures related to investment and operation of the CCS facility is, on the other hand, included in the financial analysis in Chapter 5.

Plant energy efficiency - $\boldsymbol{\eta_P}$:

$$\eta_P = \frac{LHV_{H2} * \dot{m}_{H2}}{LHV_{NG} * \dot{m}_{NG} + \dot{W}_{net}} \tag{3.1}$$

Thermal Efficiency - $\boldsymbol{\eta_T}$:

$$\eta_T = \frac{LHV_{H2} * \dot{m}_{H2}}{LHV_{NG} * \dot{m}_{NG}} \tag{3.2}$$

Where LHV is the lower heating value, $\dot{m}_{H_2}$ is the mass flow rate of the product hydrogen and $\dot{m}_{NG}$ is the total NG inlet, including both process feed and eventual furnace feed. $\dot{W}_{net}$ is the net power consumption of the production process. The dedicated power consumption of the CCS is not included in the efficiencies, since the value should enable a comparison of the production processes specifically.

The thermal efficiency is a ratio describing the energy preserved in the product hydrogen compared to the NG feed. As all excess heat is supplied by additional NG, a plant energy efficiency similar to the thermal efficiency implies a process with little power demand.

4.3.1.5 Aspen HYSYS Simulation

The hydrogen production systems are modelled with the chemical process software Aspen HYSYS version 8.6. HYSYS is specialized in hydrocarbon processing and it is a comprehensive tool, enabling design and optimization of steady state processes. Peng-Robinson (PR) is chosen as the equation of state, which, similar to Soave-Redlich-Kwong, is well known for high performance in gas and condensate systems. PR and all the HYSYS components used is further defined and elaborated in Appendix B.

4.3.2 Steam Methane Reforming (SMR)

As mentioned in Section 2.2.2, steam methane reforming is a widely used method for converting natural gas to syngas for hydrogen production. The SMR design and production results is further elaborated and analysed in this section. The HYSYS model and component designs can be seen in Appendix B.

Table 3 - SMR design parameters

	Value	Units
Gas-heated reformer:		
Temperature:	700	°C
Pressure:	25	Bar
S/C ratio:	0.25	Mole-H_2O/Mole-C[6]
SMR reactor:		
Temperature:	950	°C
Pressure:	24	Bar
S/C ratio:	3	Mole-H_2O/Mole-C[6]
High Temperature WGS:		
Temperature:	320	°C
Pressure:	23	Bar
Low Temperature WGS:		
Temperature:	190	°C
Pressure:	22.5	Bar
CO_2 Absorption:		
CO_2 recovery rate:	95%	mole/mole
CO_2 purity:	99.999%	mole/mole
PSA:		
H_2 recovery rate:	90%	mole/mole
H_2 purity:	99.999%	mole/mole
Hydrogen Product:		
Temperature:	25	°C
Pressure:	20	Bar

4.3.2.1 Pre-treatment and Gas-Heated Reformer

In SMR, desulphurized natural gas is first expanded from 50 to 25.5 bar and mixed with steam prior to the gas-heated reformer (GHR). S/C ratio is in the GHR set to 0.3, sufficient to reform all the heavier hydrocarbons. The GHR feed is heated to 400°C, with a reforming pressure of 24.75 bar[7]. The reformed gas is leaving the GHR at a temperature of 700°C. The reforming efficiency of heavier hydrocarbons is greater at "lower" temperatures around 600-700°C [7]. The heat demand in the GHR is supplied as

---

[6] Mole-C is the amount of carbon atoms in the hydrocarbons entering the reformer.
[7] Interview with Jostein Sogge, Statoil

mentioned in Section 2.2.1 from the SMR product. After the GHR process, the gas is again mixed with steam prior to the SMR, as seen from the system flowchart in Figure 5. S/C ratio is set to 3, this to get an efficient reforming and to avoid carbon formation on the reformer catalysts [8]. The gas is heated to 700°C prior to the SMR columns.

4.3.2.2 SMR Reactor

The SMR process is reforming natural gas at 950°C and 24 bar. As mentioned in Section 2.2.2, the gas conversion rate is in SMR favoured by low pressures and high temperatures. SMR becomes more expensive at lower pressures due to higher volume flows and the need of larger reactor columns. The pressure used in industrial processing plants are therefore between 20-35 bar [8]. The reformer temperature reaches 950°C and the required heat is supplied by a furnace burning NG and the PSA tail gas with air. The reformed gas leaves the reformer with H_2/CO ratio of around 4.3. The reformer product is then cooled down to 320°C before entering the WGS column. The cooling in done by heat exchanging the SMR product stream with the GHR as mentioned, and by heating the water input in both the GHR and SMR.

4.3.2.3 WGS and Hydrogen Purification

WGS conversion is as mentioned in Section 2.3 favoured by low temperatures, while the reaction kinetics is favoured by high temperatures [8]. The WGS is conducted in two stages, a high temperature shift (320°C) for fast reactions and a low temperature shift (190°C) for high conversion. WGS is the last gas conversion step in the SMR process and the gas consists of mainly H_2 and CO_2. The WGS product is cooled down to a favourable 25°C prior to the CO_2 absorption and the PSA. Separators are installed prior to the CO_2 absorption column and the PSA to avoid condensate in the processes. CO_2 is removed in an absorption column with a recovery rate of 95% and leaves with a purity of 99.99%. Further, the PSA recovers 90% of the hydrogen, with a purity of 99.999%, as described in Section 2.5.1 [8]. The pressure drop of the purified hydrogen through the PSA is 2 bar and the hydrogen product leaves the PSA with a pressure of 20 bar and a temperature of 25°C. The tail gas containing all the remaining hydrocarbons, nitrogen, water and hydrogen exits the PSA at a pressure of 2.5 bar and 25°C. The tail gas is then heated up to 500°C and fed as fuel to the furnace.

---

[8] Interview with Rahoul Anantharaman, SINTEF Energy Research

4.3.2.4 Furnace

The furnace is as mentioned supplying the SMR with the required heat by burning NG and the tail gas with air. The required air is heated and supplied at a temperature of 335°C and a pressure of 1.2 bar while the NG and tail gas is heated to a temperature of 500°C before entering the furnace. Post combustion, the flue gas leaves the furnace at a temperature of 1000°C and at atmospheric pressure. The flue gas is cooled down to 100°C supplying heat to the reforming system.

4.3.2.5 Process Optimization – SMR

In this thesis, an optimized system has a satisfying energy efficiency, natural gas demand and low CO_2 emissions, as well as being cost-effective. There are three main variables to adjust in SMR in order to achieve the desired specifications: reformer temperature, reformer pressure and S/C ratio in the reformer feed. As mentioned earlier in this section, SMR conversion is favoured by high temperatures, low pressures and high S/C ratios. On the other hand, higher temperature and more steam implies a higher heat demand in the reactor. A lower pressure results in increased volumetric flow rate and lower recovery rate in the PSA. In addition, there are technical boundary conditions in the optimization. Due to the risk of carbon formation on the reforming catalyst, S/C ratio of 3 is set as a minimum value[9]. The reformer operates at a maximum of 950°C due to material limitations[9]. Pressure levels between 20 – 35 bar is common in SMR plants, as well as a minimum of 20 bar is required for a satisfying hydrogen recovery rate in the PSA [4].

The optimal temperature was found to be at the maximum 950°C, due to the superior conversion rate. Further, a S/C ratio of 3 was set as well as a reactor pressure of 24 bar, the minimum value sufficient to keep the PSA pressure at 20 bar. The system was fully heat integrated by utilizing the SMR product and hot flue gas to produce steam pre-heat the feed streams of the reactor and furnace. This reduced the NG demand, hence increased the plant efficiency. Sensitivity to deviation from optimal conditions is discussed in 4.4.3.

4.3.3 Steam Methane Reforming, Improved (SMR+)

In order to further reduce the carbon emissions, the natural gas feed to the furnace is replaced by produced hydrogen. Thus, the CO_2 emissions per produced hydrogen is further reduced by 60 percent.

---

[9] Interview with SINTEF Research Scientist Rahoul Anantharaman

The carbon captured accounts for 90 percent of the produced CO_2, making SMR+ an interesting carbon-lean solution.

Table 4 - SMR+ design parameters

	Value	Units
Gas-heated reformer:		
Temperature:	700	°C
Pressure:	25	Bar
S/C ratio:	0.25	Mole-H_2O/Mole-C[10]
SMR reactor:		
Temperature:	950	°C
Pressure:	24	Bar
S/C ratio:	3	Mole-H_2O/Mole-C[10]
High Temperature WGS:		
Temperature:	320	°C
Pressure:	23	Bar
Low Temperature WGS:		
Temperature:	190	°C
Pressure:	22.5	Bar
CO_2 Absorption:		
CO_2 recovery rate:	95%	mole/mole
CO_2 purity:	99.999%	mole/mole
PSA:		
H_2 recovery rate:	90%	mole/mole
H_2 purity:	99.999%	mole/mole
Hydrogen Product:		
Temperature:	25	°C
Pressure:	20	Bar

4.3.3.1 Differences between SMR+ and SMR

The SMR+ hydrogen production plant consists of exactly the same components as the SMR plant described in sections 4.3.2.1 - 4.3.2.4. The difference in the production methods is the input to the furnace. In SMR+, some of the hydrogen produced is burned in the furnace instead of burning NG. This is done to reduce the CO_2 emission in the production plant. For a production capacity of 500 tonnes of hydrogen/day using SMR+, an extra 184 tonnes are produced every day to supply the reformer with a sufficient amount of heat. This can be seen in Table 13. Hence, the plant is in reality producing 684 tonnes of hydrogen/day. Due to less available heat, the SMR+ feed stream is heated to 650°C, compared to 700°C in SMR.

---

[10] Mole-C is the amount of carbon atoms in the hydrocarbons.

4.3.3.2 Process Optimization – SMR+

As mentioned earlier, the concept of SMR+ is to replace the furnace NG feed with produced hydrogen in order to reduce CO_2 emissions. Thus, the optimal SMR conditions are used in SMR+ as well. It is possible to achieve higher energy efficiencies with SMR+, but that would result in increased emissions and the concept would be pointless.

4.3.4 Partial Oxidation (POX)

Fundamentally different from SMR is the partial oxidation method of hydrogen production. As explained in Section 2.2.3, a POX system combusts natural gas with limited supply of oxygen, producing hydrogen and carbon monoxide. As the method is applicable on practically all hydrocarbon feedstock, there is no need for a GHR in the POX system.

Table 5 - POX design parameters

	Value	Units
POX reactor:		
Temperature:	1186	°C
Pressure:	24	Bar
O/F ratio:	0.656	Mole-H_2O/Mole-NG
High Temperature WGS:		
Temperature:	320	°C
Pressure:	23	Bar
Low Temperature WGS:		
Temperature:	190	°C
Pressure:	22.5	Bar
CO_2 Absorption:		
CO_2 recovery rate:	95%	mole/mole
CO_2 purity:	99.999%	mole/mole
PSA-1 and PSA-2:		
H_2 recovery rate:	90%	mole/mole
H_2 purity:	99.999%	mole/mole
Hydrogen Product:		
Temperature:	25	°C
Pressure:	20	Bar

4.3.4.1 ASU

The air separation unit (ASU) needed in POX and ATR is in this thesis modelled as a black box with a specific power consumption of 0.35 kWh/Nm^3 of oxygen, based on a conventional cryogenic ASU by Linde Kryotechnik [28]. An oxygen purity of 100% is assumed as well as atmospheric pressure and a temperature of 25°C at the ASU outlet. Although the oxygen purity would be lower in practical applications, nitrogen and other inert gases are not affecting the simulations, hence their inclusion is not necessary.

4.3.4.2 POX

First, the natural gas (NG) is expanded from 50 to 24.5 bar and heated up to 500°C prior to the POX reformer. There is no need for desulphurization when producing hydrogen with POX, due to the reforming process being non-catalytic and hence sulphur will not damage the reactor. There is also no need for a pre-reformer due to POX's ability to reform heavier hydrocarbons. Oxygen produced in the ASU is heated to 250°C and compressed in two stages to 24.5 bar before fed into the POX reformer. The reformer is modelled as an adiabatic reactor, and since the POX reaction is exothermic, the reforming product leaves the reformer at a temperature of 1186°C. All the NG hydrocarbons are reformed, as described in Section 2.2.3, resulting in mainly H_2, CO, H_2O leaving the reformer. The product stream is cooled down to 320°C prior to WGS.

4.3.4.3 WGS and Purification

WGS is, as in SMR and SMR+, done in two temperature stages. This, as mentioned in Section 4.3.2.3, to get fast reactions and high conversion. The two temperature stages convert the gas at 320°C and 190°C at a pressure of 23 and 22.5 bar. The fluid leaving the WGS is then cooled down to 25°C prior to the CO_2 absorption and PSA. The CO_2 absorption is also done similarly to SMR and SMR+ and absorb CO_2 with a recovery rate of 95% and with a purity of 99.999%. A separator is installed prior to the absorption column and the PSA to prevent condensate entering the columns. The hydrogen purification is done with two PSA stages, in order to recover more of the hydrogen produced. The tail gas after the first PSA is still containing much hydrogen, and since the tail gas is not utilised in POX as in SMR (furnace) the tail gas is fed to another PSA and more hydrogen is recovered. Both the PSA stages purify hydrogen with a recovery rate of 90% and produces hydrogen with a purity of 99.999%. The PSA systems are operating and delivering hydrogen at a temperature of 25°C and at 20 bar. Produced tail gas is burned in a furnace to provide additional heat to the system, resulting in some CO_2 emissions.

4.3.4.4 Process Optimization – POX

In POX, the oxygen-to-fuel (O/F) ratio decides the temperature in the reactor, not an external heat supply. Therefore, the system is optimized by varying oxygen flow rate and pressure level in the reactor. In this thesis, the "fuel" value used in the O/F ratio is the flow rate of the main NG feed entering the system. There is no dedicated steam feed into the POX reactor, although some steam is added prior to the reactors. More oxygen results in more combustion, higher conversion and a higher temperature. Too much oxygen, and the total combustion reaction will begin to dominate and less hydrogen will be produced. 1500°C is set as a upper limit in the reactor outlet [4], due to material limitations. As with SMR, the system pressure balance between energy efficiency and volumetric flow rate.

The pressure in the POX reactor is set to 24 bar, to keep the PSA pressure above 20 bar. Further, the system is optimized by adjusting the O/F ratio to maximize the energy efficiency. At optimal conditions the temperature is 1186°C in the reformer product and the O/F ratio is 0.656.

4.3.5 Autothermal Reforming (ATR)

As described in Section 2.2.4, ATR is a combination of non-catalytic POX and SMR. Table 6 shows the main design parameters of the system, and the rest of this section will describe the system layout and optimization steps in detail.

Table 6 - ATR design parameters

	Value	Units
Gas-heated reformer:		
Temperature:	700	°C
Pressure:	25	Bar
S/C ratio:	0.25	Mole-H_2O/Mole-C[11]
ATR reactor:		
Temperature:	1020	°C
Pressure:	24	Bar
S/C ratio:	1.5	Mole-H_2O/Mole-C[11]
O/F ratio:	0.616	Mole-H_2O/Mole-NG
High Temperature WGS:		
Temperature:	320	°C
Pressure:	23	Bar
Low Temperature WGS:		
Temperature:	190	°C
Pressure:	22.5	Bar
CO_2 Absorption:		
CO_2 recovery rate:	95%	mole/mole
CO_2 purity:	99.999%	mole/mole
PSA-1 and PSA-2:		
H_2 recovery rate:	90%	mole/mole
H_2 purity:	99.999%	mole/mole

---

[11] Mole-C is the amount of carbon including all the hydrocarbons.

Hydrogen Product: Temperature: Pressure:	 25 20	 °C Bar

4.3.5.1 ASU

The ASU used in the ATR is modelled similarly as in POX, described in Section 4.3.4.1. The ASU has a specific power consumption of 0.35 kWh/Nm^3 of oxygen, producing close to pure oxygen [28].

4.3.5.2 GHR and ATR

First, desulphurized gas is expanded to 25 bar, mixed with steam and heated to 400°C prior to the GHR. The GHR in ATR is also modelled similarly as in SMR and SMR+, described in Section 4.3.2.1. The GHR feed is pre-heated to 400°C at a pressure of 24.5 bar. A S/C ratio of 0.25 is set, sufficient to reform the heavier hydrocarbons. The GHR heat demand is supplied by cooling the ATR product stream, demonstrated in Figure 8. At a temperature of 700°C, the GHR product is mixed with more steam before entering the ATR. The steam has a temperature of 350°C and the final temperature of the feed gas entering the ATR becomes 563°C. As seen from Table 6, the S/C ratio in the ATR feed is set to 1.5. The large amount of steam in the process is needed to prevent carbon formation.

Oxygen is fed to the ATR reactor as a separate stream at a temperature of 250°C and at a pressure of 24.5 bar. The oxygen compression is done in a two-stage compressor with intercooling. As mentioned in Section 2.2.4, ATR is a combination of non-catalytic POX and SMR. The ATR reactor is adiabatic and the heat required by the SMR reactions is supplied by the POX reactions. The temperature of the reforming product is directly dependent on the amount of oxygen fed to the ATR. The oxygen-to-fuel (O/F) ratio is in the ATR set to 0.616, as seen in Table 6, and the temperature of the reforming product becomes 1020°C. In this thesis, the “fuel” value used in the O/F ratio is the flow rate of the main NG feed entering the system. The reforming pressure is set to 24 bar. The ATR process optimization is further elaborated in Section 4.3.5.4. Further, the ATR product stream is cooled down to 320°C prior to the first WGS stage. The ATR product is cooled by the GHR between 1000 – 750°C and with water between 750 - 320°C. Prior to WGS, the gas stream is also mixed with more steam, as seen from Figure 8, resulting in higher conversion of CO in the WGS reactors.

4.3.5.3 WGS and Purification

WGS is, as in SMR, SMR+ and POX, done in two temperature stages to achieve fast reactions and high conversion, as mentioned in Section 4.3.2.3. The two temperature stages convert the gas at 320°C and 190°C at a pressure of 23 and 22.5 bar. After the WGS, the gas stream is cooled down to 25°C prior to the CO_2 absorption and PSA. The CO_2 absorption is done in the same way as in SMR, SMR+ and POX, with a recovery rate of 95% and with a purity of 99.999%, as seen from Table 6. A separator is installed prior to both the absorption column and the PSA to prevent condensate entering the columns. The hydrogen purification in ATR, as well as in POX, done with two PSA columns, this to recover more of the hydrogen produced. The tail gas after the first PSA is, as in POX, compressed and fed to a second PSA to recover more hydrogen. The system flowchart can be seen in Figure 7. Both the PSA columns purify hydrogen with a recovery rate of 90% and produces hydrogen with a purity of 99.999%. The PSAs are operating and delivering hydrogen at 25°C and 20 bar. As with POX, the final tail gas stream is burned in a furnace to produce additional heat to the system.

4.3.5.4 Process Optimization - ATR

The main process design variables in ATR are the O/F ratio, the S/C ratio and pressure, affecting the overall system similarly as in SMR and POX. More oxygen favours more partial oxidation, providing more heat for the steam reforming reactions. Too much oxygen results in total combustion, less hydrogen production and temperatures above a maximum of 1150°C [4]. Due to soot formation, a S/C ratio below 1.5 is not possible with current technology[12]. The same pressure limitations as in SMR exists in ATR, with a required PSA pressure above 20 bar.

All variables is adjusted in order to achieve a maximized plant energy efficiency, defined in Section 4.3.1.4. An important note with ATR is that, regardless of oxygen flow rate, the global maximum energy efficiency was found at a S/C ratio below 1.5, which is a minimum value due to reactor operation. Hence, the S/C ratio was set to 1.5 and the process was then optimized by adjusting the oxygen flow rate. The O/F ratio was found to be 0.616 on a mole basis. Because of the internal combustion, the oxygen ratio also determines the reactor temperature, at 1020°C. Similar to SMR, the reforming in ATR is also favoured by low pressures. Therefore, the pressure has been set to a minimum of 24 bar in order to keep the process stream above 20 bar in the final PSA unit.

Further optimization of the system, looking at the possibility of recompressing the process stream after the reactor, would open for pressures below 24 bar. This is not done in this thesis due to limited cost data of such a compression, as it would imply a significant increase of the volumetric flow rate in the reactor.

---

[12] Interview with SINTEF Research Scientist Rahoul Anantharaman

4.3.6 Electrolysis of Water (EL)

As a benchmark in the comparison of the different hydrogen production methods, electrolysis of water represents a clean, zero-emission alternative. In future scenarios, if the electricity prices continue to drop, electrolysis can potentially be the most cost-efficient solution for large-scale production. Therefore, electrolysis is included in the thesis, although not simulated. The specifications of the electrolysis plant used in this report is listed in Table 7. It is important to highlight that the specific plant power consumption is the average power consumption of all components in the facility, including compressors, pumps and the effect of cell stack degeneration. Normally, suppliers list the power consumption only of the electrolyser stacks with newly activated catalysts. Typically, the catalysts are replaced every 7-9 years with a degeneration in performance at around 10% at the time of re-activation[13]. The power consumption is further elaborated in Appendix B.

Table 7 - Technical specifications of electrolysis [29].

	Electrolysis	Unit
η_P **(LHV-basis):**	62.0	
Specific Plant Power consumption:	4.85	kWh/Nm^3
Specific Plant Power consumption:	53.9	kWh/kgH$_2$
Total power demand:	961.54	MW
Electricity demand:	8.0	TWh/year
H_2 Produced:	500	Tonnes/day

It is important to highlight the significant electricity demand of a large-scale electrolysis facility. With a specific power consumption, including auxiliary components, of 53.9 kWh per kilogram, the annual demand is 8.0 TWh, operating 347 days a year. In comparison, the total energy consumption in Norway was 234 TWh in 2014 [30].

4.3.7 Combined Reforming and Electrolysis (CRE)

Based on the systems described in this chapter, one additional system is evaluated. What if the ASU in an autothermal reactor is replaced by electrolysis, co-producing hydrogen? That is the concept of the combined reforming and electrolysis (CRE) system. Keeping the 500 tonnes per day capacity, but

---

[13] Interview with Sales Director of NEL-Hydrogen, Henning Langås, 28/10 – 2016.

split the production in two parallel systems. With the electrolysers producing the amount of oxygen the ATR reactor demands, the resulting split of production is approximately 30% from EL and 70% from ATR. This further reduces the carbon footprint of ATR as well as it improves the flexibility to feedstock cost variations. The electrolysers are assumed to produce the exact stoichiometric amount of oxygen per amount of hydrogen. Key design parameters are listed in Table 8.

Table 8 - CRE design parameters

	Value	Units
Gas-heated reformer:		
Temperature:	700	°C
Pressure:	25	Bar
S/C ratio:	0.25	Mole-H_2O/Mole-C[14]
ATR reactor:		
Temperature:	1004	°C
Pressure:	24	Bar
S/C ratio:	1.5	Mole-H_2O/Mole-C[11]
Oxygen-to-NG ratio:	0.607	Mole-H_2O/Mole-NG
High Temperature WGS:		
Temperature:	320	°C
Pressure:	23	Bar
Low Temperature WGS:		
Temperature:	190	°C
Pressure:	22.5	Bar
CO_2 Absorption:		
CO_2 recovery rate:	95%	mole/mole
CO_2 purity:	99.999%	mole/mole
PSA-1 and PSA-2:		
H_2 recovery rate:	90%	mole/mole
H_2 purity:	99.999%	mole/mole
Hydrogen Product:		
Temperature:	25	°C
Pressure:	20	Bar

4.3.7.1 Process Optimization - CRE

The ATR system in CRE is very similar to the one described in Section 4.3.5, only replacing the air separation unit, and reducing the output. The EL system will be identical to Section 4.3.6. The main deviation is that the process optimization of CRE is done based on the overall efficiency, including the electrolysers. This results in a slightly lower O/F ratio due to the relatively low efficiency of the

---

[14] Mole-C is the amount of carbon including all the hydrocarbons.

electrolysis plant. The S/C ratio remains at 1.5 and the O/F ratio is found to be 0.607. The exact split of production is 362 and 138 tonnes per day in ATR and Electrolysis, respectively.

4.4 Technical Results and Discussion

Presenting an overview of the different production methods, this section will evaluate which method is preferable for a large-scale facility in Norway from a technical point of view. The key performance parameters evaluated, as mentioned in the beginning of this chapter, are energy efficiency and CO_2 emissions. The natural gas process feed is also key, due its impact on the sizing of the plant. It is important to highlight that economic viability has been taken into consideration while designing the systems.

Table 9 - Overview of the simulation results, comparing the individual production systems. All efficiencies are LHV-based.

	Unit	SMR	SMR+	POX	ATR	EL	CRE
Plant Energy efficiency, η_P:	-	0.82	0.78	0.78	0.82	0.62	0.75
Thermal Efficiency, η_T:	-	0.82	0.78	0.81	0.84	-	-
Natural Gas Consumption:	Std m^3/h	78826	82844	79753	76776	-	55630
Specific Natural Gas consumption:	Std m^3NG/kgH_2	0.158	0.167	0.160	0.154	-	0.111
Reformer conversion rate[15]:	Mole-H_2/mole-NG	3.40	3.40	1.97	2.36	-	2.36
H_2/CO ratio in the reforming product:	Mole/mole	4.12	4.12	1.71	2.69	-	2.73
S/C ratio in the reformer[16]:	Mole/mole	3	3	0	1.5	-	1.5
O/F ratio in the reformer:	Mole/mole	0	0	0.656	0.616	-	0.607
Power Demand (excl. CCS):	MW	2.03	2.30	29.8	27.1	962	335.2
Heat Demand:	GJ/h	1897.0	2445.3	754.6	887.7	-	642.7
Water Demand[17]:	Kg/h	108550	139421	60075	63667	208565	104068
CO_2 Captured:	Tonnes/day	3047	3913	3931	3 816	-	2752
CO_2 Emitted:	Tonnes/day	1198	547	363	318	-	244
H_2 Produced:	Tonnes/day	500	500	500	500	500	500

---

[15] The amount of hydrogen in the reformer product per mole NG fed to the reforming system. NG fed to furnace is not included.

[16] Mole-C is the amount of carbon including all the hydrocarbons.

[17] Water demand is the process water supplied minus the water recirculated in the system.

4.4.1 Energy Efficiency

With regards to plant energy efficiency, ATR and SMR represent the best alternatives. Here, it is important to mention the general consensus regarding SMR as the most energy efficient method to produce hydrogen from natural gas. Our simulations show that ATR is equally efficient. One possible explanation to this is that, as with POX, the non-catalytic partial oxidation occurring within the reactor chamber does not necessarily reach equilibrium in real operation. HYSYS, on the other hand, assumes instant equilibrium. Not achieving equilibrium, more oxygen would be necessary to provide enough heat for the steam reforming and the efficiency would drop. SMR+ shows a decrease in energy efficiency in order to increase the CO_2 capture. Compared to natural gas reforming electrolysis has a considerably lower energy efficiency. Combined with ATR, the result improves, but is still inferior. It is important to highlight that the use of lower heating value (LHV) in the calculation of efficiencies affect the value in electrolysis more than in the reforming processes, due to the fact that the feed NG also use LHV. On a HHV-basis, SMR and electrolysis have a plant energy efficiency of 0.87 and 0.73, respectively.

4.4.2 CO_2 emissions

As can be seen in Figure 11, ATR represents the traditional natural gas reforming alternative with the lowest carbon dioxide emissions. Although SMR and ATR produces a similar amount of CO_2 the internal combustion of ATR enables superior carbon capture and hence a significantly reduced footprint, compared to SMR. SMR+ and POX also seem to be good alternatives to produce carbon-lean hydrogen with a significant reduction from the standard SMR. The alternatives involving electrolysis are naturally producing far less CO_2, but are on the other hand consuming more electricity. As a result of Norway's vast hydropower resources, electricity is considered zero-emission energy, as showed in the figure. Elsewhere this is not necessarily the case, affecting the viability of the solution.

In order to further reduce emissions, improvement of the CO_2 recovery rate in the absorption column can be important. 95% is used in this analysis, leaving room for improvement, especially in ATR, SMR+ and POX, where the only emissions come from the burned tail gas. In SMR, post-combustion CCS will be important in the future, to approach zero-emission. Pre-combustion CCS is limited to around 70% capture in energy efficient SMR.

Mitigating climate change is one of the main reasons as to why hydrogen production is an interesting prospect. Hence, targeting close to zero emissions is important. On the other hand, the technology has to be economically viable in order to be implemented. As will be highlighted in the financial analysis in Chapter 5, analysing these production methods provides a cost of increased CO_2 capture, which is beneficiary in future investment decisions.

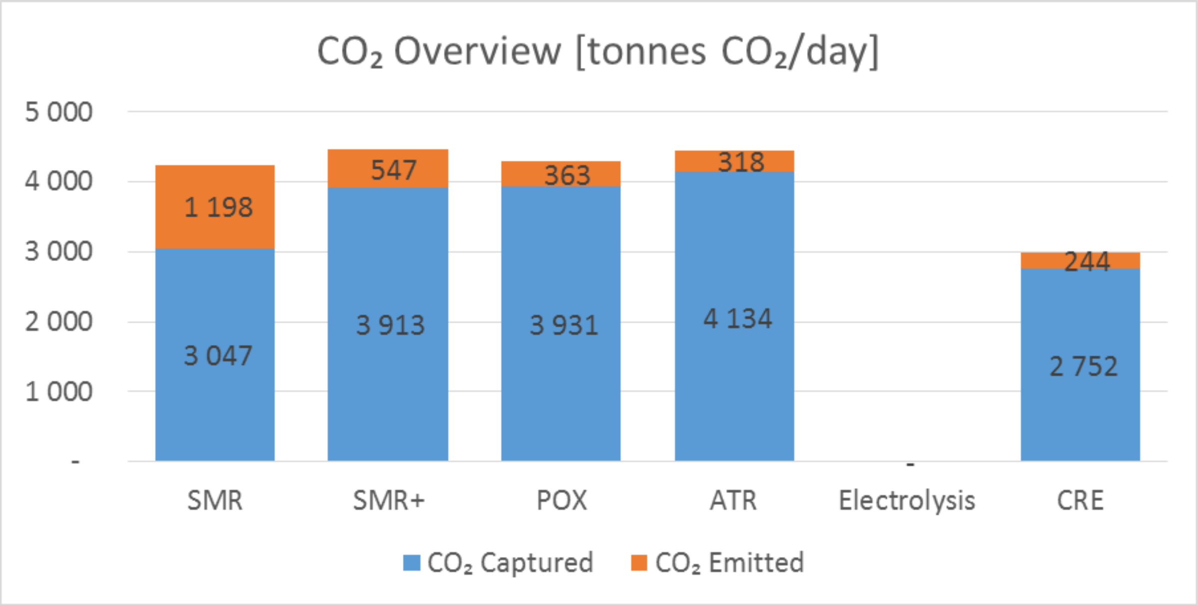

Figure 11 - CO_2 overview. This block diagram shows the amount of carbon dioxide captured from the syngas stream. The emitted CO_2 of ATR and CRE is calculated from the carbon composition of the PSA tail gas.

Figure 11 presents the CO_2 capture and emissions of the different systems. Excluding post-combustion CCS, SMR is the inferior hydrogen production method with regards to carbon footprint. Electrolysis from Norwegian, renewable energy is assumed carbon-free, enabling a zero-emission product. It is also important to mention the risks of carbon storage. Knowledge of the effect a breach in storage reservoir can cause is limited. The by-product of electrolysis, on the other hand, is pure oxygen. CRE represents a solution with further 30% reduction in emission compared with ATR, as well as reducing the needed CCS with 30%.

4.4.3 SMR Results and Discussion

As Table 9 shows, SMR has an energy efficiency of 0.82, a conversion rate of 3.47, as well as a low power demand. On the other side, it has the most CO_2 emissions of the systems analysed in this thesis. This section will elaborate on the results of the SMR simulations, as well as discuss the systems sensitivity to changes in design variables.

Table 10 provides a simulation overview, providing information of the stream properties and composition through the production process. As can be seen, the GHR work as a pre-heater as well as it reforms most of the heavier hydrocarbons. Although some hydrogen is produced in the GHR, more than 70% is produced directly in the SMR reactor.

Table 10 - SMR Simulation Overview. This table shows the stream properties and composition through the production process. It is helpful to look at Figure 5 to get the overview while studying this table.

	NG Feed	GHR Feed	SMR Feed with steam	WGS Feed	CO_2 Absorption and PSA Feed	Tail Gas	Hydrogen Product	Air to Furnace	NG to Furnace	Flue Gas
Temperature [°C]:	50	400	700	320	25	25	25	335	500	1000
Pressure [Bar]:	50	25.25	24.5	23.5	22.5	2.5	20	1.2	50	1.2
Vapour fraction:	1.0	1.0	1.0	1.0	1.0	1.0	1.0	1.0	1.0	1.0
Mole flow [kmole/h]:	2728	3546	12523	17656	14803	1579	10334	11439	606	13092
Mass flow [kg/h]:	53613	68356	213548	213550	162005	14132	20833	330022	11908	356058
Mole flow [kmole/h]:										
CH_4	2327.48	2327.48	2771.88	208.20	208.20	208.20	0.00	0.00	516.94	0.00
H_2	0.00	0.00	906.43	9272.33	11482.22	1148.22	10334.00	0.00	0.00	0.00
CO	0.00	0.00	355.18	2253.12	43.18	43.18	0.00	0.00	0.00	0.00
CO_2	60.29	60.29	163.78	832.12	3036.16	151.81	0.00	0.00	13.39	1134.67
H_2O	0.00	818.38	8315.64	5081.02	24.34	18.78	0.00	0.00	0.00	2892.03
C	0.00	0.00	0.00	0.00	0.00	0.00	0.00	0.00	0.00	0.00
C_2H_6	192.32	192.32	1.30	0.00	0.00	0.00	0.00	0.00	42.71	0.00
C_3H_8	74.34	74.34	0.00	0.00	0.00	0.00	0.00	0.00	16.51	0.00
i-Butane	14.87	14.87	0.00	0.00	0.00	0.00	0.00	0.00	3.30	0.00
n-Butane	25.64	25.64	0.00	0.00	0.00	0.00	0.00	0.00	5.70	0.00
i-Pentane	7.37	7.37	0.00	0.00	0.00	0.00	0.00	0.00	1.64	0.00
n-Pentane	7.23	7.23	0.00	0.00	0.00	0.00	0.00	0.00	1.61	0.00
n-Hexane	4.91	4.91	0.00	0.00	0.00	0.00	0.00	0.00	1.09	0.00
n-Heptane	3.55	3.55	0.00	0.00	0.00	0.00	0.00	0.00	0.79	0.00
n-Octane	1.09	1.09	0.00	0.00	0.00	0.00	0.00	0.00	0.24	0.00
N_2	8.87	8.87	8.87	8.87	8.87	8.87	0.00	9036.90	1.97	9047.74
O_2	0.00	0.00	0.00	0.00	0.00	0.00	0.00	2402.21	0.00	17.71

The table also displays how the WGS reactors shift most of the CO to CO_2. Although not included in the flowcharts, separators are located in from of both the carbon absorption column and the PSA. That explains the reduction in water content between the WGS feed and the PSA feed in the table.

In order to design a well operating system, the sensitivity to key variables requires attention. How the system responds to changes in temperature is thoroughly presented in Table 11.

Table 11 - Presentation of how SMR parameters change by changing the reforming temperature. The chosen design values are highlighted.

Property	Unit							
Temperature:	°C	700	750	800	850	900	950	1000
S/C ratio:	mole/mole	3	3	3	3	3	**3**	3
Conversion rate:	Mole_H_2/mole_NG	1.723	2.123	2.534	2.914	3.211	**3.399**	3.493

Reforming NG flow:	Sm3/h	143601	112885	91708	77731	69190	**64501**	62189
SMR flow:	Sm3/h	659223	518218	421002	356836	317628	**296101**	285488
SMR Heat demand:	GJ/h	421	522	592	642	681	**715**	747
Tail Gas flow:	kmole/h	5373	3893	2875	2206	1800	**1579**	1471
LHV Tail Gas:	kJ/kmole	650650	594643	522140	437196	353788	**289508**	250620
NG demand furnace:	Sm3/h	0	0	0	1282	9696	**14326**	18812
Total system NG demand:	Sm3/h	143601	112885	91708	79013	78886	**78826**	81001
CO_2 emission:	Tonnes/day	4415	2859	1789	1154	1181	**1198**	1327
Hydrogen produced:	kg/day	500000	500000	500000	500000	500000	**500000**	500000
Plant Energy efficiency:	-	0.448	0.571	0.704	0.817	0.819	**0.819**	0.797
Excess Heat[18]:	GJ/h	2409.9	1263.0	472.9	0.0	0.0	**0.7**	84.4

As previously mentioned, the conversion rate increases at higher reforming temperatures. Because the system is heat integrated to fit 950°C in the reactor outlet, variations in temperature will cause excess heat or additional demand. The extra heat demand is supplied by increasing the NG feed to the furnace, hence reducing the efficiency. It is important to highlight that at the temperatures with excess heat, the system is not heat integrated further than the design case. If technological development allows for temperatures up to 1000°C, one may be able to achieve even better operation, due to further improvements on heat integration. Table 11 shows that the energy efficiency is close to constant between 850 - 950°C. Therefore, the upper limit is chosen to reduce process flow which results in lower investment costs as will be discussed in Section 5.3.6.

Figure 12 highlights the sensitivity of the conversion rate and energy efficiency to temperature changes. Even though the plant energy efficiency is stable between 850 – 950°C, the conversion rate increases with temperature, which leads to lower NG feed to the process. More NG will be needed in the furnace, thus the efficiency is close to constant, but as the financial analysis will highlight, higher NG feed to the reactor implies higher CAPEX.

---

[18] Excess Heat = Total Heat Available – Total Heat Demand

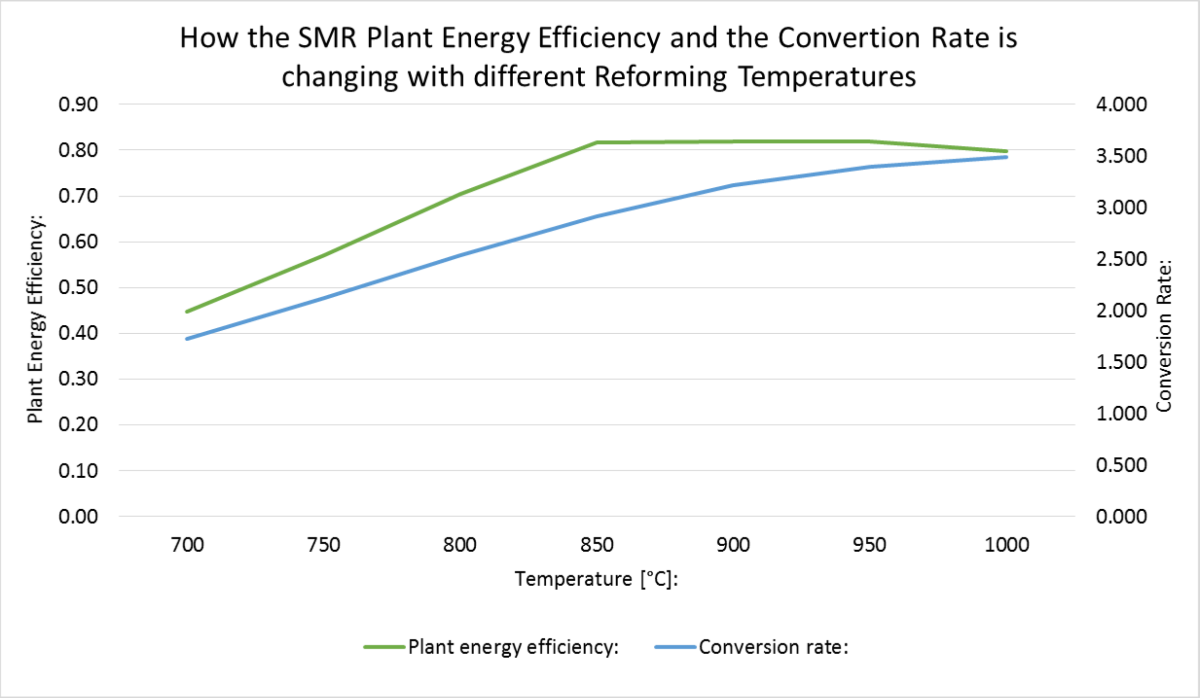

Figure 12 - How the Plant Energy Efficiency and the reforming Conversion Rate is changing with different temperatures in SMR

Adjusting the S/C ratio while keeping the temperature constant is also important to understand the system behaviour. Reducing the steam flow to a ratio of 2-2.5 will increase efficiency as shown in Table 12. This is mainly due to the reduced heat demand for the process stream to reach the set reformer temperature. As Section 4.3.2.5 explains, a S/C ratio of 3 is necessary to adequately prevent carbon and soot formation, which will reduce the activity of the catalyst. Hence, the minimum ratio of 3 was chosen. Enabling a S/C ratio below 3 will provide slightly better energy efficiency. It will also reduce the conversion rate and hence increase the NG process flow. On the other hand, a lower S/C ratio will reduce the total volume flow through the SMR, which is believed to reduce the total system CAPEX, further elaborated in Chapter 5.

Table 12 - How SMR parameters change by changing the S/C ratio in the reformer. The chosen design values are highlighted

Property	**Unit**							
Temperature:	°C	950	950	950	950	**950**	950	950
S/C ratio:	mole/mole	1	1.5	2	2.5	**3**	3.5	4
Conversion rate:	mole_H_2/mole_NG	2.334	2.769	3.056	3.254	**3.399**	3.508	3.594
Reforming NG flow:	Sm3/h	101917	80101	70429	66592	**64501**	63204	62351
SMR flow:	Sm3/h	260750	245629	251753	271870	**296101**	322261	349590
SMR Heat demand:	GJ/h	795	733	706	708	**715**	723	733
Tail Gas flow:	kmole/h	4730	2837	1958	1700	**1579**	1507	1461
LHV Tail Gas:	kJ/kmole	433555	393050	355349	317549	**289508**	269515	255212

NG demand furnace:	Sm3/h	0	0	8185	12189	**14326**	15926	17164
Total system NG demand:	Sm3/h	101917	80101	78614	78781	**78826**	79130	79516
CO_2 emission:	Tonnes/day	3743	1750	1266	1211	**1198**	1209	1227
Hydrogen produced:	kg/day	500000	500000	500000	500000	**500000**	500000	500000
Plant energy efficiency:	-	0.633	0.806	0.822	0.820	**0.819**	0.816	0.812
Excess Heat[19]:		1012.5	99.7	0.0	0.0	**0.7**	12.0	26.7

Heat integration has a large impact on the plant energy efficiency. In SMR, this is done by using heat exchangers in all the cooling processes. This allows the reformer and furnace feed streams to be heated to higher temperatures, resulting in a lower NG demand due to a lower heat demand in the reformer and more efficient combustion in the furnace.

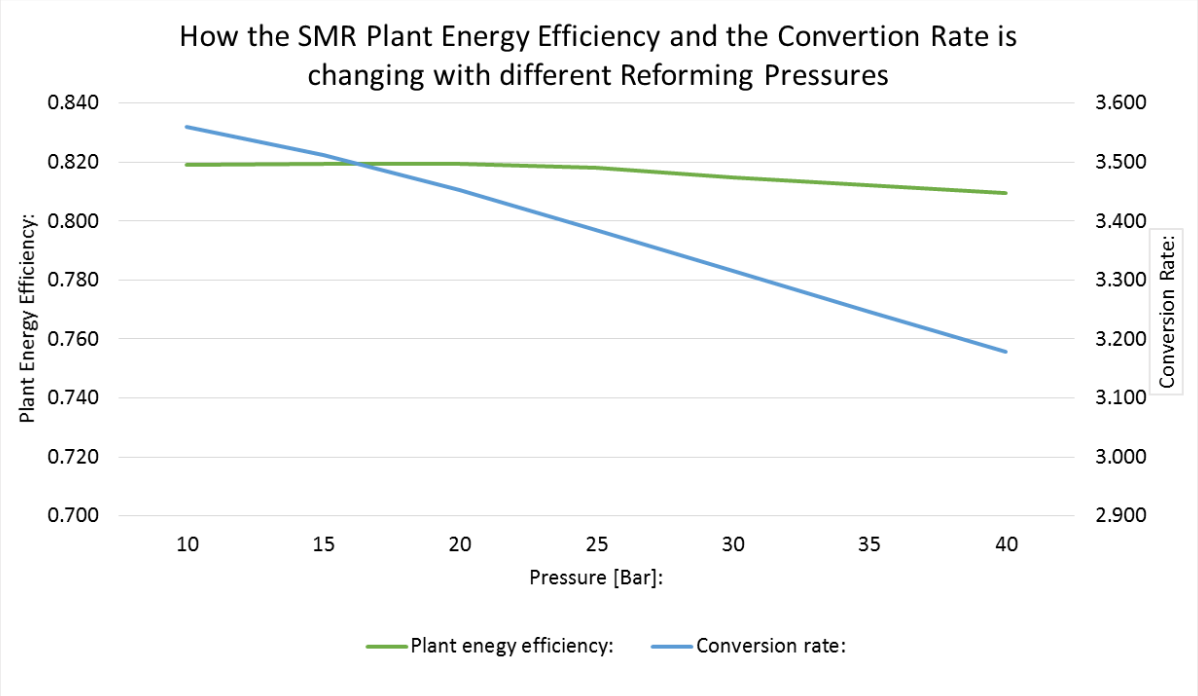

Figure 13 - How the plant energy efficiency and the conversion rate is changing with pressure in SMR

Figure 13 displays how the system pressure affects the process performance. As can be seen, the pressure merely affects the efficiency, although the conversion rate is reduced at higher pressures, This is due to the methane slip increasing the heating value of the tail gas. The process natural gas flow increases with higher pressure, but the furnace input decreases.

---

[19] Excess Heat = Total Heat Available – Total Heat Demand

Since this thesis only considers pre-combustion carbon capture, some CO_2 emission will occur in SMR. A reduced heat demand in the reformer, and thence a reduced NG input in the furnace, can reduce the emissions to some extent. If possible, a reduction in the reforming S/C ratio would reduce the reforming heat demand. In addition, a more efficient furnace would improve the heat transfer, reducing the NG input in the furnace.

SMR achieves a total plant efficiency of 0.82 on a LHV-basis, which corresponds well with existing literature. The National Renewable Energy Laboratory (NREL), which also have done a similar analysis of SMR, ended up with the same plant efficiency of 0.82 [31]. The hydrogen Roadmap made by IEA estimates the plant efficiency of SMR to be between 0.70 – 0.85, which supports the viability of the findings in this thesis. The H_2/CO ratio of the SMR reforming product of 4.3 is also supported by other journals that estimates the H_2/CO ratio in SMR to be between 3.5-5.5 [10].

4.4.4 SMR+ Results and Discussion

SMR+ is summarized by lower CO_2 emissions than SMR at the expense of higher natural gas demand and hence a lower energy efficiency. One may argue that burning a premium product, such as pure hydrogen is wasteful, but it is an interesting alternative in order to reduce the CO_2 emissions. Also as a solution for further reduction in existing SMR plants. Table 13 shows the simulation overview for SMR+, which in general operates very similarly to SMR. The main difference is the extra hydrogen produced to the furnace, increasing the total mass flow through the process.

Table 13 - SMR+ Simulation Overview

	NG Feed	GHR Feed	SMR+ Feed	WGS Feed	CO_2 Absorption and PSA Feed	Tail Gas	Hydrogen Product	Hydrogen to Furnace	Air to Furnace:	Flue Gas
Temperature [°C]:	50	400	650	320	25	25	25	500	335	1000
Pressure [Bar]:	50	25.25	24.5	23.5	22.5	2.5	20	19.75	1.2	1.2
Vapour fraction:	1.0	1.0	1.0	1.0	1.0	1.0	1.0	1.0	1.0	1.0
Mole flow [kmole/h]:	3504	4555	16085	226767	19013	2028	10334	2939	13367	16100
Mass flow [kg/h]:	68860	87796	274279	274281	208077	18151	20833	5925	385644	409715
Mole flow [kmole/h]:										
CH_4	2989.40	2989.40	3560.18	267.40	267.40	267.40	0.00	0.00	0.00	0.00
H_2	0.00	0.00	1164.21	11909.29	14747.65	1474.76	10333.99	2938.89	0.00	0.00
CO	0.00	0.00	456.19	2893.89	55.46	55.46	0.00	0.00	0.00	0.00
CO_2	77.43	77.43	210.35	1068.77	3899.60	194.98	0.00	0.00	0.00	517.85
H_2O	0.00	1051.12	10680.54	6526.01	31.26	24.13	0.00	0.00	0.00	4972.60
C	0.00	0.00	0.00	0.00	0.00	0.00	0.00	0.00	0.00	0.00
C_2H_6	247.01	247.01	1.67	0.00	0.00	0.00	0.00	0.00	0.00	0.00
C_3H_8	95.48	95.48	0.00	0.00	0.00	0.00	0.00	0.00	0.00	0.00

i-Butane	19.10	19.10	0.00	0.00	0.00	0.00	0.00	0.00	0.00	0.00
n-Butane	32.94	32.94	0.00	0.00	0.00	0.00	0.00	0.00	0.00	0.00
i-Pentane	9.46	9.46	0.00	0.00	0.00	0.00	0.00	0.00	0.00	0.00
n-Pentane	9.28	9.28	0.00	0.00	0.00	0.00	0.00	0.00	0.00	0.00
n-Hexane	6.31	6.31	0.00	0.00	0.00	0.00	0.00	0.00	0.00	0.00
n-Heptane	4.55	4.55	0.00	0.00	0.00	0.00	0.00	0.00	0.00	0.00
n-Octane	1.40	1.40	0.00	0.00	0.00	0.00	0.00	0.00	0.00	0.00
N_2	11.39	11.39	11.39	11.39	11.39	11.39	0.00	0.00	10560.00	10571.39
O_2	0.00	0.00	0.00	0.00	0.00	0.00	0.00	0.00	2807.09	37.70

Table 14 presents the sensitivity to variations in the reformer temperature. Similar to SMR, SMR+ also has a higher conversion ratio at higher temperatures. An important result is how the plant energy efficiency increases if the temperature is reduced to 850°C, at the expense of close to doubled CO_2 emissions. This occurs because the system operates as a standard SMR when the tail gas is sufficient to supply the heat demanded by the reformer. The effect of using additional hydrogen diminish, and the emissions increase. As the systems logic is based on replacing the furnace NG feed with hydrogen, it is important to keep the optimal reformer temperature and S/C ratio as in the standard SMR. If the temperature drops in the reactor outlet, the conversion rate drops and the emissions increase. That is an important result as it is the opposite of SMR, where at temperatures close to 950°C, the emissions increase with higher conversion rates. The effect of temperature changes on the emissions is also presented in Figure 14.

Table 14 - Presentation of how SMR+ parameters change by changing the reforming temperature. The design values are highlighted.

Property	Unit							
Temperature:	°C	700	750	800	850	900	**950**	1000
S/C ratio:	mole/mole	3	3	3	3	3	**3**	3
Conversion rate:	mole_H_2/mole_NG	1.723	2.123	2.534	2.914	3.211	**3.399**	3.493
Reforming NG flow:	Sm3/h	143601	112885	91708	79297	81363	**82802**	86732
SMR flow:	Sm3/h	659223	518218	421002	364028	373509	**380118**	398158
SMR Heat demand:	GJ/h	487	573	633	691	838	**955**	1081
Tail Gas flow:	kmole/h	5373	3893	2875	2251	2117	**2027**	2052
LHV Tail Gas:	kJ/kmole	650650	594643	522140	437196	353788	**289508**	250620
NG demand furnace:	Sm3/h	0	0	0	4924	42988	**69330**	96431
Total system NG demand:	Sm3/h	143601	112885	91708	79297	81363	**82802**	86732
CO_2 emission:	Tonnes/day	4415	2859	1789	1107	774	**547**	436
Hydrogen produced:	kg/day	500000	500000	500000	500000	500000	**500000**	500000
Plant energy efficiency:	-	0.448	0.571	0.704	0.815	0.794	**0.780**	0.744
Excess Heat[20]:	GJ/h	2410.0	1263.1	472.9	0.0	0.0	**0.8**	92.8

---

[20] Excess Heat = Total Heat Available – Total Heat Demand

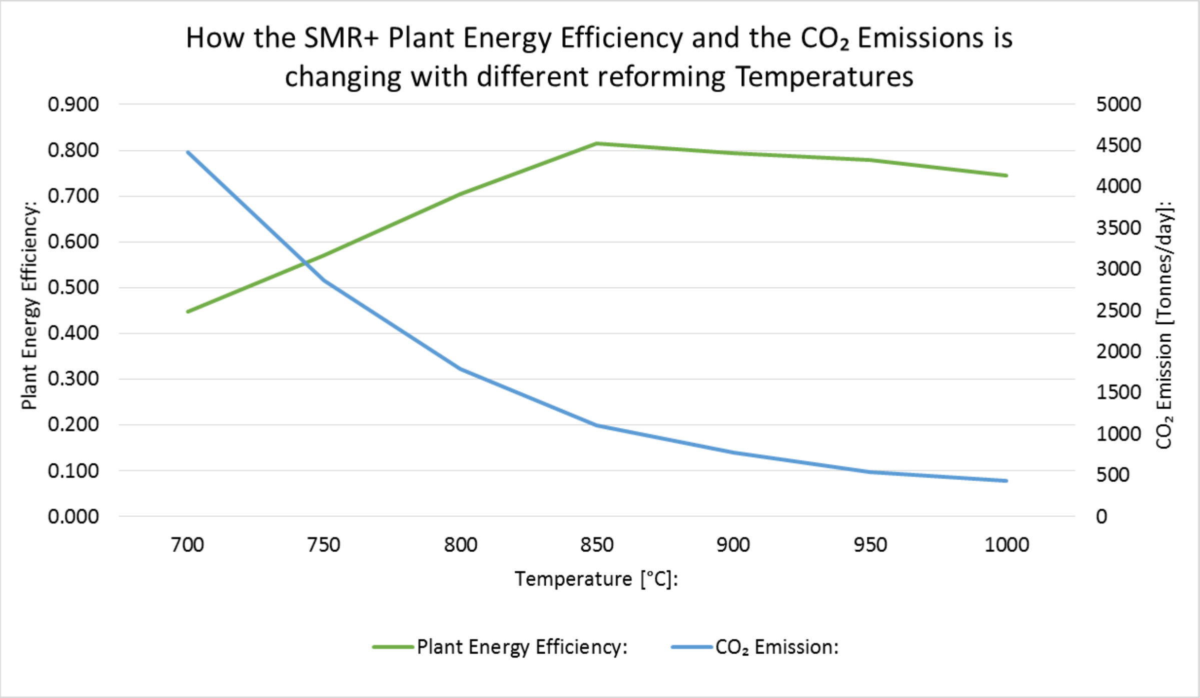

Figure 14 - Graph showing how the plant energy efficiency and CO_2 emissions are affected by changes in reformer temperature in SMR+.

In Table 15, the S/C ratio is varied, keeping the reformer temperature at 950°C. Here, the results are quite similar to SMR, with a higher conversion rate from increased steam flow. Reducing the S/C ratio, the efficiency increase, as well as the CO_2 emissions. Therefore, if SMR+ is to retain its low emissions, keeping the reformer temperature and S/C ratio on design condition is key.

Table 15 - How SMR+ parameters change by changing the S/C ratio in the reformer. The design values are highlighted.

Property	Unit							
Temperature:	°C	950	950	950	950	**950**	950	950
S/C ratio:	mole/mole	1	1.5	2	2.5	**3**	3.5	4
Conversion rate:	mole_H_2/mole_NG	2.334	2.769	3.056	3.254	**3.399**	3.508	3.594
Reforming NG flow:	Sm3/h	101917	80101	80607	82021	**82802**	83815	84730
SMR flow:	Sm3/h	260750	245629	288134	334860	**380118**	427350	475062
SMR Heat demand:	GJ/h	823	759	837	906	**955**	1001	1042
Tail Gas flow:	kmole/h	4730	2837	2241	2094	**2027**	1999	1986
LHV Tail Gas:	kJ/kmole	433555	393050	355349	317549	**289508**	269515	255212
NG demand furnace:	Sm3/h	0	0	35310	56612	**69330**	79680	87698
Total system NG demand:	Sm3/h	101917	80101	80607	82021	**82802**	83815	84730
CO_2 emission:	Tonnes/day	3743	1750	944	681	**547**	465	410
Hydrogen produced:	kg/day	500000	500000	500000	500000	**500000**	500000	500000

Plant energy efficiency:	-	0.633	0.806	0.801	0.787	**0.780**	0.770	0.762
Excess Heat[21]:	GJ/h	1012.5	99.8	0.0	0.0	**0.8**	16.4	33.8

4.4.5 POX Results and Discussion

Utilizing the partial combustion of NG, the POX reformer operates exothermically at high temperatures. At around 1300°C, the plant energy efficiency is 0.78 with a CO_2 emission level of 363 tonnes per day with maximal pre-combustion carbon capture. The O/F ratio and the pressure are the only main process design variables. Table 16 shows the simulation overview.

Table 16 - POX Simulation Overview

	NG Feed	POX NG Feed	POX O_2 Feed	POX product	WGS Steam Feed	CCS and PSA1 Feed	PSA2 Feed	Tail Gas	Hydrogen Product	Air to Burner	Flue Gas
Temperature [°C]:	50	500	250	1186	320	25	25	25	25	350	1000
Pressure [Bar]:	50	24.5	24.5	24	23.25	22.25	22	2.5	20	1.2	1.2
Vapour fraction:	1.0	1.0	1.0	1.0	1.0	1.0	1.0	1.0	1.0	1.0	1.0
Mole flow [kmole/h]:	3373	3373	2213	11189	5840	14539	1401	461	10334	1255	1635
Mass flow [kg/h]:	66290	66290	70814	137104	105199	197284	14135	12241	20833	36198	48438
Mole flow [kmole/h]:											
CH_4	2877.84	2877.84	0.00	89.56	0.00	89.56	89.56	89.56	0.00	0.00	0.00
H_2	0.00	0.00	0.00	6627.18	0.00	10438.38	1043.84	104.38	10334.00	0.00	0.00
CO	0.00	0.00	0.00	3869.24	0.00	57.99	57.99	57.99	0.00	0.00	0.00
CO_2	74.54	74.54	0.00	113.41	0.00	3917.98	195.88	195.88	0.00	0.00	343.44
H_2O	0.00	0.00	0.00	478.87	5839.51	24.60	2.32	2.32	0.00	0.00	285.84
C	0.00	0.00	0.00	0.00	0.00	0.00	0.00	0.00	0.00	0.00	0.00
C_2H_6	237.80	237.80	0.00	0.00	0.00	0.00	0.00	0.00	0.00	0.00	0.00
C_3H_8	91.91	91.91	0.00	0.00	0.00	0.00	0.00	0.00	0.00	0.00	0.00
i-Butane	18.38	18.38	0.00	0.00	0.00	0.00	0.00	0.00	0.00	0.00	0.00
n-Butane	31.71	31.71	0.00	0.00	0.00	0.00	0.00	0.00	0.00	0.00	0.00
i-Pentane	9.11	9.11	0.00	0.00	0.00	0.00	0.00	0.00	0.00	0.00	0.00
n-Pentane	8.94	8.94	0.00	0.00	0.00	0.00	0.00	0.00	0.00	0.00	0.00
n-Hexane	6.07	6.07	0.00	0.00	0.00	0.00	0.00	0.00	0.00	0.00	0.00
n-Heptane	4.38	4.38	0.00	0.00	0.00	0.00	0.00	0.00	0.00	0.00	0.00
n-Octane	1.35	1.35	0.00	0.00	0.00	0.00	0.00	0.00	0.00	0.00	0.00
N_2	10.96	10.96	0.00	10.96	0.00	10.96	10.96	10.96	0.00	991.19	1002.15
O_2	0.00	0.00	2212.92	0.00	0.00	0.00	0.00	0.00	0.00	263.48	3.16

Different from SMR and SMR+, the reformer temperature in POX is set by adjusting the oxygen feed. Increased O/F ratio provides more exothermic oxidation resulting in a higher temperature, and increased conversion up to a point where total combustion starts to dominate. Balancing on this

---

[21] Excess Heat = Total Heat Available – Total Heat Demand

optimal point of operation may be difficult, but based on the HYSYS analyses, POX is energy efficient with limited emission. Table 17 shows how the system responds to changes in O/F ratio, highlighting the optimal value of 0.656. As can be seen, the energy efficiency is equal at a ratio of 0.7, but at that temperature, the system has an additional heat demand. At the optimal O/F ratio and hence optimal reformer temperature, the conversion rate is also maximized. This unison point of operation differs significantly from SMR and SMR+ due to their balancing of S/C ratio vs. temperature. Some existing plants use an air-blown design, which result in lower CAPEX, but requires extensive downstream clean-up if producing high purity hydrogen.

Table 17 - POX parameters sensitivity to changes in O/F ratio

Property	Unit									
O/F Ratio:	Mole/mole	0.500	0.600	0.650	**0.656**	0.700	0.750	0.800	0.900	1.000
Oxygen feed:	Sm3/h	50683	50830	52041	**52323**	55751	61451	67761	81811	98086
Product Temperature:	°C	1022	1100	1173	**1186**	1320	1511	1698	2034	2300
Conversion rate:	mole_H_2/mole_NG	1.538	1.852	1.958	**1.965**	1.952	1.870	1.779	1.600	1.427
Reforming NG flow:	Sm3/h	101366	84717	80063	**79753**	79644	81934	84701	90901	98086
Total Reforming flow:	Sm3/h	152049	135548	132105	**132076**	135396	143385	152462	172712	196172
CO_2 emission:	Tonnes/day	1495	646	385	**363**	285	280	286	303	322
Water Input WGS:	kg/h	108567	106552	105382	**105199**	103409	100721	97771	91208	83607
Hydrogen produced:	kg/day	500000	500000	500000	**500000**	500000	500000	500000	500000	500000
Plant energy efficiency:	-	0.619	0.740	0.782	**0.784**	0.784	0.761	0.734	0.681	0.629
Additional Heat Demand[22]:	GJ/h	-859.9	-214.0	-16.2	**0.0**	54.7	50.1	36.2	4.0	-32.5

---

[22] Additional Heat Demand = Total Heat Demand – Total Heat Available

The reformer temperature is significantly higher in POX than in SMR and due to the absence of steam, soot formation is a familiar phenomenon. In existing facilities, the soot formation is handled with a scrubber after the reformer outlet [4].

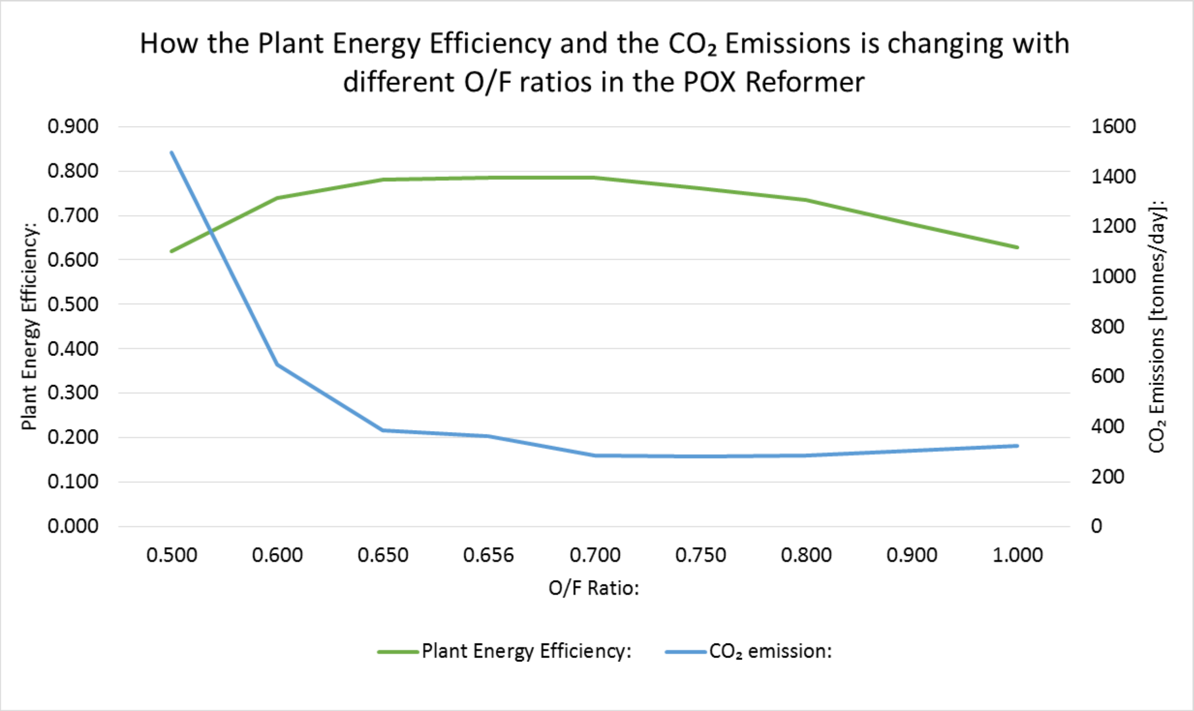

Figure 15 - Graph showing how the plant energy efficiency and CO_2 emissions are affected by changes in the oxygen-to-fuel ratio in POX.

Figure 15 shows how the O/F ratio affects the performance of the POX system. With low oxygen rates, the conversion of methane is incomplete, resulting in significant amounts of carbon not captured in the absorption column. This gives higher CO_2 emissions, since the tail gas is fed to a furnace to supply heat to the process. At higher O/F ratios, the emissions are low, due to full conversion. The plant energy efficiency starts to drop when the oxygen flow rate increase beyond 0.7 due to the energy consumption in the ASU and oxygen compression, as well as very high O/F ratios lead to total combustion.

HYSYS is not capable of including soot formation in the simulation, which gives operation results beyond realistic values. The inconclusiveness of the POX simulation was confirmed by Statoil processing specialist Jostein Sogge[23], explaining that the soot formation will reduce the efficiency. In addition, he highlighted that the lack of catalyst will affect the results even further. The HYSYS simulation assumes equilibrium, but the syngas product from POX will in practice not reach equilibrium. Therefore, the results of the POX simulations are not considered conclusive and POX is not evaluated further in this thesis.

4.4.6 ATR Results and Discussion

Combining SMR and POX, ATR operates with both oxygen and steam feed streams. Optimized with a minimal S/C ratio of 1.5 and an O/F ratio of 0.616, the plant energy efficiency is 0.82, with a conversion rate of 2.36. Table 18 shows the simulation overview, with the reformer temperature at 1020°C.

Table 18 - ATR Simulation Overview

	NG Feed	GHR Feed	ATR NG + Steam Feed	ATR O_2 Feed	WGS Feed	CO_2 Absorption and PSA1 Feed	PSA2 Feed	Tail Gas	H_2 Product	Air To Burner	Flue Gas
Temperature [°C]:	50	400	560	250	320	25	25	25	25	350	1000
Pressure [Bar]:	50	25	24.5	24.5	23.25	22.25	22	2.5	20	1.2	1.2
Vapour fraction:	1.0	1.0	1.0	1.0	1.0	1.0	1.0	1.0	1.0	1.0	1.0
Mole flow [kmole/h]:	3247	4221	9959	2000	16802	14387	1358	419	10334	907	1244
Mass flow [kg/h]:	63816	81365	165006	64007	235283	191606	13287	11393	20833	26152	37546
Mole flow [kmole/h]:											
CH_4	2770.43	2770.43	3297.76	0.00	53.34	53.34	53.34	53.34	0.00	0.00	0.00
H_2	0.00	0.00	1083.39	0.00	7653.28	10438.36	1043.84	104.38	10333.97	0.00	0.00
CO	0.00	0.00	424.96	0.00	2843.10	57.99	57.99	57.99	0.00	0.00	0.00
CO_2	71.76	71.76	194.42	0.00	1023.78	3802.53	190.10	190.10	0.00	0.00	301.44
H_2O	0.00	974.13	4946.64	0.00	5218.28	24.31	2.25	2.25	0.00	0.00	213.31
C	0.00	0.00	0.00	0.00	0.00	0.00	0.00	0.00	0.00	0.00	0.00
C_2H_6	228.92	228.92	1.54	0.00	0.00	0.00	0.00	0.00	0.00	0.00	0.00
C_3H_8	88.48	88.48	0.00	0.00	0.00	0.00	0.00	0.00	0.00	0.00	0.00
i-Butane	17.70	17.70	0.00	0.00	0.00	0.00	0.00	0.00	0.00	0.00	0.00
n-Butane	30.52	30.52	0.00	0.00	0.00	0.00	0.00	0.00	0.00	0.00	0.00
i-Pentane	8.77	8.77	0.00	0.00	0.00	0.00	0.00	0.00	0.00	0.00	0.00
n-Pentane	8.60	8.60	0.00	0.00	0.00	0.00	0.00	0.00	0.00	0.00	0.00
n-Hexane	5.84	5.84	0.00	0.00	0.00	0.00	0.00	0.00	0.00	0.00	0.00
n-Heptane	4.22	4.22	0.00	0.00	0.00	0.00	0.00	0.00	0.00	0.00	0.00
n-Octane	1.30	1.30	0.00	0.00	0.00	0.00	0.00	0.00	0.00	0.00	0.00
N_2	10.57	10.57	10.55	0.00	10.55	10.55	10.55	10.55	0.00	716.11	726.66
O_2	0.00	0.00	0.00	2000.21	0.00	0.00	0.00	0.00	0.00	190.36	2.49

---

[23] Specialist in mid- and downstream processing, Statoil.

ATR operation requires control of both oxygen and steam supply in order to maintain optimal operation. Table 19 shows the systems response to changes in oxygen input, and hence the POX part of the reforming reactions. A higher O/F ratio results in higher temperatures, due to more exothermic reactions. The plant energy efficiency has a maximum value at an O/F ratio of 0.616.

Table 19 - ATR parameters sensitivity to changes in O/F ratio

Property	**Unit**									
O/F Ratio:	Mole/mole	0.400	0.500	0.600	**0.616**	0.650	0.700	0.750	0.800	0.900
S/C Ratio:	Mole/mole	1.5	1.5	1.5	**1.5**	1.5	1.5	1.5	1.5	1.5
Oxygen feed:	Sm3/h	39701	42143	46171	**47294**	50263	55556	61397	67681	81655
Product Temperature:	°C	830	889	993	**1020**	1087	1199	1313	1424	1635
Conversion rate:	mole_H$_2$/ mole_NG	1.954	2.232	2.366	**2.357**	2.307	2.201	2.091	1.986	1.788
Reforming NG flow:	Sm3/h	99251	84287	76952	**76776**	77328	79366	81863	84601	90728
Total Reforming flow:	Sm3/h	138952	126430	123123	**124070**	127591	134922	143260	152282	172383
CO$_2$ emission:	Tonnes/day	1608	809	351	**318**	283	273	272	273	282
Water Input WGS:	kg/h	0	0	6642	**6271**	4068	0	0	0	0
Hydrogen produced:	kg/day	500000	500000	500000	**500000**	500000	500000	500000	500000	500000
Plant energy efficiency:	-	0.635	0.746	0.815	**0.816**	0.809	0.787	0.761	0.735	0.683
Additional Heat Demand[24]:	GJ/h	-867.9	-306.0	-32.4	**-26.7**	-50.1	-131.5	-230.3	-338.7	-581.5

When it comes to CO$_2$ emissions, keeping the oxygen supply at optimal conditions is important. A drop in O/F ratio to 0.5 more than doubles the CO$_2$ emissions. The reason for the increased emissions is the unconverted methane slip. Methane, which passes through the reactor, will not be affected in WGS reactors, neither will it be captured in the carbon absorption column. Hence, lower O/F ratio leads directly to more emissions. On the other hand, an increased O/F ratio leads to total combustion and more CO$_2$ production. The produced CO$_2$ will be captured and does not affect the total emissions significantly.

---

[24] Additional Heat Demand = Total Heat Demand – Total Heat Available

Changing the S/C ratio has a similar effect in ATR as in SMR. More steam gives a higher conversion rate, but demands more heat in order to operate. In ATR, this leads to lower reformer temperature, because the heat supply is fixed from the POX section of the reactor. As can be seen from Table 20, reducing the S/C ratio gives higher efficiency, even though the conversion rate drops. Ideally, ATR would operate with low S/C ratios, but due to soot and carbon formation, 1.5 is the lower limit. Hence, a S/C ration of 1.5 is chosen as the optimal point of operation.

Table 20 - ATR parameters sensitivity to changes in S/C ratio

Property	Unit							
O/F Ratio:	Mole/mole	0.616	0.616	0.616	**0.616**	0.616	0.616	0.616
S/C Ratio:	Mole/mole	0.1	0.5	1.0	**1.5**	2.0	2.5	3.0
Oxygen feed:	Sm3/h	46662	46752	46979	**47294**	47584	47964	48406
Product Temperature:	°C	1251	1160	1080	**1020**	973	934	902
Conversion rate:	mole_H_2/mole_NG	2.136	2.204	2.284	**2.357**	2.420	2.474	2.519
Reforming NG flow:	Sm3/h	75750	75896	76265	**76776**	77247	77863	78581
Total Reforming flow:	Sm3/h	122411	122648	123244	**124070**	124831	125827	126987
CO_2 emission:	Tonnes/day	280	285	299	**318**	321	335	357
Water Input WGS:	kg/h	90354	66338	36555	**6271**	0	0	0
Hydrogen produced:	kg/day	500000	500000	500000	**500000**	500000	500000	500000
Plant Energy Efficiency:	-	0.828	0.826	0.822	**0.816**	0.811	0.805	0.797
Additional Heat Demand[25]:	GJ/h	12.6	7.0	-7.1	**-26.7**	-43.2	-66.2	-93.5

The operating temperature is found to correlate well with literature, describing ranges from 900-1150°C [4]. ATR is commonly used in chemical industry, especially in methanol production, due to its favourable H_2/CO ratio of around 2. This also fits well with the results in this thesis. On the other hand, some deviation may be assumed on the energy efficiency. A majority of reports describes SMR as the most energy efficient method of hydrogen production from natural gas. Here, ATR proves equal. One explanation is that, similar as pure POX, the partial oxidation is simulated too well in HYSYS. Carbon and soot formation will slow the reaction rates as the catalyst degenerates, but that effect is not included in the HYSYS simulations. This effect is not as severe in ATR as in POX due to the steam feed to the reactor.

---

[25] Additional Heat Demand = Total Heat Demand – Total Heat Available

The changes in plant energy efficiency and CO_2 emissions due to temperature variations follow in ATR a similar curve as in POX, displayed in Figure 16. The optimal O/F ratio is a little lower in ATR than POX, but the level of energy efficiency is higher. In addition, the CO_2 emissions in ATR are lower, due to the enhanced conversion in the SMR section of the reactor, as well as a higher S/C ratio through the WGS, providing a better shift to CO_2. As in all the reformer systems, the more carbon bound in CO_2 after the WGS, the higher the capture rate and thus, lower emissions.

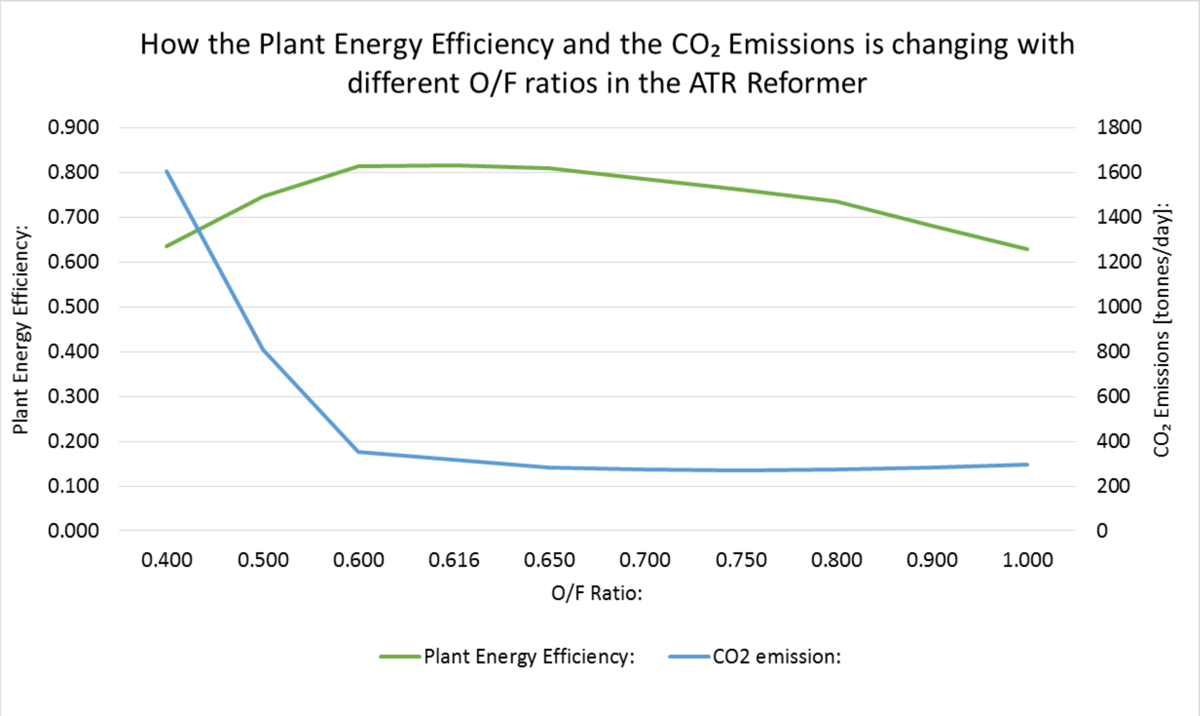

Figure 16 - Graph showing how the plant energy efficiency and CO_2 emissions are affected by changes in O/F ration in ATR.

4.4.7 CRE Results and Discussion

Combined ATR and electrolysis will operate as the traditional ATR, but with a lower production rate from natural gas and a different ASU.

Table 21 - CRE system overview

	NG Feed	GHR Feed	ATR NG + Steam Feed	ATR O_2 Feed	WGS Feed	CO_2 Absorption and PSA1 Feed	PSA2 Feed	Tail Gas	H_2 From ATR	H_2 From EL	Air To Burner	Flue Gas
Temperature [°C]:	50	400	560	250	320	25	25	25	25	80	350	1000
Pressure [Bar]:	50	25.25	24.75	24.75	23.50	22.5	22.25	2.5	20.25	20.25	1.2	1.2
Vapour fraction:	1.0	1.0	1.0	1.0	1.0	1.0	1.0	1.0	1.0	1.0	1.0	1.0

Mole flow [kmole/h]:	2353	3059	7215	1428	12156	10414	996	316	7478	2856	787	1044
Mass flow [kg/h]:	46240	58956	119577	45700	169943	138442	9806	8436	15075	5758	22712	31148
Mole flow [kmole/h]:												
CH_4	2007.39	2007.39	2390.68	0.00	51.80	51.80	51.80	51.80	0.00	0.00	0.00	0.00
H_2	0.00	0.00	781.78	0.00	5558.10	7553.22	755.32	75.53	7477.69	2856.28	0.00	0.00
CO	0.00	0.00	306.34	0.00	2037.11	41.96	41.96	41.96	0.00	0.00	0.00	0.00
CO_2	52.00	52.00	141.25	0.00	751.61	2742.13	137.09	137.09	0.00	0.00	0.00	230.85
H_2O	0.00	705.83	3586.02	0.00	3749.81	17.43	1.63	1.63	0.00	0.00	0.00	180.77
C	0.00	0.00	0.00	0.00	0.00	0.00	0.00	0.00	0.00	0.00	0.00	0.00
C_2H_6	165.87	165.87	1.12	0.00	0.00	0.00	0.00	0.00	0.00	0.00	0.00	0.00
C_3H_8	64.11	64.11	0.00	0.00	0.00	0.00	0.00	0.00	0.00	0.00	0.00	0.00
i-Butane	12.82	12.82	0.00	0.00	0.00	0.00	0.00	0.00	0.00	0.00	0.00	0.00
n-Butane	22.12	22.12	0.00	0.00	0.00	0.00	0.00	0.00	0.00	0.00	0.00	0.00
i-Pentane	6.35	6.35	0.00	0.00	0.00	0.00	0.00	0.00	0.00	0.00	0.00	0.00
n-Pentane	6.23	6.23	0.00	0.00	0.00	0.00	0.00	0.00	0.00	0.00	0.00	0.00
n-Hexane	4.24	4.24	0.00	0.00	0.00	0.00	0.00	0.00	0.00	0.00	0.00	0.00
n-Heptane	3.06	3.06	0.00	0.00	0.00	0.00	0.00	0.00	0.00	0.00	0.00	0.00
n-Octane	0.94	0.94	0.00	0.00	0.00	0.00	0.00	0.00	0.00	0.00	0.00	0.00
N_2	7.65	7.65	7.65	0.00	7.65	7.65	7.65	7.65	0.00	0.00	621.92	629.57
O_2	0.00	0.00	0.00	1428.14	0.00	0.00	0.00	0.00	0.00	0.00	165.32	2.97

The hydrogen production from ATR will be reduced by around 30%, but that will not affect the process simulations from HYSYS. The only thing that deviates is the optimization. Due to the high energy consumption of the electrolysers, the optimal O/F ratio will be lower than in ATR in order to get the best plant energy efficiency. That means a less efficient ATR process, but a better overall result. This can be seen from the results in Table 22, and is highlighted in Figure 17. Notice how fast the efficiency drops with increased O/F ratio due to the power consumption of the electrolysis. With higher O/F ratio, the rate of which EL produces hydrogen increases and thus the emissions continue to drop. The high emissions at low O/F ratios originates from the methane slip due to low conversion, similar as in POX and ATR.

Table 22 - CRE parameters sensitivity to variations in the O/F ratio, given optimal S/C ratio.

Properties	**Unit**									
O/F Ratio:	Mole/mole	0.400	0.500	0.600	0.607	0.650	0.700	0.750	0.800	0.900
S/C Ratio:	Mole/mole	1.5	1.5	1.5	1.5	1.5	1.5	1.5	1.5	1.5
Oxygen feed:	Sm^3/h	30000	31365	33524	33768	35616	38191	40862	43553	48943
Product Temperature:	°C	831	890	993	1004	1087	1199	1312	1424	1635
Conversion rate:	mole_H_2/mole_NG	1.950	2.229	2.365	2.362	2.307	2.201	2.092	1.986	1.788
Reforming NG flow:	Sm^3/h	75001	62730	55873	55630	54794	54558	54483	54441	54381
Total Reforming flow:	Sm^3/h	105001	94095	89396	89398	90411	92749	95345	97994	103324
CO_2 emission:	Tonnes/day	1218	604	256	244	201	188	181	176	169
Water Input WGS:	kg/h	0	0	4747	4666	2850	0	0	0	0
Total EL consumption:	kWh/kg_H_2	58	58	57	57	58	58	58	58	58
Hydrogen produced:	kg/day	500000	500000	500000	500000	500000	500000	500000	500000	500000
ATR Based H_2:		377220	371635	362801	361801	354233	343700	332765	321753	299694

EL Based H_2:		122780	128365	137200	138199	145765	156300	167233	178247	200306
Plant Energy Efficiency:	-	0.627	0.704	0.745	0.745	0.738	0.721	0.702	0.684	0.651
Additional Heat Demand:	GJ/h	-659.7	-230.8	-25.1	-22.0	-36.1	-90.6	-153.4	-218.1	-348.8

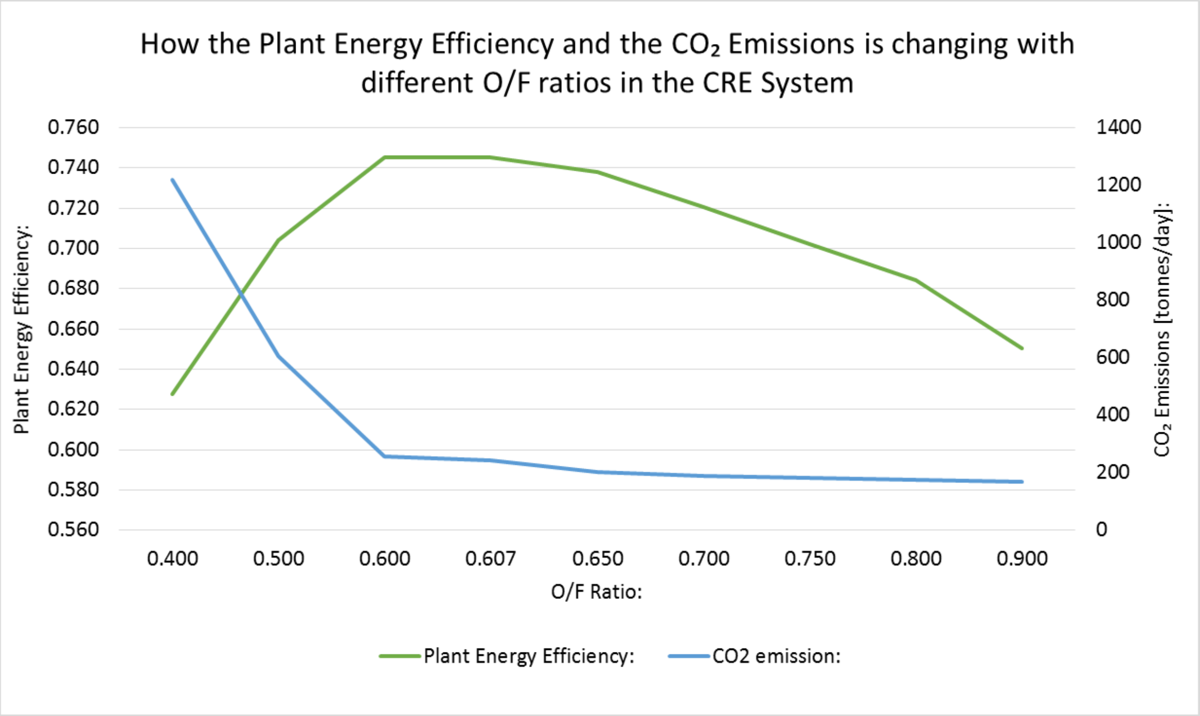

Figure 17 - Graphs showing how the plant energy efficiency and CO_2 emissions are affected by changes in the O/F ratio

The behaviour of CRE when changing the S/C ratio is identical to ATR, but with smaller response due to the split production. Table 23 shows the results of the sensitivity analysis of CRE with changes in S/C ratio.

Table 23 - CRE parameters sensitivity to variations in S/C ratio

Properties	Unit							
O/F Ratio:	Mole/mole	0.607	0.607	0.607	0.607	0.607	0.607	0.607
S/C Ratio:	Mole/mole	0.1	0.5	1.0	1.5	2.0	2.5	3.0
Oxygen feed:	Sm^3/h	33363	33421	33570	33768	33949	34172	34423
Product Temperature:	°C	1221	1136	1060	1004	960	923	892
Conversion rate:	mole_H_2/mole_NG	2.145	2.214	2.292	2.362	2.423	2.474	2.516
Reforming NG flow:	Sm^3/h	54964	55059	55305	55630	55929	56297	56710
Total Reforming flow:	Sm^3/h	88327	88480	88876	89398	89878	90469	91133
CO_2 emission:	Tonnes/day	210	215	227	244	248	260	277
Water Input WGS:	kg/h	65658	48508	26766	4666	0	0	0
Total EL consumption:	kWh/kg_H_2	57	57	57	57	57	57	57
Hydrogen produced:	kg/day	500000	500000	500000	500000	500000	500000	500000

ATR Based H_2:		363458	363222	362609	361801	361058	360145	359120
EL Based H_2:		136542	136779	137391	138199	138941	139855	140880
Plant Energy Efficiency:	-	0.754	0.753	0.750	0.745	0.741	0.736	0.731
Additional Heat Demand:	GJ/h	13.2	8.2	-4.8	-22.0	-36.6	-55.6	-77.3

5 Financial Analysis of Large-scale Hydrogen Production

In order to evaluate the systems defined in Chapter 4 to assist a potential investment decision, a financial analysis is necessary. Improved thermodynamic efficiency and operation is often related to increased investment cost and higher operation expenditures. There are few journals or reports comparing the cost of various hydrogen production methods to this level. Therefore, a variety of different sources has provided the information needed to compose this overview. The aim of this chapter is to establish a benchmark production cost of carbon-lean hydrogen. By performing a cost analysis, the CAPEX and OPEX of each system will be decomposed in order to highlight differences in how the individual designs affect the overall viability. A sensitivity analysis will highlight how the individual systems are affected by variations in feedstock cost, financial market situations and facility design. Finally, the chapter will conclude with a discussion of which system is best suited for large-scale operation in Norway. All financial and technical inputs used in this analysis are listed in Appendix A.

Due to the technical analysis and limited information on investment cost and operational expenditures, POX is not included in the financial analysis.

5.1 Financial Risk

If a large-scale production plant is to be built, the business case carries considerable risk, seen from a 2016 perspective. Significant uncertainties are related to the market development of infrastructure and political incentives for a greener transportation sector and CO_2 emission reductions in the industry. Because of a diverse market, with opportunities within transportation and industry, the risk of substitute technology such as improved batteries or biofuel, is reduced. Economies of scale related to the fuel cell industry is important in order for that market segment to reach adequate levels. The natural gas reforming technology itself is mature, with several facilities existing today. The overall performance risk could be greatly reduced by running a small-scale demo project prior to the investment decision.

5.1.1 Discount Rate

The project discount rate has been set to 10% for the investment scenarios in this thesis. The discount rate is both describing the time value of money and the risk premium attached to this specific investment. The risk free return on capital is estimated by the average long-term interest rate on Norwegian government bonds of 1.57% in 2015 [32]. The cost of capital of green energy projects in Europe was approximately 6% in 2015 [33, 17]. This implies a risk premium of around 4.5%. Because of a large-scale hydrogen export project to an uncertain market holds significantly higher risk, the risk premium is close to doubled, resulting in a discount rate of 10%. To further justify the rate, feed-in-tariffs or other subsidies are not included in the revenue stream, even though it is very likely for a project similar to that described in this thesis to receive substantial support. Especially considering the combination of CO_2 emission reductions and technology development.

As a comment, the discount rate chosen for this analysis does not necessarily reflect the actual required discount rate prior to the investment decision at a later stage.

5.2 What Is the Price Target of Carbon-lean Hydrogen Produced in Norway?

As this thesis aim to provide a benchmark for the cost of producing hydrogen in Norway, an important question arises: At what level must the breakeven price of hydrogen be in order to be cost competitive?

During the project work done in the fall of 2015, a competitive analysis on the production of hydrogen in Germany and UK was conducted in order to provide a target for the production and export cost. It was estimated that the costs of liquefaction, storage and transportation would be in the range from 0.9 €/kgH_2 of hydrogen produced to 1.9 €/kgH_2 in 2030 [20]. The market analysis done in the same study concluded that a marginal cost to market of between 2 - 4 €/kgH_2 is what can be expected of domestic production of hydrogen in UK and Germany, including traditional hydrogen production without CCS [20]. Hence, based on the conservative liquefaction, storage and transportation costs, **a production price below 2.1 €/kgH_2 is necessary in order to be competitive in a large-scale European export scenario.** One can see from the estimations, that in a scenario where domestic production in UK or Germany is 2 €/kgH_2 and transportation costs are high, export to those markets will not be a viable business case.

The Japanese government has released an import target price of imported hydrogen of 30 yen/Nm^3 which equals 2.7 €/kgH_2[26] [22]. If exported to Japan, the transport cost will increase by some factor, but this only accounts for a small part of the total cost. Hence, given a conservative liquefaction, storage and transportation cost, export to Japan does not seem viable in the future. On the other

---

[26] 1 € = 123.7 Yen, Exchange rate of 30.05.2016

hand, if cost compression allows for optimistic distribution costs, the case holds potential, given a production cost below 1.8 €/kgH_2. These are early and uncertain values, but provide a ballpark target.

5.3 Cost Analysis

The cost analysis is based on data collected from various project reports and journals, referred to throughout the chapter. Although significant uncertainty is related to the exact values listed in this section, the relative difference of the costs should provide key insights to an investment decision. Included in the cost analysis is the entire production facility, from desulfurized natural gas feed to hydrogen output at 20 bar and 25 degrees Celsius. CAPEX and OPEX of the CCS plant is also included, although the process itself is excluded in the process model. The assumptions behind the most important cost drivers are explained in sections 5.3.5 through 5.3.7. In addition, a detailed list of assumptions with references is found in Appendix A.

First, an overview of the expenditures is presented in Table 24 and Table 25, respectively. Further, the CAPEX and OPEX of the individual systems are explained in more detail, providing a deeper understanding of the differences.

Table 24 - CAPEX overview of the hydrogen production systems. All systems are designed with a daily production capacity of 500 tonnes of H_2, delivered at 20 bar.

CAPEX OVERVIEW - 500 tonnes H_2 per day

Hydrogen Production	Prefix	SMR	SMR+	ATR	Electrolysis	CRE
Hydrogen Production plant:	M€	349.0	423.9	296.2	429.3	358.1
Cell stack reinvestment:	M€	-	-	-	51.9	16.3
Air Separation Unit:	M€	-	-	64.3	-	-
Compressors:	M€	0.2	0.2	0.7	-	-
Land area:	M€	5.4	5.4	5.4	5.4	5.4
Auxiliary components:	*% of investment*	*20 %*	*20 %*	*20 %*		
	M€	69.8	84.8	72.2		44.6
Installation and Engineering:	*% of total investment*	*20 %*	*20 %*	*20 %*	*20 %*	*20 %*
	M€	83.8	101.8	86.7	96.2	80.5
Total CAPEX H_2 Production:	M€	508.2	616.2	525.6	582.8	505.0

Carbon Capture and Storage	Prefix	SMR	SMR+	ATR	Electrolysis	CRE
Carbon capture facility:	M€	117.4	139.9	137.5		109.4
Carbon transport and injection:	M€	176.2	209.9	206.2		164.0
Drilling and injection well:	M€	88.1	104.9	103.1		82.0
Total CCS CAPEX:	M€	381.7	454.8	446.8	-	355.4

Total System CAPEX:	**M€**	**889.9**	**1 071.0**	**972.4**	**582.8**	**860.4**

Table 25 - OPEX overview of the hydrogen production systems. All systems are designed with a daily production capacity of 500 tonnes of H_2, delivered at 20 bar

OPEX OVERVIEW - 500 tonnes H_2 per day

Hydrogen Production	Prefix	SMR	SMR+	ATR	Electrolysis	CRE
Specific cost of electricity:	*€/kgH_2*	*0.002*	*0.002*	*0.026*	*1.081*	*0.324*
Cost of electricity:	M€/year	0.3	0.4	4.5	187.5	56.1
H_2 Prod grid connection cost:	M€/year	0.1	0.1	0.7	24.3	8.5
Cost of natural gas:	M€/year	114.1	119.9	111.1	-	80.5
CO_2 tax:	M€/year	3.2	1.5	0.9		0.7
System OPEX rate:	*% of CAPEX/Year*	*5 %*	*5 %*	*5 %*	*5 %*	*5 %*
System OPEX:	M€/year	25.4	30.8	26.3	29.1	25.3
Total OPEX H_2 Production:	M€/year	143.1	152.6	143.5	240.9	171.1

Carbon capture and storage	Prefix	SMR	SMR+	ATR	Electrolysis	CRE
CCS cost of electricity:	M€/year	2.12	2.72	2.65		1.91
CCS grid connection cost:	M€/year	0.32	0.41	0.40		0.29
CCS System OPEX:	*% of CAPEX/Year*	*5 %*	*5 %*	*5 %*		*5 %*
	M€/year	19.1	22.7	22.3		17.8
Total OPEX CCS:	M€/year	21.5	25.9	25.4	-	20.0

Total System OPEX:	**M€/year**	**164.6**	**178.5**	**168.9**	**240.9**	**191.0**

5.3.1 Cost Breakdown SMR

As seen from Table 24, the total investment cost of the basic steam methane reforming (SMR) system is M€ 889.9. This is low compared to the other natural gas reforming systems. OPEX is dominated by the cost of natural gas, due to the minimal electricity consumption. The dedicated hydrogen production components dominate the CAPEX, while the natural gas consumption account for almost 75 percent of OPEX.

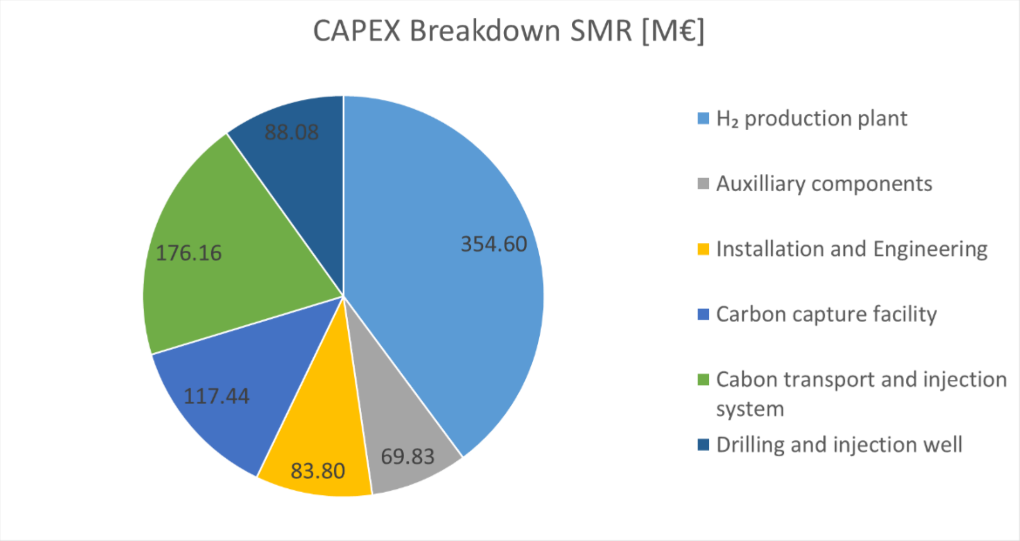

Figure 18 - CAPEX Breakdown of the SMR system. The three light grey values are related to hydrogen production. The three dark grey values are related to CCS

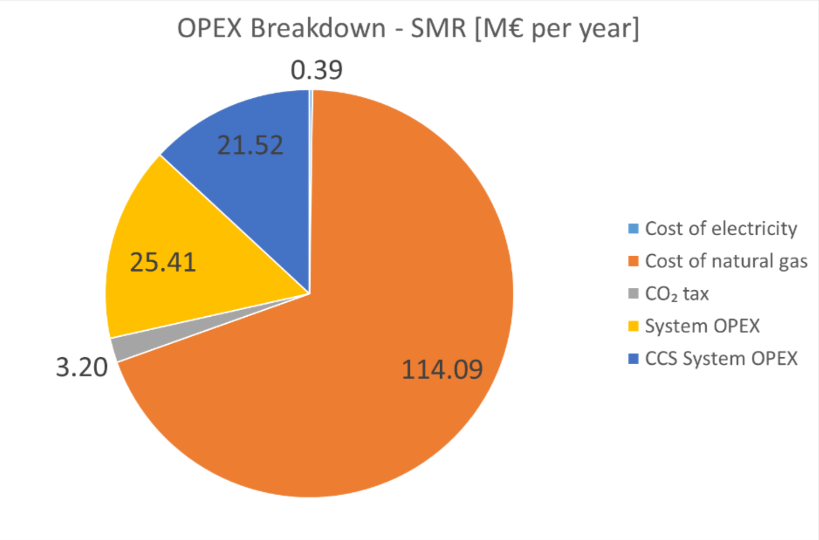

Figure 19 - OPEX breakdown of the SMR system. The cost of natural gas dominate with close to 65% of the expenditures

5.3.2 Cost Breakdown SMR+

In order to further reduce emissions, SMR+ use hydrogen instead of natural gas in the furnace to provide heat for the reformer, as mentioned in Section 4.3.3. This affects the cost significantly. The hydrogen demand implies a higher yield, hence more natural gas through the reformer. Since the reformer investment cost is based on hydrogen output, this is largely affected by this design change. The natural gas consumption only slightly increases. The cost picture as a whole is similar to SMR.

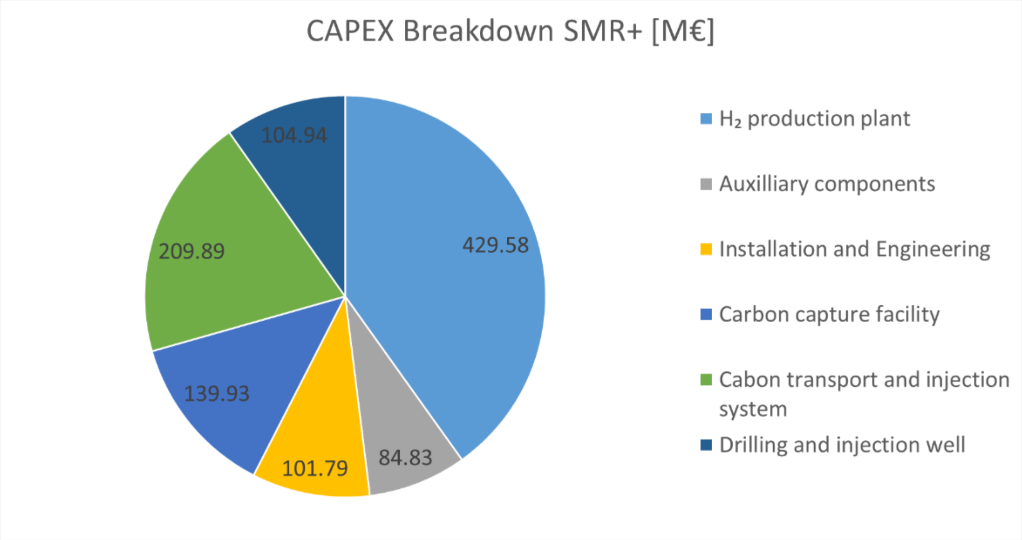

Figure 20 - CAPEX Breakdown of the SMR+ system. Notice the significant increase in H_2 production plant investment cost. This is due to the increased natural gas process input and hence a larger reactor.

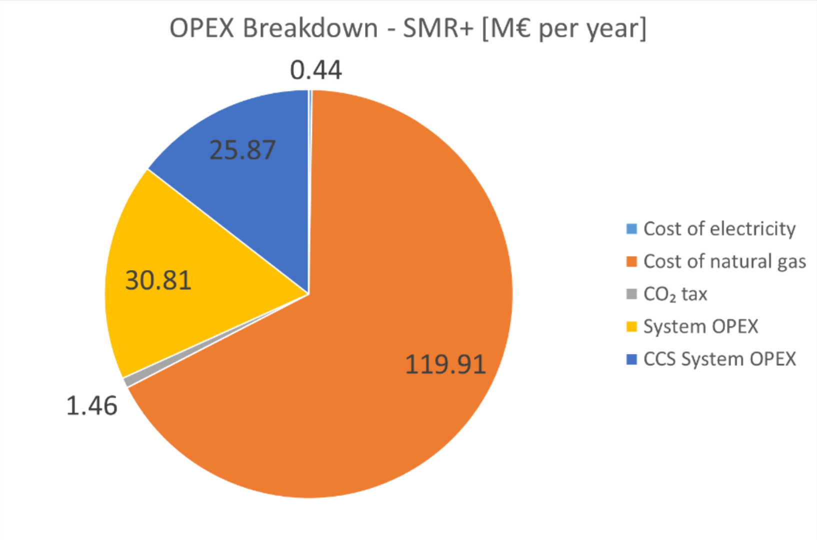

Figure 21 - OPEX Breakdown of the SMR+ system. The natural gas cost dominate as in SMR. The general cost level has increased evenly.

5.3.3 Cost Breakdown ATR

The cost breakdown of ATR differs from SMR and SMR+ mainly due to the different reformer design and the need for an air separation unit (ASU). The ASU represents a significant capital investment and consumes a fair amount of power, affecting the operating expenditures as well. On the other hand, the ATR reformer has a simpler design, reducing the investment cost of the reactor itself. OPEX is still dominated by natural gas cost.

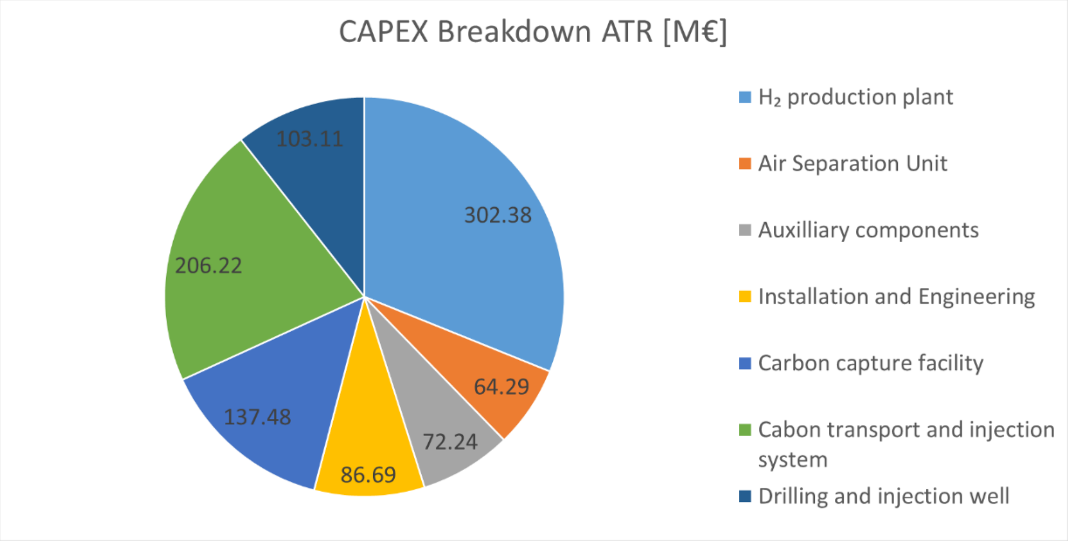

Figure 22 - CAPEX Breakdown of the ATR system. Differs from SMR mainly on the less expensive reformer and the inclusion of an air separation unit.

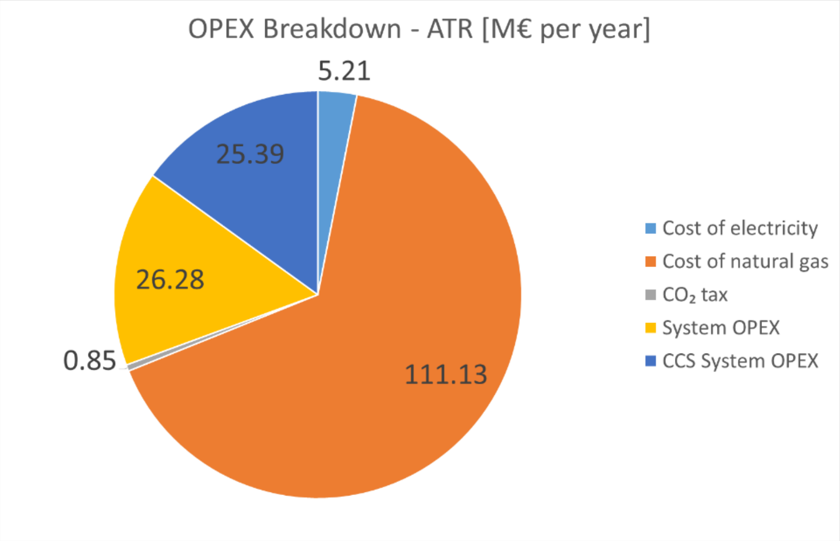

Figure 23 - OPEX Breakdown of the ATR system. The natural gas dominate among the expenditures, but here, cost of electricity impacts to a larger extent.

5.3.4 Cost Breakdown CRE

Although visually different from the traditional reforming, the combination system is very similar to ATR in capital expenses. Instead of a large reformer and an air separation unit, CRE uses a smaller reformer and electrolysis to produce hydrogen. This distributes the hydrogen production CAPEX on ATR plant and electrolysis plant. The same effect on OPEX, as the large natural gas piece is split into electricity cost and natural gas cost. CRE has a lower CAPEX compared with pure reforming, but OPEX is increased due to lower plant energy efficiency.

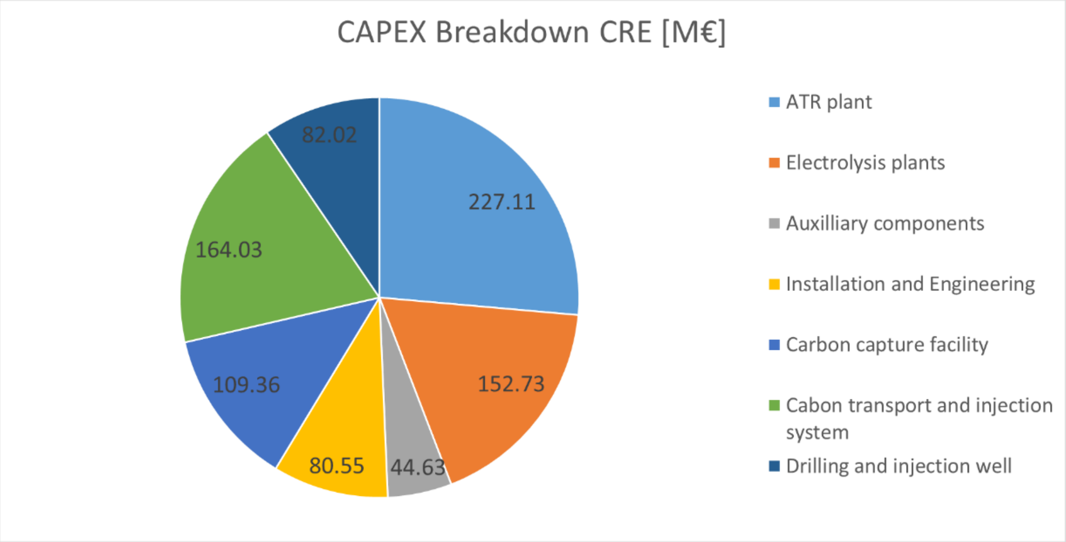

Figure 24 - CAPEX breakdown of the combined reforming and electrolysis system.

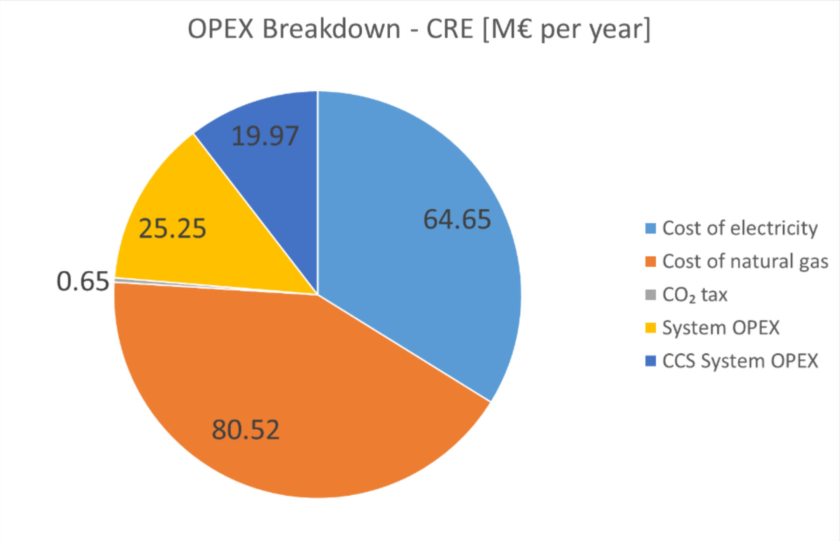

Figure 25 - OPEX breakdown of the combined reforming and electrolysis system. Here, the cost of natural gas and electricity are close to equal

5.3.5 Energy Input Costs

OPEX of all the production systems is dominated by energy input expenditures, where the main drivers are the costs of natural gas or electricity. Both variables are highly volatile and thus difficult to predict, which results in uncertainty. The cost of natural gas is set to 0.174 €/Sm^3, based on the average internal gas price of Statoil in 2015 [34]. The internal gas price reflects a market price where marketing and distribution costs are deducted. The electricity price in Norway is set to be 20.03 €/MWh. This is based on the monthly averages of NASDAQ commodity ENOYR 17, 18 and 19 from April to May of 2016[27] [35]. Any taxation on power consumption is not included in this thesis. The grid connection cost is set to be 230 NOK/kW installed capacity, based on the Norwegian national grid tariff of 2016 [36].

5.3.6 Production Facility Costs

CAPEX of the SMR systems are based on European averages of large-scale steam methane reformers of 400 €/kW capacity, Higher heating value (HHV) of hydrogen output, in a 300 MW facility [1]. Further, SMR is scaled based on hydrogen output with a coefficient of 0.8[28], assuming normal operation. The formula used in scaling capital expenditures is explained in Appendix A. The reason for the relatively poor scaling is due to the modular reactor design. SMR+ is further scaled from SMR to account for the increase in process NG feed. For ATR, the CAPEX is based on a cost analysis report on gas-to liquid systems done by the U.S. department of energy in 2013 [37]. Due to a simple and less modularized design, the ATR reactor cost can be scaled with a factor of 0.7[28]. The cost basis of SMR is the system total investment, while ATR is given with each component, hence the more detailed cost breakdown.

Similar for all the reactor cost estimations is that the effect of changing water input is not directly included in the results. The components are either scaled based on hydrogen output or natural gas input. The reason for this is the limited information of the actual S/C ratios used in the reference systems. By adding this effect, a more optimal design could have been found. Since this is similar for all the systems, it would not have a large effect on the relative cost estimations.

---

[27] The estimation of electricity price was done based on a recommendation by Professor Magnus Korpås, NTNU.

[28] The scaling coefficients have been estimated in cooperation with Jostein Sogge, Statoil

The cost of the electrolysis plant is based on the available data from NEL-Hydrogen, 600€/kW installed capacity of a 50 MW plant producing 26 tonnes per day at 15 bar [38]. Because of strict modularity, the electrolysis plant is scaled by a factor of 0.9.

Similar for all reforming systems is an additional 20 percent added to cover auxiliary components e.g. water systems, heat integration and power system. This is not included in the electrolyser system, due to the overall cost used in the thesis is listed as a total plant investment cost. Installation and engineering costs account for an additional 20% of system CAPEX. OPEX related to the hydrogen production other than NG and electricity is a standard 5% of CAPEX.

5.3.7 Carbon Capture and Storage Costs

CCS is a prerequisite for the success of fossil-based hydrogen production. The technology is used in the Norwegian oil and gas sector already, storing extracted CO_2 from reservoir gas. The cost estimations are based on approximate investment costs of the CCS system at Hammerfest LNG, provided by Professor II and Statoil researcher Jostein Pettersen. At the gas field "Snøhvit" in the Barents Sea around 700 000 tonnes of CO_2 is captured and sequestrated annually. The CCS-system consists of a separating unit followed by a compression stage. CO_2 is then transferred through a pipeline to a subsea injection unit. All the components are included in the cost analysis, including the investment in the drilling of an injection well. The professor estimated the total investment cost to be 2 600 M€ for the reference case, with OPEX equalling 5% of the total investment, annually. The cost is scaled to the different CO_2 with a coefficient of 0.7, also provided by the professor.

The average carbon emission price of 2016 is 69.98 NOK/tonne CO_2, where further specific emission tax is excluded due to the overall emission reduction a facility of this scale represents [39]. Some expect that a more intensive taxation of carbon emissions will be introduced in the future, in order to meet emission reduction targets. How the different systems will respond to that, is presented in Section 5.7.3.

5.4 Breakeven Price of Hydrogen

In order to determine the most cost-efficient hydrogen production method, the breakeven price is estimated for each system. The breakeven price is also known as the levelized cost of hydrogen and defined in the following way:

$$Breakeven\ Price = \frac{Sum\ of\ expenditures\ over\ lifetime}{Sum\ of\ hydrogen\ produced\ over\ lifetime} = \frac{\sum_{t=1}^{n} \frac{CAPEX_t + OPEX_t}{(1+r)^t}}{\sum_{t=1}^{n} \frac{H2_t}{(1+r)^t}}$$

In a given cost scenario, the sales price of hydrogen for which the net present value is zero, is equivalent to the breakeven price. As elaborated in Section 5.1.1, the discount rate for this project is set to be 10%. The lifetime of the project is set to 25 years and the reliability of the production is set to 95%, equal to 347 days of full production, annually. In addition, all CAPEX are assumed paid in the first year of operation.

Figure 26 shows the breakeven price of the different hydrogen production systems, based on the cost data presented in Section 5.3. The sensitivity analysis in Section 5.7 will provide estimations on optimistic and conservative scenarios as well, creating a range within which the breakeven price of hydrogen should be, given the assumptions of this thesis.

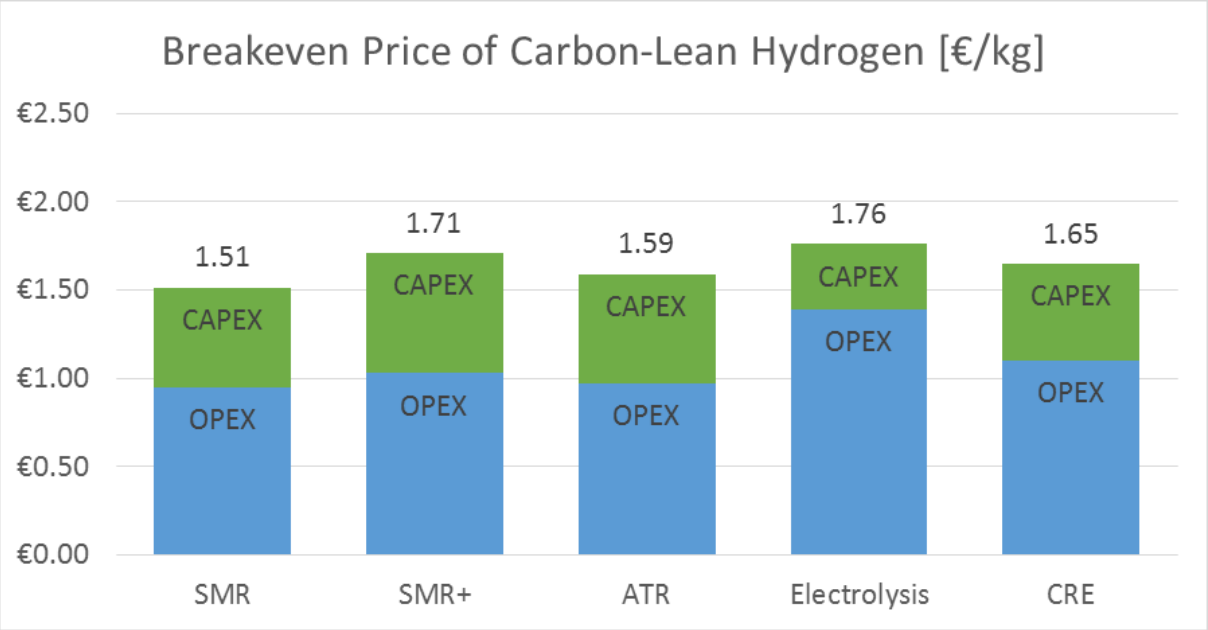

Figure 26 - Block diagram showing the breakeven price of carbon-lean hydrogen. Includes all auxiliary components, including CCS. 500 tonnes of H_2 daily, delivered at 20 bar. The blue and green colours indicate the share of which OPEX and CAPEX contribute throughout the lifetime, respectively. 10% discount rate and 25 years lifetime.

It is interesting that the difference in breakeven price is so small, across the various production methods. SMR appears to be the most cost-efficient system, with a breakeven price of 1.51 €/kgH_2, but all the other systems are included within a 17% price increase. ATR is second, at a price of 1.59 €/kgH_2, although providing a considerable reduction of CO_2 emissions compared to SMR.

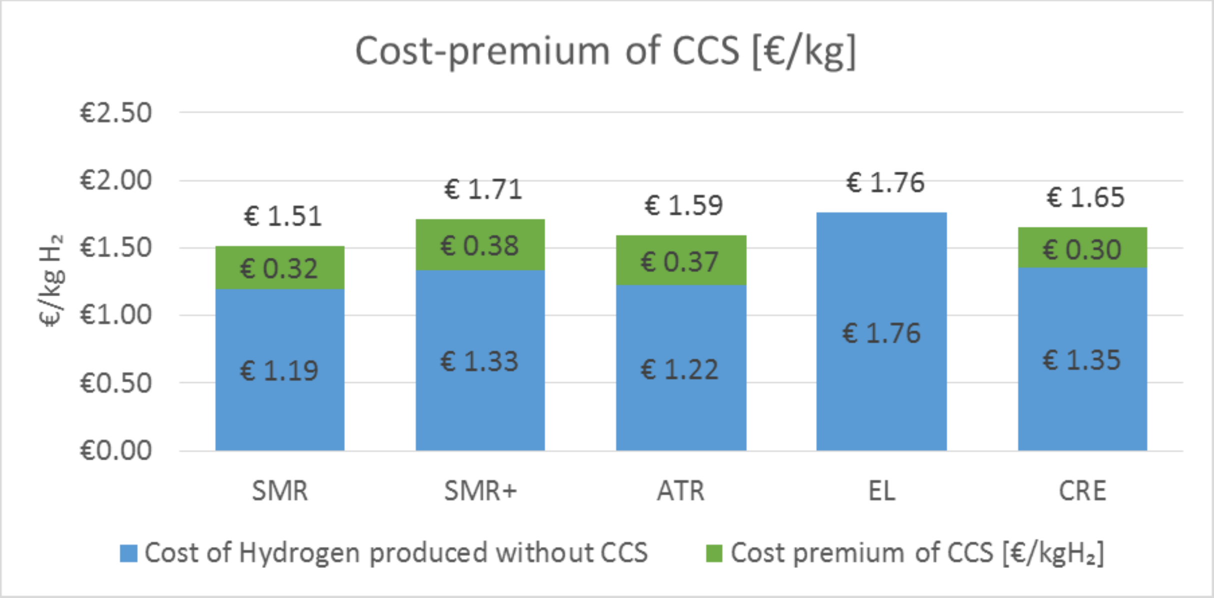

Figure 27 - Block diagram showing the breakeven price of carbon-lean hydrogen, highlighting the additional cost CCS represents in the different systems. Keep in mind the amount of CO_2 captures is different for each system.

Looking at the breakeven price of production, it is interesting to highlight the price premium CCS represents in each system. As shown in Figure 27, CCS represents approximately 20 percent of the total cost. Section 5.2 estimates a competitive production cost to be below 2.1 €/kgH_2, in a European export scenario. As the results of this analysis show, all the systems provide carbon-lean hydrogen with a breakeven price under 2.1 €/kgH_2. Whether the industry will accept a 20 percent increase in cost to produce carbon-lean hydrogen, compared to traditional hydrogen, is hard to predict, and may be affected by several factors like feed-in-tariffs and available subsidies.

As these results show, the estimations of the breakeven price of carbon-lean hydrogen in Norway ranges from 1.51 – 1.76 €/kgH_2. Further in this chapter, these results will be compared to other recent studies and an optimistic and conservative scenario is defined in order to provide cost ranges for each production system.

5.5 Cost Comparison with H2A Report by National Renewable Energy Laboratory

Validating results from analyses like the ones performed in this thesis can be difficult, due to the variation in source literature and uncertainty in estimations. One effective way of testing the realism in the results is to compare them with existing journals. Throughout the technical analysis, this is done in order to ensure realistic process operation. This section will present the highlights from a project carried out by the National Renewable Energy Laboratory (NREL) in the U.S. called H2A (Hydrogen analysis project), a comprehensive techno-economic analysis of hydrogen production from 2009 [31]. Figure 28 presents the results of the H2A project, with values given in 2005$. For simplicity, the NREL report is referred to as the H2A report and the current master thesis is referred to as "this thesis".

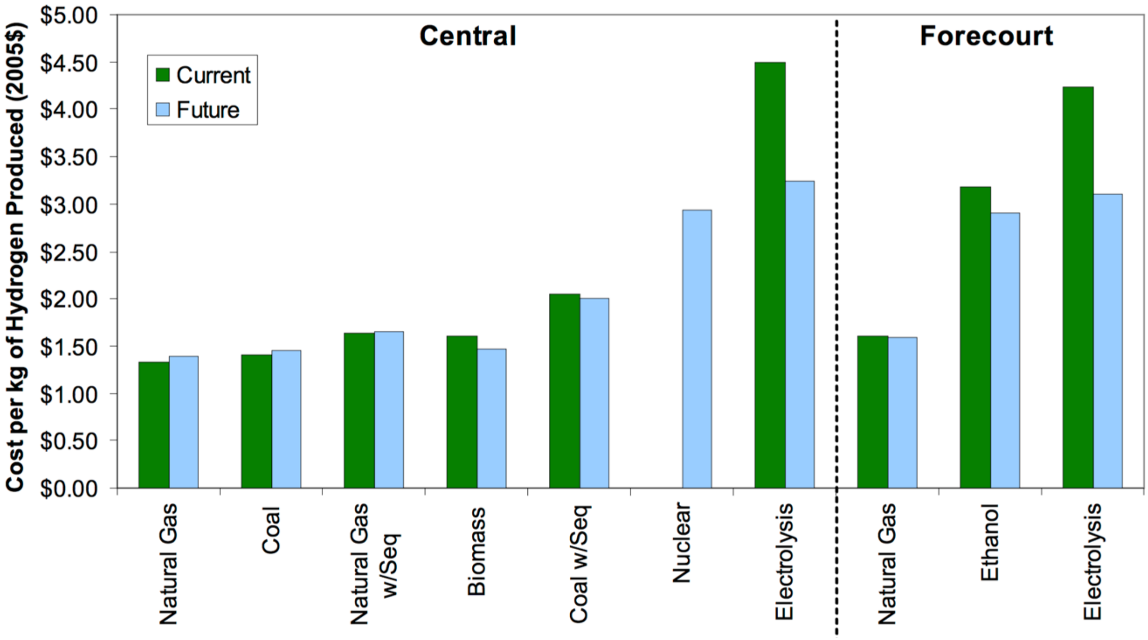

Figure 28 - Results of the H2A analysis of hydrogen production methods. The Future estimations are based on 2025 projections [31]. Keep in mind that the values are displayed in 2005$. The conversion factor to 2016$ is 1.225 [40].

The first apparent information from Figure 28 is that hydrogen production from a hydrocarbon feedstock is significantly more cost-efficient than electrolysis. Even though this is likely to be the case, as the results of the analysis in this thesis also indicates, the large difference can also be explained by scale of production and feedstock cost. This is also the main reason for the significant cost reduction in the future scenario, combined with a higher energy efficiency. Another interesting detail, although not covered in this thesis, is the competitiveness of hydrogen produced from biomass.

Table 26 - Cost comparison of this thesis with the results of H2A. Here, the breakeven price of hydrogen from H2A is converted from 2005$ to 2016€, based on the standard currency exchange rate used as well as a US inflation calculator [40], [31].

	SMR without CCS		SMR with CCS		Electrolysis	
	H2A Report	This Thesis	H2A Report	This Thesis	H2A Report	This Thesis[29]
Breakeven price of hydrogen:	€ 1.48	€ 1.19	€ 1.81	€ 1.51	€ 4.27	€ 1.94
OPEX percentage of hydrogen cost:	83.5%	73.1%	75.5%	62.9%	79.5%	74.7%

Table 26 shows a comparison between the analysis of SMR and electrolysis carried out in H2A report and the results from this thesis, given in Section 5.4. SMR without CCS is also included, in order to display the cost-premium it represents.

As can be seen from the table, the H2A report presents more expensive estimates. For SMR the difference can be explained by two factors: First, the design output of SMR in H2A is 341 tonnes of hydrogen per day, compared to 500 used in this thesis. The upscaling will result in further reduction of CAPEX per hydrogen produced. Second, the average natural gas price used by NREL is 0.25 €/Nm^3 (converted to 2016€) which is almost 50% more than the 0.17€/Nm^3 internal gas price from Statoil used in this thesis. This also explains the higher OPEX percentage of the breakeven price for the H2A results. If the natural gas price is adjusted to the value in H2A, the breakeven price of SMR with CCS increase to 1.80 €/kg, with an OPEX split of 68.9%, which is highly comparable.

On the electrolysis system, the deviation of the results is large, but it has a simple explanation: the cost of electricity. The electricity price used in H2A is 60.6 €/MWh, more than three times the 20.03 €/MWh used in this thesis. With an OPEX percentage of 75-80%, the cheap and available hydropower in Norway directly causes the price of hydrogen to be less than half of what similar technology can provide in the US. That result is very interesting. Because NREL used 51 tonnes per day capacity on the electrolysis system, the value from this thesis is also adjusted to that production volume. The change in production capacity increase the breakeven price, due to scale effects, from €1.76 per kg to

---

[29] The production capacity is changed from 500 tonnes per day to 51, in order to more comparable.

€1.94. If 60.6 €/MWh is used in this thesis, the breakeven price of hydrogen from electrolysis is 4.13 €/kg, only 3 percent less than H2A.

This section shows that the cost estimations of SMR and electrolysis are comparable to similar studies carried out in the past, improving the viability of the results. A very interesting discovery is the immense effect the low-cost, Norwegian energy resources have on the production cost of hydrogen.

5.6 Environmental Impact

Producing hydrogen brings socio-economic benefits, which create an added value not taken into account in the cost analysis. The Norwegian hydrogen production presented in this thesis, can reduce global CO_2 emissions, contribute to technology development and create jobs. In the cost analysis Section 5.3, the value of large-scale hydrogen production was assessed from a business perspective while the value of avoided CO_2 emissions are not fully taken into account. This chapter will discuss the value of reduced carbon emissions and whether the project has sufficient positive impact on the environment to outweigh the cost of CCS.

5.6.1 CO_2 Emissions

Most of the hydrogen production today is based on conversion of fossil resources without carbon capture and storage (CCS) [1]. All the CO_2 produced is therefore vented out in the atmosphere contributing to global warming. In December 12th 2015 more than 200 countries signed the Paris climate agreement and have committed to start the transition towards a low-emission society. The solution presented in this thesis can contribute to achieve the emission target as it cost-efficiently produces CO_2-lean hydrogen. Governments need concrete, large-scale projects in order to meet targets, and as Table 27 shows, even the production method with the highest CO_2 emissions studied in this thesis can cut global emissions by 2.98 million tonnes per year. The unavoidable emissions from the SMR plant adds up to 23.9 grams of CO_2 per km in a Toyota Mirai, assuming 100km per kg of hydrogen[30]. In comparison, the new vehicle emission target of EU in 2021 is 95 g/km, and an extremely low-emitting vehicle is defined as below 50 g/km [41].

---

[30] Some emissions may be caused by distribution, but as the project work of 2015 showed, not a large addition.

Table 27 - Annually CO_2 Captured and Avoided

	Value	Unit
CO_2 Captured SMR:	1.06	Million tonnes/year
CO_2 Captured SMR+:	1.45	Million tonnes/year
CO_2 Captured ATR:	1.36	Million tonnes/year
CO_2 Captured CRE:	0.95	Million tonnes/year
CO_2 Avoided[31] SMR:	2.98	Million tonnes/year
Annual emission of CO_2 equivalents in Norway:	53.8	Million tonnes/year [24]

Table 28 shows the CO_2 emissions per kWh produced electricity from a large gas turbine, with and without a combined cycle, and from a proton exchange membrane fuel cell (PEMFC) using hydrogen from SMR and ATR with CCS.

Table 28 - CO_2 emitted per kWh electricity produced.

Electricity Production Method	Value	Unit
PEMFC with hydrogen produced from SMR with CCS[32]:	0.12	$kgCO_2/kWh_{el}$
PEMFC with hydrogen produced from ATR with CCS:	0.04	$KgCO_2/kWh_{el}$
Large gas turbine [42] :	0.43	$kgCO_2/kWh_{el}$
Large Combined Cycle Gas Turbine (CCGT) power plant [42]:	0.29	$kgCO_2/kWh_{el}$

The CO_2 emissions from producing the same amount of electricity in a large NG fired CCGT power plant is almost six times the emissions when producing electricity with hydrogen from ATR. To reform NG to hydrogen before producing electricity is therefore an effective way of reducing CO_2 emissions.

The results of this analysis show that despite a higher cost, hydrogen production with CCS triggers great environmental benefits. The avoidance of CO_2 emissions by the utilization of the produced hydrogen are significant. The estimated energy efficiency of producing electricity from NG via hydrogen is approximately 50% using SMR[33], while a Large gas turbine efficiency of max 39% and Large

---

[31] CO_2 avoided using hydrogen from SMR+CCS as fuel in FCV replacing petrol vehicle. Assumed petrol engine efficiency of 30% and PEMFC efficiency of 60%.

[32] Assuming PEMFC efficiency of 60% [52]. SMR and ATR systems defined in Chapter 3.

[33] ATR Efficiency of 82%. PEMFC efficiency of 60%. Bare in mind that distribution of hydrogen is not included here. Neither is distribution of natural gas or power in the turbine cases.

gas fired CCGT power plant efficiency of max 58% is assumed [42]. Hence, for a given quantity of NG, a state-of-the-art CCGT power plant produces 16% more electricity compared to power production from hydrogen, but emits 240% more CO_2.

Table 29 shows SMR compared to ATR with different levels of emissions. Because the carbon recovery is variable, the cost of CCS can be reduced by lowering the recovery rate. ATR version 2 has the similar emission level as SMR. An important detail to be found from Table 29 is the cost of improved CCS in the ATR system. If boosting the capacity from ATR version 2 to ATR, 6 eurocents will be added per kg of hydrogen in order to avoid approximately 900 tonnes of CO emissions every day. That is substantial. Eliminating CCS entirely, the breakeven price of ATR is estimated to be 1.22 €/kg of hydrogen. Hence, from maximum emissions to 92% capture, the price premium of CCS is 0.37 €/kg. A 30% price increase, including CO_2 tax. This may indicate a need for policy support in order to be cost-competitive with traditional hydrogen.

Table 29 - This table shows how the breakeven price of ATR will differ when varying the CCS capacity. ATR 2 is a case with similar carbon capture as SMR. ATR 3 has similar emission level as SMR

	SMR	ATR	ATR 2
Breakeven Price €/kg H_2:	€ 1.51	€ 1.59	€ 1.53
CO_2 emissions [tonnes per day]:	1 198	318	1 198
CO_2 captured [tonnes per day]:	3 047	3 816	2 936

5.7 Sensitivity Analysis

A study of how the different systems respond to changes in initial conditions is important in order to get a complete overview. In projects with a lifetime of 25 years and initiation within a minimum of 5 years, it is difficult to estimate correct conditions. This sensitivity analysis consists of three parts. First is a technical case presentation, estimating an optimistic and a conservative scenario of the different systems, providing a range within the system should be operating. Further, the effect of changes in specific financial variables are tested, keeping all other variables constant. At the end is a presentation of how the systems are affected by a selection of technical design conditions.

5.7.1 Optimistic Case and Conservative Case Scenarios

In order to get a more nuanced view of the different systems, an optimistic and conservative scenario was defined. The main changes are on CAPEX scaling coefficients and hydrogen yield of the production processes. The specific details of the scenarios are listed in Appendix A.

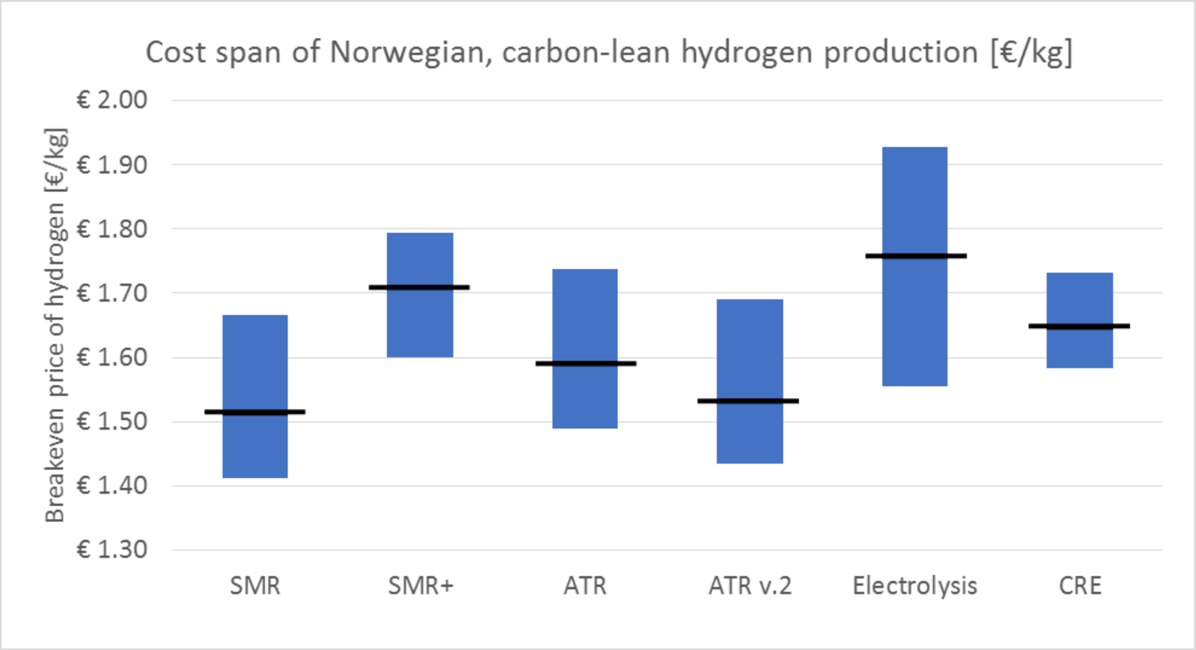

Figure 29 - Range of Breakeven price of hydrogen production.

The results of the scenario analysis is presented in Figure 29. As the diagram indicates, SMR is the most cost-efficient production method for carbon-lean hydrogen. ATR version 2 system is included, in order to show the effect of increased emissions has on the viability. The new version, similar to the one in Table 29, has the same emission level as SMR, by adjusting the rate at which the absorption column captures the CO_2.

Since the simulations done in Chapter 4 are assumed steady state with reactions reaching equilibrium, the results are ideal, given the chosen input parameters. In real operation, catalysts will enable reactions to approach equilibrium, but not perfectly, as in the simulations. Because of this, variation of the recovery of hydrogen in the PSA is included in the optimistic and conservative cases.

5.7.2 Changes in energy input Cost

Although considerable uncertainties are related to investment costs and maintenance, variations in feedstock costs are certain to occur and will affect the overall viability of the different systems significantly. In hydrogen production, the volatile prices of energy input, in the form of natural gas and electricity, dominate. Worldwide, the electricity price has been closely related to the cost of fossil resources. With the recent developments in renewables, this is not necessarily the case in the future, hence a scenario with high cost natural gas and cheap electricity is possible, and vice versa. In Norway, the electricity price is not directly affected by the natural gas price. On the other hand, with an increasing export capacity of power to northern European countries, a rapid increase in fuel costs may promote further export and lower supply in the home market. This section will present how the different systems react to changes in energy input cost.

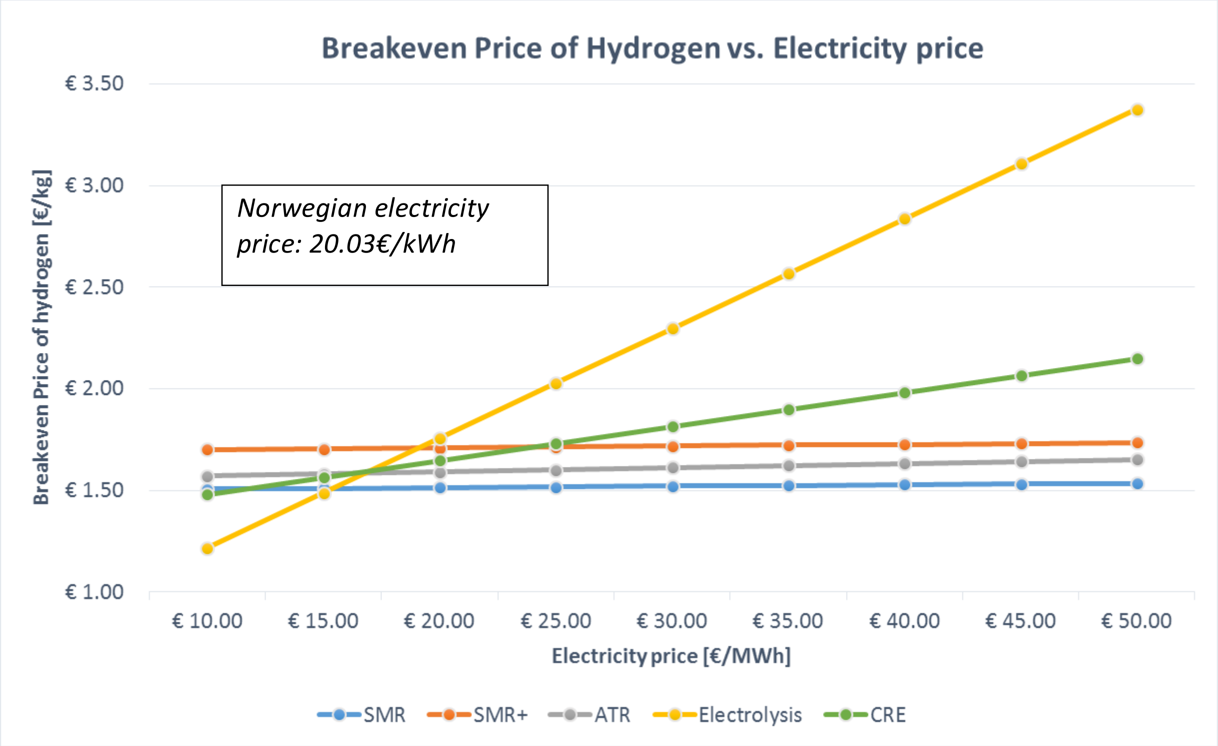

Figure 30 - Breakeven price of hydrogen with changes in the electricity price.

As can be seen from Figure 30 electrolysis is highly affected by the changes in electricity cost. Note that below approximately 16 €/MWh it is the most cost-efficient hydrogen production method for the 500 tonnes/day capacity. The average electricity price used in this thesis is 20.03 €/MWh [35]. This is based on the NASDAQ commodities ENOYR16-19 as mentioned in Section 5.3.5. It is evident that the price used is low compared to 33.88€/MWh, which was the average price of power intensive industry in the first quarter of 2016 [43]. The latter price would have resulted in a breakeven price of 2.51, 1€ more expensive than the price of hydrogen from SMR at the same electricity price. This is significant, and implies caution. Electrolysis industry is included in the power intensive segment, although one can argue that hydrogen production is fundamentally different from metal processing using the same "electrolysis". In the case of hydrogen, it is energy storage for distribution or export. Either way, the price of electricity is volatile and provides high risk in the case of such large-scale production of hydrogen.

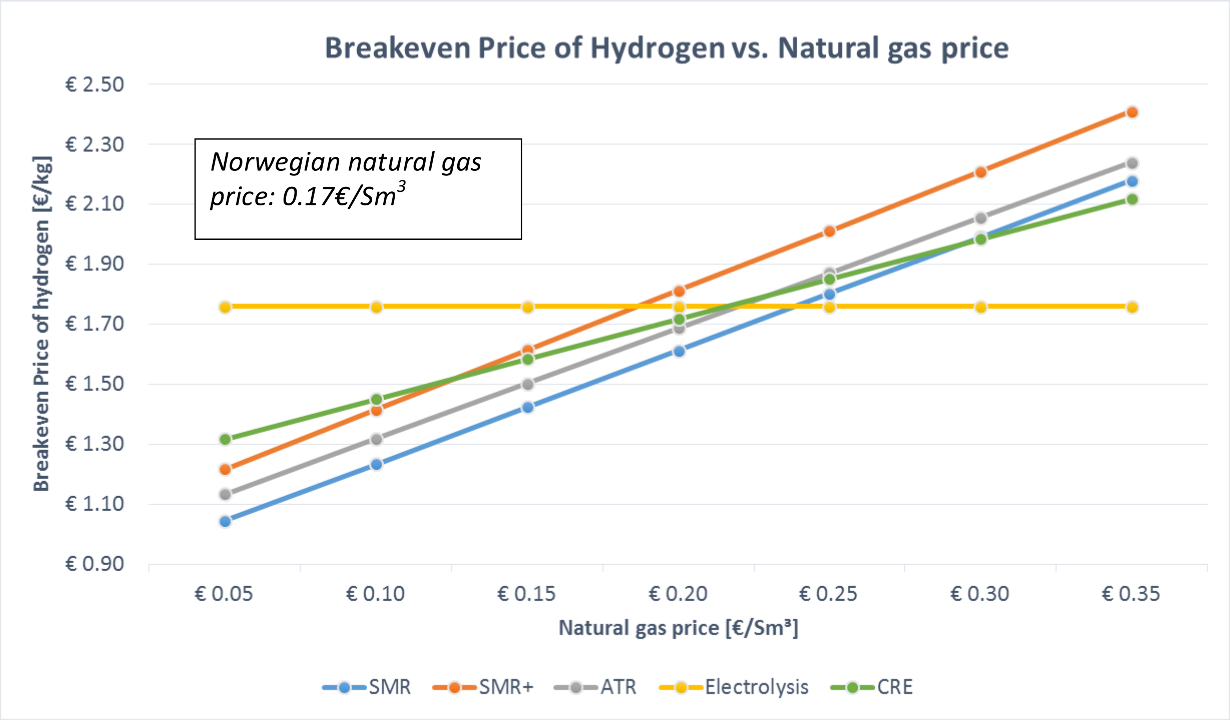

Figure 31 - Breakeven price of hydrogen vs. natural gas price.

Figure 31 plots how the systems respond to changes in natural gas cost. Here, an important value is the cost at which electrolysis out-compete the reforming processes. This occurs at a price around 0.24 €/Sm^3. Assuming the price of natural gas increase to this level, from the current 0.17/Sm^3, it is fair to assume that it will have some effect on the electricity price as well. Therefore, a scenario where the energy input costs vary with the same rate of change is shown in Figure 32.

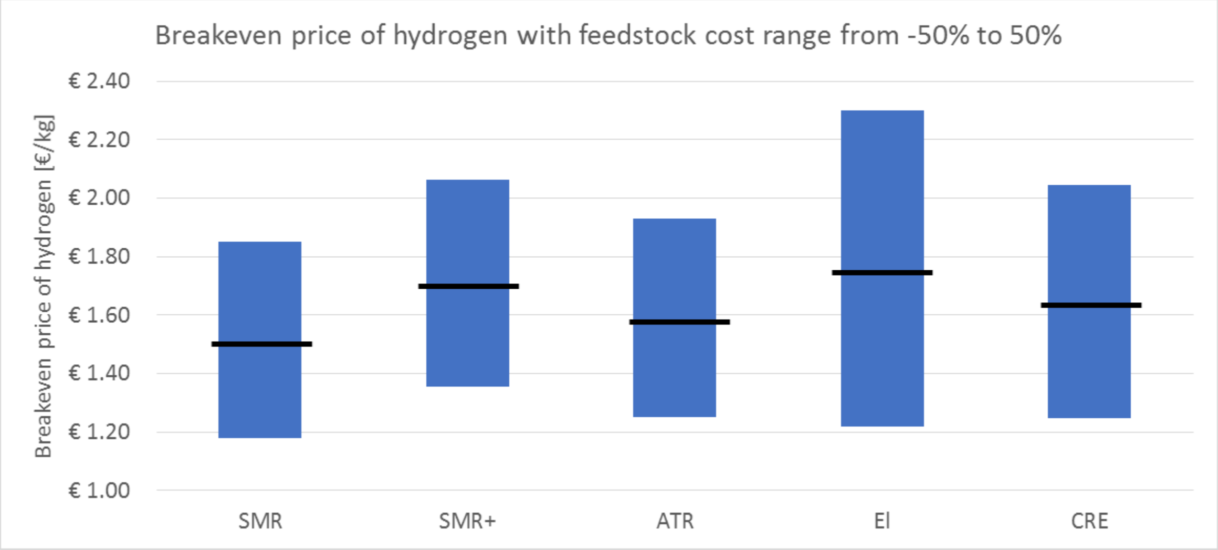

Figure 32 - Breakeven price of produced hydrogen, given natural gas and electricity prices fluctuate at the same rate

Figure 32 clearly shows that in a scenario where the cost of natural gas and electricity changes similarly, the reforming systems are more stable in the response, meaning higher risk for pure electrolysis. The price target of hydrogen for export was estimated to be 1-2 €/kg in order to be cost-competitive, as stated in Section 5.2. As can be seen from Figure 32, only SMR and ATR will produce hydrogen within this target range even with a natural gas price increase of 50%.

As the figures in this section show, CRE is never the most cost-efficient hydrogen production system. If the electricity price drops, electrolysis will be the preferable method. If the electricity price increases, natural gas reforming alone will be superior. The effect of natural gas price changes will be similar, with reforming methods dominating at low NG prices and electrolysis at high feedstock prices. Although never the best alternative, CRE is also never the worst, meaning that given future NG and electricity price fluctuations, CRE has a more stable response. This may reduce the risk of sudden price increases and is an important strength of the combination system.

5.7.3 Carbon Tax

With European politics focusing on effective measures to reduce emissions, it is natural to study the systems response to an increasing price of CO_2 emissions. The results of this sensitivity analysis, shown in Figure 33, is very interesting. First of all, a carbon price close to 60 €/tonneCO_2 is needed in order to make carbon-lean hydrogen cost-competitive with hydrogen from traditional SMR without CCS. That is a significant value, considering the current average carbon price in Europe is 7.7€/tonneCO_2. That is an 800% increase. Interestingly, the emission permits in Europe cost 30€/tonne of CO_2 equivalents in 2008 [44]. Another interesting result is that even with a carbon price of 100 €/tonne CO_2 SMR still produce hydrogen at a lower cost than electrolysis.

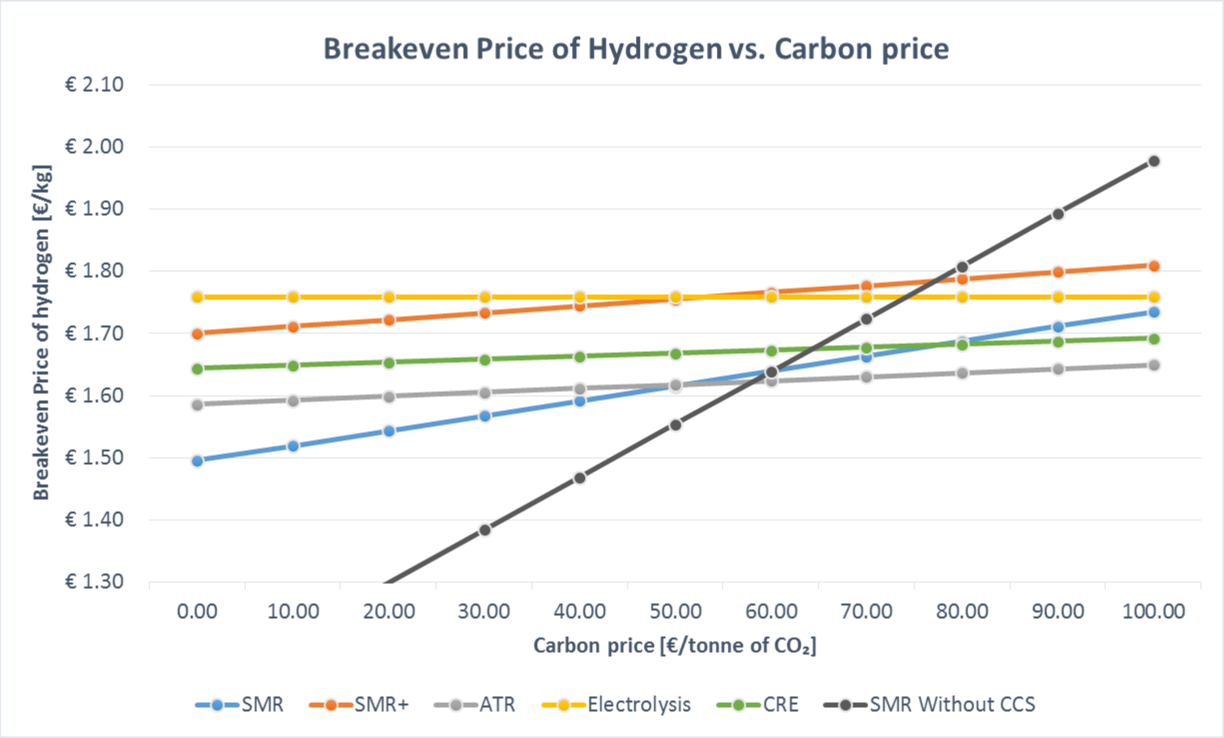

Figure 33 - Breakeven price of hydrogen vs. cost of CO_2 emissions. SMR without CCS is added in order to see how high the carbon price must be in order for carbon-lean hydrogen to be cost-competitive

5.7.4 System Design Variations

In this section, the specific competitiveness of individual systems will be analysed by changing key performance variables. First, a study of how the production volume affect the overall viability is presented. This is important for many reasons. If a large-scale production facility is to be made, a pilot project with lower production capacity is an effective way to reduce overall risk. Also, in order to determine which method to choose, the market demand is decisive. If the total demand will be 500 tonnes per day, five distributed electrolysis plants may be a better alternative than one large centralized SMR facility. By small, medium and large-scale production, 0-25, 25-100 and above 100 tonnes of hydrogen per day is used in this thesis, respectively.

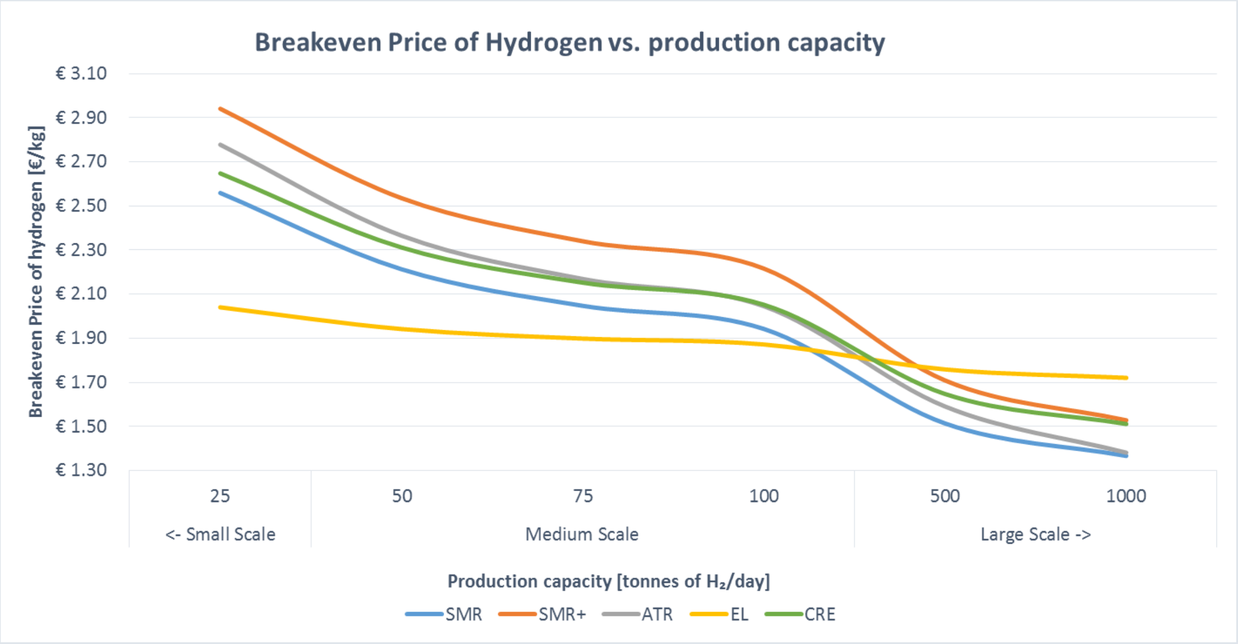

Figure 34 - Breakeven price of hydrogen vs. production capacity. Mind the change on the x-axis from 100 to 500 tonnes/day.

As Figure 34 clearly indicates, electrolysis is the best available option for small to medium scale carbon-lean hydrogen production. This is unexpected, based on the current production worldwide, but the main explanation is the low cost electricity available in Norway. Due to modularity, the scale effects of electrolysis are limited. The cost of electricity, on the other hand, has a large effect on the production cost, as seen in Figure 30. If the electricity price stays on the levels projected, electrolysis will be a favoured production method to supply most of the domestic demand. But only slight variations in the electricity price can change the overall picture.

Another interesting detail to read from Figure 34 is the relative cost difference of ATR and SMR. SMR is considered as the favourable method of hydrogen production from natural gas. The reason as to why is based on high conversion rates and the expensive oxygen production plant required by ATR. In large-scale operation, this relative investment cost difference diminishes due to economies of scale, improving the cost-competitiveness of ATR. Important, as it represents an alternative with 70% less CO_2 emissions.

Figure 35 shows how the energy efficiency of the electrolysis plant affect the breakeven price. The plant analysed in this thesis has a plant energy efficiency of 76%. Some improvements to the overall efficiency can be assumed due to research and development, but as can be seen from the figure it has to be close to the theoretical maximum in order to be the most cost efficient method for large-scale. Since the natural gas systems are mature technologies limited to incremental improvements as well, the overall system competitiveness will mainly be based on CAPEX level and feedstock costs in the near future.

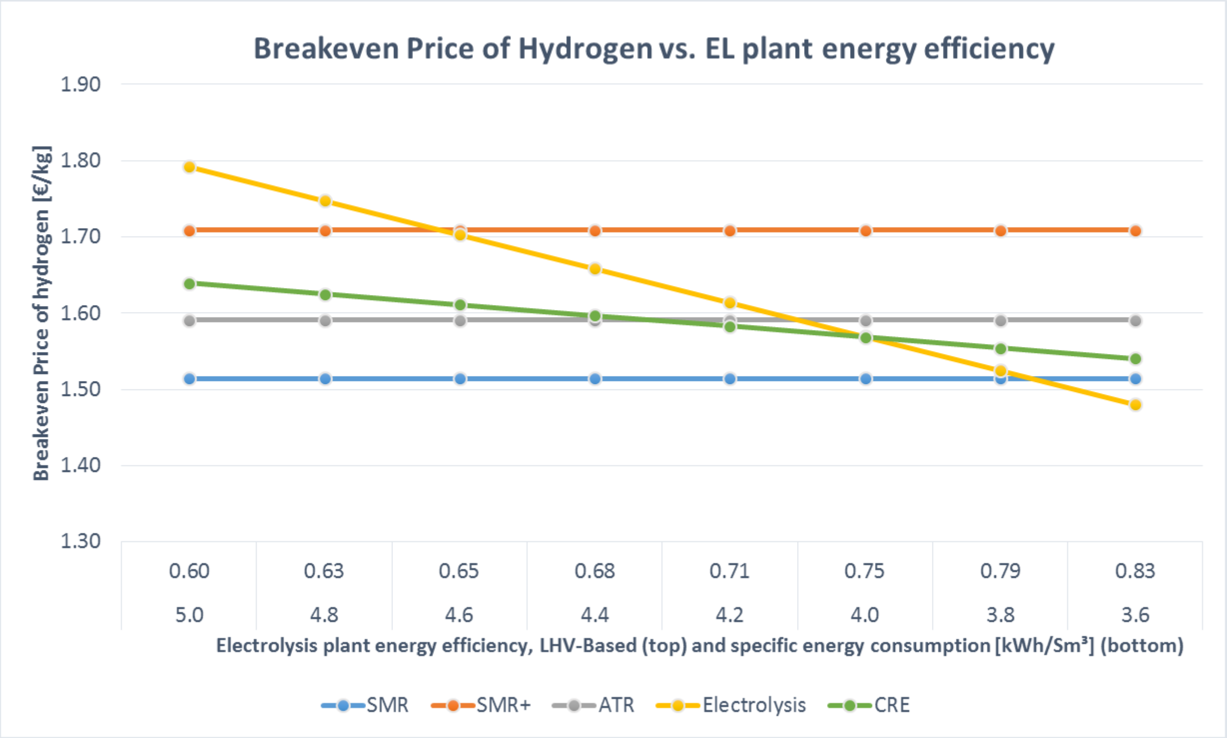

Figure 35 - Breakeven price of hydrogen vs. energy efficiency of the electrolysis plant.

5.7.5 Financial Market Changes

The financial markets are challenging to predict. Therefore, a display of how the breakeven price of hydrogen change with the overall financial situation is done. Figure 37 A and B show the results in a strict and in a calm financial market scenario, respectively. In a strict financial market, in this case defined with a discount rate of 15% due to high risk, a high OPEX to CAPEX ratio is preferred. This benefits electrolysis, which is more competitive here, than in the calm, low risk scenario.

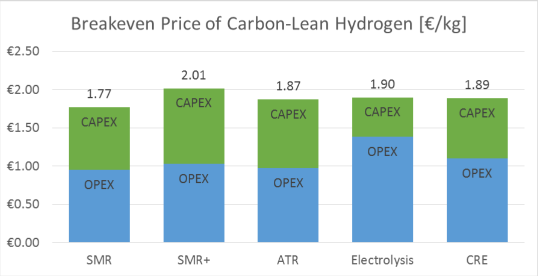

Figure 37 - Breakeven price of Carbon-lean Hydrogen. Strict financial market. 15% discount rate. 20 years lifetime

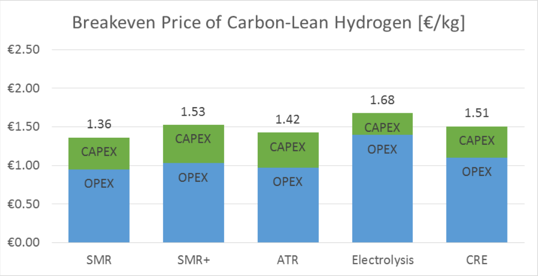

Figure 36 - Breakeven price of Carbon-lean Hydrogen. Calm financial market. 7% discount rate. 30 years lifetime

5.8 Techno-Economic Evaluation of Large-scale Hydrogen Production in Norway

Estimating which hydrogen production method is the most cost-efficient is difficult. As this thesis states carbon capture as a prerequisite for the broad acceptance of hydrogen as an energy carrier of the future, the decision is even more complicated. The two most important questions to answer in this section are: What is the cost of producing carbon-lean hydrogen in Norway, and what is the price premium of further reduced emissions?

Chapter 4 provides a thorough technical analysis of large-scale hydrogen production, showing benefits and disadvantages with the different systems available. Focusing on energy efficiency, natural gas consumption and carbon emissions, the analysis covers the important factors in a choice of technology. As can be seen in Chapter 4, ATR and SMR are the leading technologies with regards to plant energy efficiency. It is important to highlight the limitations of steady state simulations like the ones performed in this thesis, but the results enable comparison and provide preliminary estimations.

Given the feedstock prices used in this thesis, the breakeven price of hydrogen, in a 500 tonnes/day facility, ranges from 1.51 €/kg with SMR, to 1.76 €/kg with electrolysis. For production capacities below around 150 tonnes/day, electrolysis is preferred. An interesting result is the small deviation in the production cost of the different methods. One can assume that a benchmark cost of hydrogen produced under normal, Norwegian conditions will be in this range. This assumption is also strengthened by the comparison with the H2A report in Section 5.5. In Section 5.2, a price target between 1 and 2 €/kg was defined as a prerequisite for economic viability in an export scenario. This thesis shows that hydrogen produced from natural gas, electrolysis or a combination all meet the cost target.

Carbon-lean hydrogen can be produced large-scale in Norway at a breakeven price of 1.50-1.75 €/kg

As can be seen below in

Table 30, even with equal emission levels, SMR has the lowest production cost. However, the difference to ATR is barely 2 percent, meaning ATR could very well prove to be better. Since the current estimated production cost of carbon-lean hydrogen from ATR and SMR are close to identical, it is not possible to conclude with a preferred method. An argument in the favour of ATR is the opportunity to increase the CCS rate.

Table 30 - Key figures from the technical and financial analyses.

KEY FIGURES IN THIS Thesis						
	Unit	**SMR**	**SMR+**	**ATR**	**Electrolysis**	**CRE**
Production Technology:		Steam methane Reforming	Steam methane reforming	Autothermal reforming	Alkaline electrolysis	Combined autothermal reforming and electrolysis
H_2 Production rate:	kg/day	500 000	500 000	500 000	500 000	500 000
Annual Consumption of Natural Gas:	Sm^3/day	78 826	82 844	76 776	-	55 630
Grid Power demand:	MW	15	19	43	962	349
Total Plant energy efficiency (LHV-based):		82%	78%	82%	62%	74%
Electricity price:	€/MWh	20.03	20.03	20.03	20.03	20.03
Natural gas price:	€/Sm^3	0.17	0.17	0.17	0.17	0.17
Total CAPEX:	M€	889.0	1071.0	972.4	582.8	860.4
Total OPEX:	M€	164.6	178.5	168.9	240.9	191.0
Breakeven Price of hydrogen:	**€/kg**	**1.51**	**1.71**	**1.59**	**1.76**	**1.65**
CO_2 Emissions:	Tonnes of CO_2 per day	1 198	547	318	-	244
CO_2 Stored:	Tonnes of CO_2 per day	3 047	3 913	3 816	-	2 752
Price premium of CCS:	€/kg H_2	0.32	0.38	0.37	-	0.30
Specific cost of CCS:	€/kgCO_2	0.053	0.049	0.048	-	0.055

Many factors will affect the real price of hydrogen production, like government subsidies, quote and the chosen company's technological history. The most important result of this thesis is to show that there are viable alternatives to produce carbon-lean hydrogen in Norway, either from natural gas, electrolysis or in combination. In an unstable energy market, with large variations in feedstock costs, the combined reforming and electrolysis method can prove effective. As well as it provides a good opportunity for technology development in a variety of areas.

In order to minimize carbon footprint, ATR, CRE or pure electrolysis represents the best solutions. Although SMR represents a solution with more CO_2 emissions, given no post combustion CCS, it will also contribute to a significant emission reduction in the energy value chain. ATR has a high flexibility with regards to CCS capacity, enabling an impressive 92% capture rate solely with pre-combustion, and still proving economically viable. The price premium of carbon capture is lowest in SMR, as seen in Table 30, but that is the result of limited capture. A levelized cost of 0.048 € per kg of captured CO_2 in ATR proves the effectiveness hydrogen represents as a mean to cut emissions. And that value does not include the avoided CO_2 the use of hydrogen would imply if replacing other energy carriers.

6 A Case Study Approach to Hydrogen Production Combining Gas Reforming and Electrolysis

To this point, the thesis has presented and evaluated different systems for large-scale hydrogen production, both technically and economically. The results indicate that both SMR and ATR are cost-efficient hydrogen production methods in a future, carbon-lean energy system. With this taken into consideration, the breakeven price of CRE is not significantly higher than ATR, 1.65 €/kgH_2 to 1.59€/kgH_2. Further, the sensitivity analysis demonstrates that CRE is less responsive to changes in energy input costs, compared to either pure ATR or pure EL. As Figure 30 shows, at a grid electricity price below approximately 16 €/MWh, CRE is less expensive than ATR. Therefore, this chapter will evaluate the potential for CRE to reduce the electricity cost, by utilizing excess wind power, and thus become a more cost-efficient alternative than ATR.

Due to the available natural gas from the Heidrun gas field and the recent confirmation of Statkraft plans for the biggest wind farm in Europe, located around Fosen and Snillfjorden [45], Mid-Norway was chosen as the case location in this study. Here, stranded natural gas, abundant wind resources and available carbon storage alternatives create one of the most advantageous locations for large-scale hydrogen production in Norway.

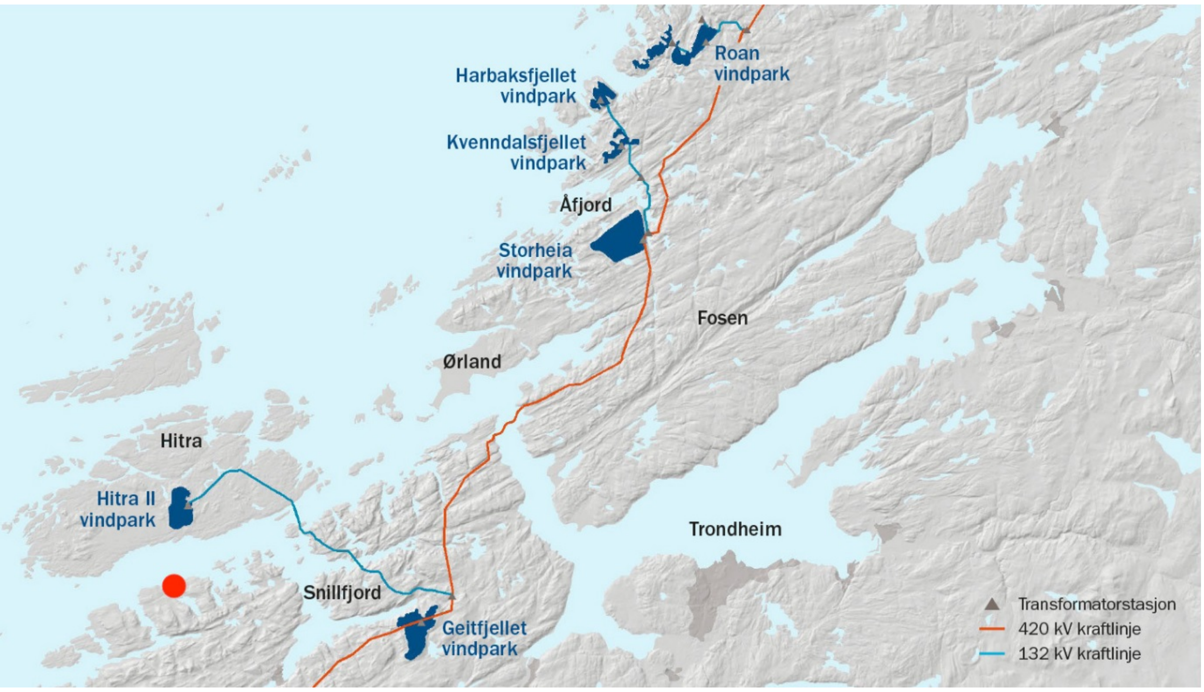

Figure 38 - The map shows the location of the Fosen/Snillfjorden wind farms. The red dot marks the location of Tjeldbergodden Industrial Complex and the Heidrun gas-receiving terminal. Photo: Statkraft [45].

Hydrogen storage has not been included, specifically, in both the technical and financial analysis of these cases, due to the use of the models evaluated in Chapter 4 and 5, but the implications of hydrogen storage is discussed in the end of this chapter.

Following, two sets of cases will be evaluated; a set of stationary production cases and a set of fluctuating production cases. The stationary cases will provide the reference values in order to measure the potential gain of allowing fluctuations. The only feedstock boundary of the case studies is the capacity of natural gas from the Heidrun field available. Power demand beyond the capacity of the wind farm will be supplied by the grid.

6.1.1 Tjeldbergodden Industrial Complex

Tjeldbergodden industrial complex consists of three parts; a natural gas receiving terminal from the Heidrun field, a methanol plant and an air separation facility [46]. Tjeldbergodden has an annual production capacity of approximately 900 000 tonnes of methanol, an impressive 25% of the total European capacity. An important factor for choosing this location for the case study is the existing syngas production already in operation. The methanol plant utilizes a two-step reforming benefitting from both the cost-efficiency of SMR, as well as the flexible H_2/CO ratio of ATR [47]. The processing facility at Tjeldbergodden is not utilizing the full NG capacity of the Haltenpipe pipeline from Heidrun. The maximum NG capacity is 7 MSm^3/day where approximately 2.2 MSm^3/day are used in the methanol plant [48] [20]. Hence, around 4.8 MSm^3/day potential capacity is available for other use.

6.1.2 Fosen and Snillfjorden Wind Farm

In 2020, the largest onshore wind project in Europe will be in operation. Distributed at six locations along the coast of Mid-Norway, the Fosen and Snillfjorden wind farm will represent an installed capacity of 1000.8 MW, delivered by 278 individual 3.6 MW wind turbines [45]. The total scheduled production is 3400 GWh, implying a capacity factor of 0.388 [49].

6.2 Stationary Production

6.2.1 Stationary Case 1, Natural Gas-based Co-production of Hydrogen:

Stationary case 1 will use the maximum available NG at Tjeldbergodden in the hydrogen production. Using the CRE system, additional hydrogen is produced by electrolysis, while providing the required oxygen to the reformer. In this case study, all power will be supplied by the grid, at the average electricity price used throughout the thesis. The results of the study are listed in Table 31.

Table 31 - Stationary case 1 results. The full natural gas capacity is used, with electrolysers supplying oxygen as well as producing additional hydrogen

Stationary case 1	Value	Unit
Natural gas demand:	4.8	MSm^3/day
Natural gas available:	4.8	MSm^3/day
Design capacity electrolysis:	1117	MW
Annual Average capacity wind farm:	388	MW
Maximum capacity wind farm:	1000.8	MW
Operating days:	347	Days/Year
Natural gas price:	0.17	€/Sm^3
Electricity price:	20.03	€/MWh
H_2 produced by electrolysis:	497	Tonnes/day
H_2 produced by ATR:	1301	Tonnes/day
Total hydrogen production:	1798	Tonnes/day
Total CAPEX:	2262.8	M€
Total OPEX:	638.5	M€
Breakeven price of hydrogen:	1.42	€/kgH_2
Specific production cost from electrolysis:	1.76	€/kgH_2

As Table 31 shows, the available natural gas at Tjeldbergodden enables a production of 1800 tonnes of hydrogen/day. This results in a breakeven price of 1.42 €/kg of hydrogen, a 15% reduction from the capacity evaluated in Chapter 5. Since the limited NG enables CRE to produce additional hydrogen compared to reforming alone, the potential for CRE to achieve lower production cost exists. Table 32 shows that this is not the case. Even with lower production capacity, ATR is even better relative to CRE, compared to results in Chapter 5. Hence, CRE would not be the preferable alternative for stationary production of this size.

Table 32 - Stationary case 1: Benchmark breakeven price of hydrogen production, given the same feedstock demands

	SMR	ATR	Unit
Hydrogen produced:	1268	1303	Tonnes/day
Breakeven price:	1.33	1.33	€/kg

This case study shows that the NG available at Tjeldbergodden is sufficient to supply a considerable future hydrogen market, with almost three times the NG required of the systems in Chapter 4 and 5. Although an unrealistic production capacity, the result demonstrates the vast potential of the energy resources available in this geographical area.

6.2.2 Stationary Case 2, Wind-based Co-production of Hydrogen:

An alternative to case 1 is to design the production based on the annual average power production from the Fosen/Snillfjorden wind farm. When finalized, the total wind power capacity will be 1000 MW. With an estimated capacity factor of 0.388, the average annual power production is 388MW, which will be the design capacity of the electrolysis plant in this case study. As in stationary case 1, all electricity will be supplied by the grid, at the average electricity price. The oxygen produced will be the design parameter for the autothermal reforming plant part of the production.

Table 33 - Stationary case 2 results. The system is designed based on the annual average power supply from the wind farm. The parallel ATR system is designed based on the produced oxygen.

Stationary case 2	Value	Unit
Natural gas demand:	1.67	MSm^3/day
Natural gas available:	4.8	MSm^3/day
Design capacity electrolysis:	388	MW
Annual Average capacity wind farm:	388	MW
Maximum capacity wind farm:	1001	MW
Operating days:	347	Days/Year
Natural gas price:	0.17	$€/Sm^3$
Electricity price:	20.03	€/MWh
H_2 produced by electrolysis:	173	Tonnes/day
H_2 produced by ATR:	452	Tonnes/day
Total hydrogen production:	625	Tonnes/day
Total CAPEX:	1017.4	M€
Total OPEX:	233.3	M€
Breakeven price of hydrogen:	1.59	$€/kgH_2$
Specific production cost form ATR	1.50	$€/kgH_2$
Specific production cost from electrolysis:	1.83	$€/kgH_2$

Table 33 presents the results from the case study. The breakeven price of CRE with these boundary conditions is 1.59 €/kgH_2, which is close to the values of SMR and ATR using the same NG feed, seen in Table 34. The specific production cost of the hydrogen produced by electrolysis is 1.83 €/H_2, highlighting the relative cost-difference of ATR and EL in the combination system. 1.59 €/kgH_2 is the reference price used in the fluctuating cases of Section 6.3.

Table 34 - Stationary case 2: Benchmark breakeven price of hydrogen production, given same feedstock demands

	SMR	ATR	Unit
Hydrogen produced:	440	452	Tonnes/day
Breakeven price:	1.53	1.56	€/kg

6.3 Fluctuating Production:

An alternative to the stationary case 2 is to let the electrolysis part of the total production be dependable on the available wind power supplied by the Fosen/Snillfjorden wind farm. In other words, design the electrolysers such that the process is able to utilize periods of strong winds and hence potentially lower electricity prices. This will on the other hand increase the CAPEX of the electrolysers due to required increase in the electrolyser production capacity. The study does not take into account the challenges of fluctuation in real time operation, but examines the overall economic viability of such a system in terms of increased CAPEX versus reduced cost of electricity.

The ATR part of the CRE system is in all the fluctuating cases assumed to produce hydrogen at a constant rate, and cases will produce the same total amount of hydrogen as the stationary case 2. It is reasonable to assume a lower electricity price when utilizing excess power from the wind farm, but the exact value is hard to predict. Therefore, the electricity price required for the breakeven price to reach the reference price from stationary case 2, 1.59 €/kgH_2, is estimated.

6.3.1 Fluctuating Case 1: Partly Flexible Electrolysis

This case enables the production facility to utilize some of the excess wind power when demand is low, but limits the installed electrolyser capacity to 600 MW, approximately 60 percent of the maximum wind power capacity. The results of this case study are listed in Table 35.

Table 35 - Fluctuating case 1: Partly flexible electrolysis with an electrolysis capacity of 600MW. Highlights from the simulation is presented here. Showing the Breakeven price of the hydrogen produced as well as the required electricity price to equal the reference price of stationary case 2.

	Value	Unit
Electrolyser design capacity:	600	MW
Electrolyser design production capacity:	267	Tonnes/day
Average H_2 produced by electrolysis:	173	Tonnes/day
Operating days:	347	Days/year
EL price:	20.03	€/MWh
Result:		
Breakeven price of hydrogen:	1.67	€/kgH_2
Specific production cost from ATR:	1.50	€/kgH_2
Specific production cost from electrolysis:	2.11	€/kgH_2
Wind power supply factor[34]:	0.81	
Electricity price to reach reference price:	14.75	€/MWh
Electricity price to reach the ATR breakeven price of 1.53 €/kgH_2:	10.77	€/MWh

As can be seen from Table 35, the breakeven price of this case design is 1.67 €/kgH_2, given the average electricity price used in this thesis. In order to achieve a breakeven price equal to the reference price in stationary case 2, an electricity price of 14.75 €/MWh is necessary. Whether or not this price is achievable is hard to predict, but in order for the CRE system to be less expensive than ATR, the electricity price must be lower than this value.

The wind power supply factor is 0.81, which means that 81% of the annual required power in the electrolysis plant is directly supplied by the wind farm. The wind data used to calculate the wind power supply factor is presented in Appendix C. The remaining 19% of the power produced by the wind farm is delivered to the grid, while the grid distributes this same amount of the power to the electrolysers in periods of calm weather.

6.3.2 Fluctuation Case 2: Flexible Electrolysis.

This case study evaluates the scenario where the electrolysis plant is designed to meet the full capacity of the wind farm. Such a high capacity implies a significant increase in CAPEX, but enables the plant to

---

[34] The wind power supply factor is the power directly supplied by the wind farm, divided by the total power demand of the electrolysis plant. The wind data used to calculate the wind power supply factor is presented in Appendix C.

leverage on all the available low-cost electricity in periods of relatively high supply. Table 36 shows the results of the case study.

Table 36 - Fluctuating case 2: Flexible electrolysis, with capacity of 1000MW. Highlights from the simulation is presented here. Showing the Breakeven price of the hydrogen produced as well as the required electricity price to equal the reference price of stationary case 2.

	Value	Unit
Electrolyser design capacity:	1000.8	MW
Electrolyser design production capacity:	445	Tonnes/day
Average H_2 produced:	173	Tonnes/day
Operating days:	347	Days/year
EL price:	20.03	€/MWh
Result:		
Breakeven price of hydrogen:	1.81	€/kgH_2
Specific production cost from ATR:	1.50	€/kgH_2
Specific production cost from electrolysis:	2.63	€/kgH_2
Wind power supply factor[35]**:**	1	
Electricity price to reach reference price:	5.24	€/MWh
Electricity price to reach the ATR breakeven price of 1.53 €/kgH_2:	1.26	€/MWh

As seen in Table 36, the breakeven price is 1.81 €/kgH_2 if using the original electricity price. Since this case utilizes the full capacity of the wind farm, the maximum possible reduction in the electricity price is achieved. The electricity price required to reach the reference price of 1.59 €/kgH_2 is estimated to be 5.24 €/MWh, a 74% reduction from the original grid electricity price.

6.4 Is Combined Reforming and Electrolysis a Competitive Solution?

This chapter evaluates whether or not the CRE system can utilize excess wind power to reduce the electricity cost and thus become more cost-efficient than ATR. The results in Chapters 4 and 5 indicate that producing hydrogen exclusively from natural gas reforming constitutes the most economically viable business cases. This section will discuss whether or not the results of the case studies provide a different conclusion.

---

[35] The wind power supply factor is the power directly supplied by the wind farm, divided by the total power demand of the electrolysis plant. The wind data used to calculate the wind power supply factor is presented in Appendix C.

The stationary case 1 shows that the energy resources available at Tjeldbergodden are sufficient for large-scale production of hydrogen, with the feedstock to produce around 1300 tonnes of hydrogen/day using ATR.

As seen in Figure 39 the wind power supply factor is 0.81 for the 600MW fluctuating case. Since the cost of intermediate oxygen and hydrogen storage is not taken into account in this study, the stationary case 2 is equivalent to a fluctuating case with a 388MW electrolyser capacity, providing a wind power supply factor of 0.73. Hence, an 11% increase in the wind power supply factor will need to provide a 25% electricity price reduction to equal stationary CRE (from 20.03 to 14.75 €/MWh).

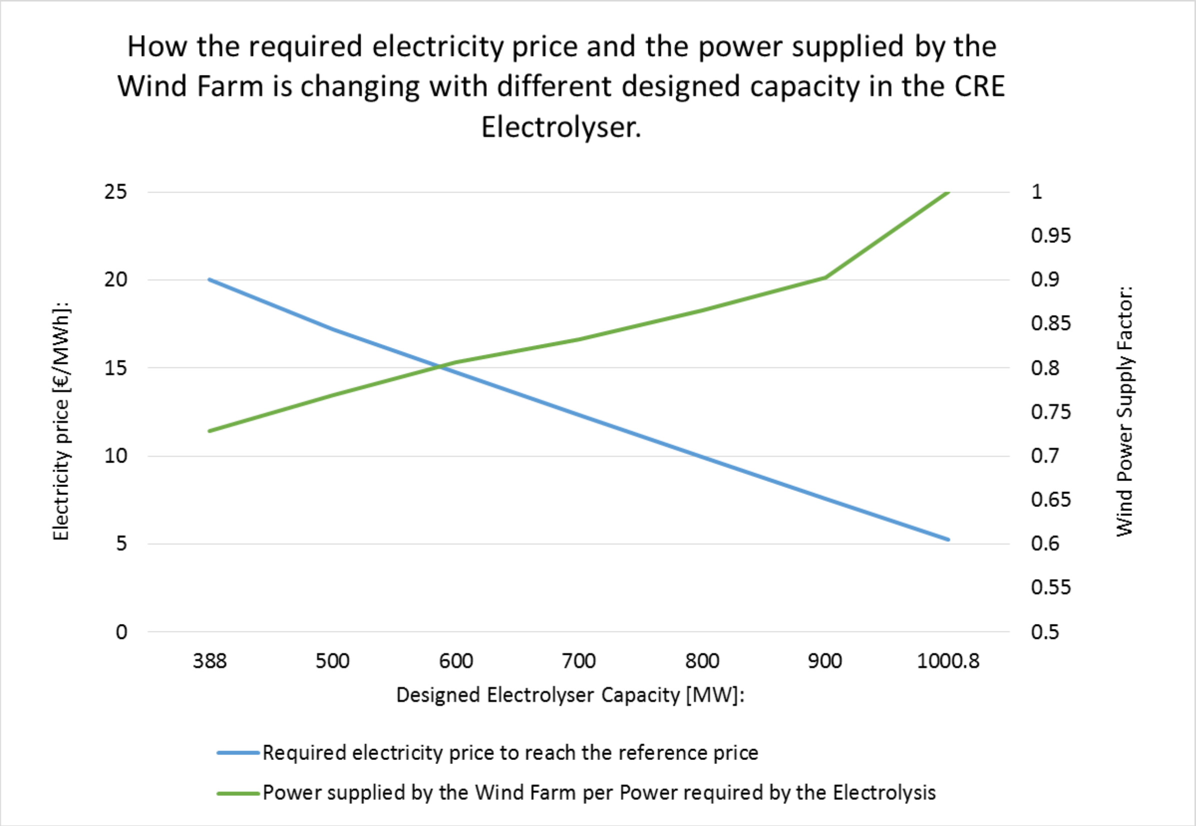

Figure 39 - Graph showing how the electricity price required to reach the reference price and the power supplied by the wind farm are affected by changes in the designed electrolyser capacity.

Most importantly, the results from the case studies show that a CRE system designed to utilize excess wind power will need significant reductions in electricity price in order to be cost-competitive. If the system is designed for the maximal capacity of the wind farm, the electricity price has to be reduced by almost 75% (from 20.03 to 5.24 €/MWh), only to achieve the same breakeven price as stationary CRE. This relation is presented in Figure 39. In order to reach the breakeven price of ATR, the required electricity price is 1.26€/MWh, a reduction of 94%. Therefore, the results of the case studies indicate that, given the boundary conditions in this thesis, a combined electrolysis and reforming (CRE) system utilizing excess wind power is not likely to be cost-competitive with either stationary CRE powered by the grid or traditional reforming.

It is important to highlight that the estimated electricity price reductions do not include the cost of intermediate oxygen and hydrogen storage required in the fluctuating production facilities. The constant natural gas reforming occurring simultaneously, demands a steady flow of oxygen, which implies a need for a storage system. This would increase the cost even further making the fluctuating cases even less viable.

7 Conclusion

Hydrogen is a promising energy carrier with the potential to reduce CO_2 emissions from fossil resources, integrate renewables with society and replace fossil fuels in the transportation sector. The idea of a hydrogen-based energy chain is not new, but with recent developments in renewable industries and political support, the conditions are improving significantly.

This thesis provides a technical and a financial analysis of available, mature systems capable of large-scale operation, in order to evaluate the potential of large-scale production of hydrogen in Norway. It is difficult to provide general conclusions to business cases with such uncertain boundary conditions, especially with regards to feedstock cost and market development, but based on the assumptions thoroughly stated through the thesis, the following points summarize the key findings.

Key findings in the thesis:

- *ATR and SMR are the most energy efficient alternatives for carbon-lean hydrogen production, both with a plant energy efficiency of 82%. ATR has the most potential of further emission reductions.*

- *SMR is the most cost-efficient method for large-scale operation in Norway, producing carbon-lean hydrogen at a breakeven price of 1.51 €/kg in a 500 tonnes/day facility*

- *The price premium of 72% reduction in CO_2 emissions using SMR with CCS is 0.32 €/kg H_2. Compared to SMR, ATR represents an additional cost of 0.08€/kg H_2 in order to further reduce the CO_2 emissions with 70%.*

- *Given the assumed feedstock prices, electrolysis is the most cost-efficient alternative for production rates up to around 150 tonnes of hydrogen per day, while SMR is the best alternative for large-scale production.*

- *Combined electrolysis and reforming (CRE) is not likely to become the most cost-efficient alternative, but is less sensitive to variations in feedstock costs.*

- *The results of the case studies indicate that, given the boundary conditions in this thesis, a combined electrolysis and reforming (CRE) system utilizing excess wind power is not likely to be cost-competitive with either stationary CRE powered by the grid or traditional reforming.*

Five systems were fully evaluated in this thesis: SMR, SMR+, ATR, Electrolysis and CRE. All proved to be economically viable for domestic consumption as well as for export scenarios, given the assumed cost level. Due to key technical factors not simulated and lack of financial data, POX was not included in the financial analysis. Electrolysis is the only zero emission alternative evaluated, and it proves superior in small to medium scale production plants up to 150 tonnes of hydrogen per day, given that the price of electricity and natural gas remains at the level used in this thesis.

A case study of hydrogen production using the combined reforming and electrolysis (CRE) system at Tjeldbergodden was conducted. The results showed that the energy resources available is enough to produce 1800 tonnes per day. A more important result from the case studies was that utilizing excess power from a wind farm is not likely to reduce the electricity cost sufficiently in order to be economically viable.

The results of this thesis indicate that hydrogen production can utilize the vast energy resources and CCS possibilities in Norway to create viable, low-carbon energy value chains.

8 Proposals for Further Work

Multiple large-scale hydrogen production plants exist around the world today, but the combination of low-cost resources in Norway as well as a focus on minimizing CO_2 emissions creates new challenges. The motivation for this thesis was the opportunity of refining Norwegian resources to create low-emission value chains and in order for that to become a reality, significant research remains. In the case of small-scale production intended for domestic consumption, the required technologies exist today, although the market is yet to develop. For large-scale production intended for export, storage and transportation technologies are under development, but they still require considerable attention.

This section will provide specific proposals for further research in two categories: One group of specific areas within the production process, which require in-depth research or cost-estimation, and one group of areas within the export value chain.

8.1.1 Proposals for further research within the hydrogen production processes:

- **Process control and off-design analysis.** This thesis assumes a base case reliability of 95%, meaning that the plant operates at full capacity 347 days of the year. Both reactor temperature and steam-to-carbon ratio requires intelligent control systems in order to operate optimally. How does the system operate in off-design conditions? Transient operation may also occur, especially due to the direct connection to the gas-receiving terminal. How can the system handle start and stop?

- **Batch process simulation**. The connection between the carbon absorption column and the PSA, both batch processes, is not simulated in this thesis. Both systems are assumed “black boxes” with a base-case 95% recovery rate in the absorption and 90% in the PSA. These systems are very important in order to provide high capture and high yield. Deviations from the base case will result in large response in the business case.

- **Production design, sizing and planning.** Detailed cost-estimation of the entire facility and evaluation of possible policy support and governmental subsidies. An export focus seems most viable, resulting in the need for inclusion of a liquefaction plant, storage and an offloading terminal. All of which include developing technologies.

- **Demo plant.** Construction of a demo facility can to provide key operational experience and reduce the risks related to full-scale operation. Combined with the fuelling of a ferry or in cooperation with ATB in Mid-Norway, this could also assist in the pursuit of further industrial and governmental support.

8.1.2 Proposals for research within the export value chain:

- **Hydrogen storage and transportation.** Several studies on different technologies and methods for hydrogen storage and transportation have been conducted, but a well structured overview of the alternatives is difficult to apprehend. In the case of Norwegian export, SINTEF conducted a paper in 2008, which can be used as inspiration. One goal can be to perform a techno-economic analysis in order to benchmark the cost of storage and transport from Norway to Europe or Japan. Another can be a more detailed technical study of the different alternatives, estimating energy efficiencies, carbon footprint, viability and optimization.

- **Market study of future hydrogen consumption in Norway.** Although transportation is the most visible future consumer through media, the annual, industrial demand for hydrogen was more than 50 million worldwide in 2015, emitting more than 500 million tonnes of CO_2. Projects like Tizir smelting plant in Tyssedal is an example of emerging potential hydrogen demand in the Norwegian industry as well. A study of the existing industrial hydrogen demand in Norway, as well as estimating a future carbon-lean hydrogen demand can be an important part of the development of production technology in the years to come.

References

[1] IEA, “Technology Roadmap - Hydrogen and Fuel Cells,” OECD/IEA, 2015.

[2] Global CCS Institute, “www.globalccsinstitute.com,” 17 12 2015. [Online]. Available: http://www.globalccsinstitute.com/projects/sleipner%C2%A0co2-storage-project. [Accessed 10 06 2016].

[3] Global CCS Institute, “www.globalccsinstitute.com,” 17 12 2015. [Online]. Available: http://www.globalccsinstitute.com/projects/sn%C3%B8hvit-co2-storage-project. [Accessed 10 06 2016].

[4] K. Liu, C. Song and V. Subramani, Hydrogen and Syngas Production and Purification Technologies, USA: Wiley, 2010.

[5] J. Dunleavy, “Sulfur as a Catalyst Poison,” Johnson Matthey, Billingham, 2006.

[6] J. C. Molburg and D. R. D., “Hydrogen from Steam-Methane Reforming with CO2 Capture,” Annual International Pittsburgh Coal Conference, Pittsburgh, 2003.

[7] ThyssenKrupp Industrial Solutions, “Thyssenkrupp-industrial-solutions.com,” 2016. [Online]. Available: http://www.thyssenkrupp-industrial-solutions.com/fileadmin/documents/brochures/uhde_brochures_pdf_en_7.pdf. [Accessed 2016].

[8] M. Voldsund, K. Jordal and R. Anantharaman, “Hydrogen production with CO2 capture,” Science Direct .

[9] International Energy Agency, “Hydrogen Production & Distribution,” IEA Energy Technology Essentials, 2007.

[10] IEA Greenhouse - "SMR, POX and ATR", “ieaghg.org/,” March 2015. [Online]. Available: http://www.ieaghg.org/docs/General_Docs/IEAGHG_Presentations/18_-_S._Santos_IEAGHGSECURED.pdf. [Accessed 07 Des 2015].

[11] A. Smith and J. Klosek, “A review of air separation technologies and their integration with energy conversion processes,” *Fuel Processing technology 70,* 2001.

[12] R. Chaubey, S. Satanand, O. J. Olusola and M. Sudip, “A review on development of industrial processes and emerging techniques for production of hydrogen from renewable and sustainable sources,” Renewable and Sustainable Energy Reviews - Elsevier, 2013.

[13] D. Berstad, R. Anantharaman and P. Nekså, “Low-Temperature CO2 capture technologies - Applications and potential,” SINTEF Energy Research, Trondheim, 2013.

[14] Statoil, “Statoil.com,” 10 12 2013. [Online]. Available: http://www.statoil.com/no/TechnologyInnovation/NewEnergy/Co2CaptureStorage/Pages/default.aspx. [Accessed 15 03 2016].

[15] Miljødirektoratet, “Miljøstatus.no,” [Online]. Available: http://www.miljostatus.no/tema/klima/norske-klimagassutslipp/co2-utslipp/. [Accessed 2016].

[16] Sintef, NTNU, “Nasjonale rammebetingelser og potensial for hydrogensatsingen i Norge,” Sintef, 2016.

[17] K. H. Storaker and A. Goodwin, “Hydrogen in the Maritime Sector,” Norwegian School of Economics, Bergen, 2015.

[18] Sysla Grønn, “Syslagronn.no,” 2015. [Online]. Available: http://syslagronn.no/2015/10/16/syslagronn/startskudd-for-storskala-hydrogenproduksjon_64587/. [Accessed 2016].

[19] L. Nohrstedt, “nyteknik.se,” 04 04 2016. [Online]. Available: http://www.nyteknik.se/energi/nya-satsningen-stal-utan-kol-6537738. [Accessed 23 05 2016].

[20] V. Åtland and D. Jakobsen, “Value chains for hydrogen export from Norway,” NTNU, Trondheim, 2015.

[21] New Energy World, “Generic estimation scenarios of market penetration and demand forecast for “premium” green hydrogen in short, mid and long term,” 2015.

[22] Kawasaki Heavy Industries, “Feasibility Study of CO2 free hydrogen chain,” Kawasaki, 2012.

[23] EEA, “eea.europa.eu,” 14 12 2015. [Online]. Available: http://www.eea.europa.eu/data-and-maps/indicators/transport-final-energy-consumption-by-mode/assessment-5. [Accessed 15 12 2015].

[24] Statistisk sentralbyrå, “ssb.no,” 09 02 2015. [Online]. Available: https://www.ssb.no/energi-og-industri/statistikker/elektrisitet/maaned/2015-02-09. [Accessed 15 12 2015].

[25] Green car congress, “www.grenncarcongress.com,” 14 03 2016. [Online]. Available: http://www.greencarcongress.com/2016/03/20160314-khi.html. [Accessed 30 05 2016].

[26] Toyota, “2016 Toyota Mirai Product Information,” Toyota, 2015.

[27] SSB, “SSB.no,” 22 04 2016. [Online]. Available: https://www.ssb.no/transport-og-reiseliv/statistikker/klreg/aar/2016-04-22. [Accessed 22 05 2016].

[28] Linde Kryotechnik, “Enhanced Cryogenic Air Separation,” Linde Group, 2009.

[29] NEL Hydrogen, “Efficient electrolysers for hydrogen production,” Nel-Hydrogen AS, Notodden, 2016.

[30] SSB, “SSB.no,” 06 05 2015. [Online]. Available: https://www.ssb.no/energi-og-industri/statistikker/energiregn/aar-forelopige/2015-05-06. [Accessed 12 05 2016].

[31] T. Ramsden, D. Steward and J. Zuboy, “Analyzing the Levelized cost of Centralized and Distributed Hydrogen Production Using the H2A production Model, Version 2,” National Renewable Energy Laboratory, Virginia, 2009.

[32] Norges Bank, “Norges-bank.no,” 06 06 2016. [Online]. Available: http://www.norges-bank.no/Statistikk/Rentestatistikk/Statsobligasjoner-Rente-Arsgjennomsnitt-av-daglige-noteringer/. [Accessed 06 06 2016].

[33] Damodoran Online, “pages.stern.nyu.edu,” 05 01 2015. [Online]. Available: http://pages.stern.nyu.edu/~adamodar/New_Home_Page/datacurrent.html. [Accessed 09 05 2016].

[34] Statoil ASA, “Statoil.com,” 01 10 2015. [Online]. Available: http://www.statoil.com/no/InvestorCentre/AnalyticalInformation/InternalGasPrice/Pages/default.aspx. [Accessed 09 12 2015].

[35] Nasdaq, “nasdaqomx.com,” 13 05 2016. [Online]. Available: http://www.nasdaqomx.com/commodities/market-prices. [Accessed 13 05 2016].

[36] Statnett, “www.statnett.no,” 25 09 2015. [Online]. Available: http://www.statnett.no/Drift-og-marked/Nettleie-og-tariffstrategi/Tariffer-i-sentralnettet/. [Accessed 20 05 2016].

[37] U.S. Department of Energy, “Analysis of Natural Gas-to Liquid Transportation Fuels via Fischer-Tropsch,” DOE, 2013.

[38] NEL-Hydrogen, “50 MW Hydrogen Plant,” NEL-Hydrogen AS, Notodden, 2016.

[39] Norges Miljøverndirektorat, “miljodirektoratet.no,” [Online]. Available: http://www.miljodirektoratet.no/no/Tema/klima/CO2-priskompensasjon/Kvotepris-for-stottearet-2014/. [Accessed 30 05 2016].

[40] Coin News media group LLC, “usinflationcalculator.com,” 17 05 2016. [Online]. Available: http://www.usinflationcalculator.com. [Accessed 21 05 2016].

[41] European Commission - "Reducing CO2 emissions from passenger cars", “ec.europa.eu,” 10 12 2015. [Online]. Available: http://ec.europa.eu/clima/policies/transport/vehicles/cars/index_en.htm. [Accessed 17 12 2015].

[42] Eurelectric and VGB, “Efficiency in Electricity Generation,” Eurelectric & VGB, 2003.

[43] Statistisk Sentralbyrå, “ssb.no,” 31 05 2016. [Online]. Available: http://www.ssb.no/elkraftpris. [Accessed 04 06 2016].

[44] Reuters, “Reuters.com,” 04 05 2016. [Online]. Available: http://www.reuters.com/article/europe-carbon-germany-idUSL5N181906. [Accessed 30 05 2016].

[45] Teknisk Ukeblad, “www.tu.no,” 23 02 2016. [Online]. Available: http://www.tu.no/artikler/na-skjer-det-europas-storste-vindkraftanlegg-bygges-pa-fosen/277306. [Accessed 05 05 2016].

[46] Statoil, “Statoil.com,” 14 08 2008. [Online]. Available: http://www.statoil.com/en/OurOperations/TerminalsRefining/Tjeldbergodden/Pages/default.aspx. [Accessed 06 05 2016].

[47] P. J. Dahl, T. S. Christensen, S. Winter-Madsen and S. M. King, “Proven autothermal reforming technology for modern large-scale methanol plants,” Haldor Topsøe A/S, Copehagen, 2014.

[48] Gassco, “www.gassco.no,” [Online]. Available: https://www.gassco.no/en/our-activities/pipelines-and-platforms/haltenpipe/. [Accessed 06 05 2016].

[49] Statkraft, “Faktaark Fosen Vind,” Statkraft, 2016.

[50] L. Nord, “Pre-combustion CO2 capture: Analysis of integrated reforming combined cycle,” NTNU, Trondheim, 2010.

[51] H. M. Kvamsdal and M. Thor, “Tjeldbergodden power/methanol - CO2 reduction efforts SP 2: CO2 capture and transport,” SINTEF, 2005.

[52] International Energy Agency, “Technology Roadmap - Hydrogen and Fuel Cells,” International energy Agency, Paris, 2015.

Appendices

A. Financial Analysis – elaboration

Equation for scaling

In the cost estimations, scaling is actively used in order to estimate the cost of the current component or facility based on a reference case. The equation used, is written below.

$$C_x = C_b\left(\frac{S_x}{S_b}\right)^{\alpha}$$

α – Scaling factor

C_b – Base cost

C_x – Cost for a plant of size x (S_x)

S_b – Base size

Currency table:

Table 37 - Currency table - Averages February-March 2016

Currency table	
NOK to EURO:	0.11
US Dollars to Euro:	0.90

Sensitivity Analysis

Scenario sensitivity

Here, the details behind the optimistic and conservative cases are explained.

Steam Methane Reforming:

Table 38 - Definition of the optimistic, base and conservative care simulations for SMR

	Optimistic Case	Base Case	Conservative Case
Prereformer:			
Reformer + WGS:	CAPEX of the reformer is scaled from 400USD/kW with a	CAPEX of the reformer is scaled from 400USD/kW with a	CAPEX of the reformer is scaled from 600USD/kW

	scaling coefficient of 0.7.	scaling coefficient of 0.8.	with a scaling coefficient of 0.9.
PSA:	Assuming hydrogen recovery of 95%.	Assuming hydrogen recovery of 90%.	Assuming hydrogen recovery of 80%.
CCS CAPEX scaling:	0.6	0.7	0.8
Compressors/Pumps:	Assuming adiabatic efficiency: Pump: 85%, Compressor: 80%	Assuming adiabatic efficiency: Pump: 75%, Compressor: 75%	Assuming adiabatic efficiency: Pump: 70%, Compressor: 70%
Reliability factor:	95%	95%	90%
Installation factor:	10%	20%	30%

Autothermal Reformer:

Table 39 - Definition of the optimistic, base and conservative care simulations for ATR

	Optimistic Case	Base Case	Conservative Case
Prereformer:			
Reformer + WGS:	CAPEX of the reformer is scaled with a scaling coefficient of 0.6.	CAPEX of the reformer is scaled with a scaling coefficient of 0.7.	CAPEX of the reformer is scaled with a scaling coefficient of 0.8.
PSA:	Assuming hydrogen recovery of 95%.	Assuming hydrogen recovery of 90%.	Assuming hydrogen recovery of 80%.
CCS CAPEX scaling:	0.6	0.7	0.8
Compressors/Pumps:	Assuming adiabatic efficiency: Pump: 85%, Compressor: 80%	Assuming adiabatic efficiency: Pump: 75%, Compressor: 75%	Assuming adiabatic efficiency: Pump: 70%, Compressor: 70%
Reliability factor:	95%	95%	90%
Installation factor:	10%	20%	30%

Explanation to the scaling of ATR: Since the CAPEX of the ATR reformer is based on a much larger facility, the scaling coefficient work opposite than with SMR. Hence, the CAPEX has been scaled down to the SMR source facility with 0,7 and scaled up to ATR size with 0,6 and 0,8 for the optimistic and conservative case, respectively.

Electrolysis:

Table 40 - Definition of the optimistic, base and conservative care simulations for Electrolysis

	Optimistic Case	Base Case	Conservative Case
Plant scaling factor:	0,8	0,9	0,95
Reliability factor:	95%	95%	90%
Installation cost factor:	10%	20%	30%
Plant Electricity consumption [kWh/Nm^3]:	4,7	4,85	5,0

List of inputs and assumptions used for cost estimations in Excel

Table 41 - List of inputs used for the cost-estimations and net present value calculations in EXCEL

General Input	Value	Unit	Descriction	Source
Lifetime facility:	25	Years		
Operating days:	347	Days/Year	Reliability of 95%	
Daily production capacity:	500 000	kg	As a result of an evaluation performed in the Project work 2015	
Production rate:	823	MW	Based on Higher Heating value of the hydrogen gas produced	
Area space required:	90 000	m3	Based on the melkøya LNG plant and scaled with a 0,7 factor to the production volume evaluated in this thesis.	
SMR Base case production rate:	300.00	MW	HHV H_2. This is used as the base case for cost estimations of the SMR plant.	IEA Technology Roadmap
ASU Base case production rate:	496 600.00	kgO$_2$/h	Based on GLT report	
ASU power consumption:	0.35	kWh/Nm3 O$_2$	Based on data sheet from Linde Kryotechnic	http://www.ieaghg.org/docs/oxyfuel/OCC1/Plenary%201/Beysel_ASU_1stOxyfuel%20Cottbus.pdf
ATR and Prereformer Base case :	339 400.00	kgNG/hr	Based on GLT report	
PSA Base case:	14 900.00	kgNG/hr	Based on GLT report	
WGS Base case:	1 000.00	MW (HHV H_2)	Hydrogen production plant, from coal gasification.	
CO_2 compression work:	0.10	kWh/kg CO_2	Based on a simple model in HYSYS, compressing 1 million tonnes per year from 1 to 150 bar.	
CCS Base case capacity:	700 000	tonnes/year	Based on the melkøya LNG plant	Assumtions by professor Jostein Pettersen
Electrolysis Base Case capacity:	26 000	kg/day	NEL-Hydrogen brochure of large scale facility	
Electrolysis cell stack consumption:	50 000	kW		

Electrolysis plant specific power consumption:	4.85	kWh/Nm3 H_2	Based on NEL brochure and information from Akzo Nobel.	
Electrolyser cell stack catalyst lifetime:	9.00	years	Based on the average lifetime of a cell stack catalyst. Span from 60000 - 90000 hours	IEA Technology roadmap

Chemical Properties	Value	Unit	Description	Source
HHV H_2:	39.50	kWh/kg		
LHV H_2:	33.39	kWh/kg		
Density H_2:	0.09	kg/Sm3		
Density NG:	0.83	kg/Sm3		
MM H_2:	2.02	kg/kmole		
LHV NG:	12.91	kWh/kg		
HHV Petrol:	9.47	kWh/L		

Process input	Value	Unit	Description	Source
NG Temperature:	50.00	deg C		SINTEF Report
NG Pressure:	50.00	bara		SINTEF Report
Process Water Temperature:	15.00	deg C		
Water Pressure:	1.01	bara		
Oxygen T:	15.00	deg C		
Oxygen Pressure:	20.00	bara		

Cost input	Value	Unit	Description	Source
Base case SMR Plant:	400.00	$/KW	Based on the investment cost of a 300 MW (HHV H_2 produced)plant. Including WGS and PSA	IEA Technology roadmap p. 28
Base case ATR reformer:	406 582 000.00	$	Based on a GTL cost analysis report, 2 500 tonnH_2/day capacity, including cost of engineering and contingencies	National Energy Technology Laboratory, Analysis of Gas-to-Liquid Transportation fuels via Fisher Tropsch, 2013
Base case POX Plant:				
Base case total CO_2 capture plant Investment:	800 000 000	NOK	Cost of expansion of process facility to include capture, compression, drying, condensation and pumping of CO_2. Capacity: 700 000 t/y	Assumtions by Professor Jostein Pettersen, based on Statoil Snøhvit
Base case total CO_2 transport investment:	1 200 000 000	NOK	Cost of pipeline, 8 inches, 140 km from shore to subsea injection unit. 200 bara design pressure, 400 m water depth. Cap: 700 000 t/y	Assumtions by Professor Jostein Pettersen, based on Statoil Snøhvit
Base case total CO_2 injection well system:	600 000 000	NOK	Cost of drilling and completion of CO_2 injection well. Capacity 700 000 t/y	Assumtions by Professor Jostein Pettersen, based on Statoil Snøhvit
Auxilliary Component factor:	0.20	%/Production CAPEX	This factor is added to include feedwater systems, cooling systems, electrical system, controll systems, buildings and improvements to site	National Energy Technology Laboratory, Analysis of Gas-to-Liquid Transportation fuels via Fisher Tropsch, 2013
Installation factor:	0.20		When costs of plants and systems are given, this factor is added to cover the expenses related to engineering and intallation	
Electricity price from NASDAQ:	20.03	€/MWh	Average of NASDAQ Commodities ENOYR 17,18 and 19 on from 18.04 to 16.05 2016. (20.03)	http://www.nasdaqomx.com/commodities/market-prices
Electricity price:	0.18	NOK/kWh	Converted to NOK per kWh. In comparison, the average el price in Trondheim from 14.04 to 13.05 2016 was 0,23 NOK/kWh (NORDPOOL).	https://www.ssb.no/energi-og-industri/statistikker/elkraftpris/kvartal/2016-02-25
Electricity Grid price:	230.00	kr/kW/year	Statnett Tariffs for national grid connection. Based on the max power consumption needed.	http://www.statnett.no/Drift-og-marked/Nettleie-og-tariffstrategi/Tariffer-i-sentralnettet/
Natural Gas price in Euros:	0.174	€/Sm3	For sensitivity analysis	

Natural Gas price:	1.58	NOK/Sm3	Average internal price of natural gas reported by Statoil in 2015. Estimated price when marketing and transportation costs are deducted. (1.58)	http://www.statoil.com/no/InvestorCentre/AnalyticalInformation/InternalGasPrice/Pages/default.aspx
CO_2 tax rate in euros:	7.70	€/tonnes of CO_2	For sensitivity analysis	
CO_2 tax rate :	69.98	NOK/tonne CO_2	Average european quota for carbon emissions. (69,98NOK/Tonne)	http://www.miljodirektoratet.no/no/Tema/klima/CO_2-priskompensasjon/Kvotepris-for-stottearet-2014/
Price of industry area:	550.00	NOK/m3		http://www.finn.no/finn/b2b/commercialproperty/plots/object?finnkode=64408682&searchclickthrough=true
Base case CAPEX Water Gas Shift:	40 000 000.00	$	Based on a report paper from Princeton, 1000MW (HHV H_2)capacity. Converted from 2002 USD with factor of 132,37% (usinflationcalculator.com)	PRODUCTION OF HYDROGEN AND ELECTRICITY FROM COAL WITH CO_2 CAPTURE. Kreutz, Williams, Socolow
Base case CAPEX Cryogenic ASU :	299 725 000	$	Based on a GTL cost analysis report, 496000 kgO_2/hr, including cost of both engineering and contingencies	National Energy Technology Laboratory, Analysis of Gas-to-Liquid Transportation fuels via Fisher Tropsch, 2013
Base case CAPEX Pressure Swing Adsorption:	12 469 000	$	Based on a GTL cost analysis report, 142000 kgH_2/day, including cost of both engineering and contingencies	National Energy Technology Laboratory, Analysis of Gas-to-Liquid Transportation fuels via Fisher Tropsch, 2013
Base case CAPEX Prereformer:	322 704 000	$	Based on a GTL cost analysis report, 2486000 kgH_2/day, including cost of both engineering and contingencies	National Energy Technology Laboratory, Analysis of Gas-to-Liquid Transportation fuels via Fisher Tropsch, 2013
Base case CAPEX Electrolysis:	€ 30 000 000	€	Based on 26 tonnes/day Plant by NEL-Hydrogen. Produced to 15 bar pressure	http://wpstatic.idium.no/www.nel-hydrogen.com/2015/04/NEL_Hydrogen_50MW.pdf
Reinvestment cost catalyst replacement :	20.00 %	% of CAPEX	Based on information from DNV GL	
H_2 and O_2 Compressor CAPEX:	70	USD/kW	Based on current performance of a 180 bar hydrogen compressor. This is a very conservative value	IEA Technology roadmap
OPEX Rate NG Reforming system:	5 %	% of CAPEX/year		
OPEX Rate CCS System:	5 %	% of CAPEX/year		

Financial Inputs				
USD to Euro:	0.90		Average currencies from february-march 2016	Oanda.com
NOK to Euro:	0.11		Average currencies from february-march 2016	Oanda.com
Discount rate:	0.10		Ref. Project work	

Scaling factors				
SMR:	0.80			Statoil, Jostein Sogge
ATR:	0.70			Statoil, Jostein Sogge
POX:	0.70			Statoil, Jostein Sogge
CCS system:	0.70			Statoil/NTNU Professor Jostein Pettersen
WGS:	0.70			
ASU:	0.70			
PSA:	0.90			
Electrolysis plant:	0.90			

B. Technical Analysis

Equation of state

The Peng Robinson equation of state was chosen for the simulations in Aspen Hysys, due to its common use in hydrocarbon process simulation. A test versus Soave-Redlich-Kwong and Kabadi-Danner was done in order to check for deviations, and the results prove very consisten.

$$P = \frac{RT}{V_m - b} - \frac{a\alpha}{V_m^2 + 2bV_m - b^2}$$

$$a = \frac{0.4572R^2T_c^2}{P_c}$$

$$b = \frac{0.07780RT_c}{P_c}$$

$$\alpha = (1 + (0.37464 + 1.54226\omega - 0.26992\omega^2 - 0.26992\omega^2)(1 - T_r^{0.5}))^2$$

Where:

ω is the acentric factor of the different components

P_c is the critical pressure

T_c is the critical temperature

R is the ideal gas constant = 8.314413 J/mol-K

Table 42 - Test of EOS, with a given natural gas input to the SMR process.

	Peng Robinson	Soave-Redlich-Kwong	Kabadi-Danner
Natural gas input [kg/h]:	54 000.000	54 000.000	54 000.000
Hydrogen produced [kg/h]:	20 983.729	20 987.444	20 979.031
Relative difference to PR [%]:	-	0.018	0.022

Electrolysis – technical details

The power consumption of the electrolysis plant used in this report is the average consumption of the entire facility during the lifetime of the operation. This includes the electrolyser cell stacks, rectifier, feed water pump, lye pump and product hydrogen compressor. The sources are Henning Langås, Nel-Hydrogen and [34] [12].

Table 43 - Electrolysis plant power consumption

	Value	Unit
Plant power consumption, new facility:	4.7	kWh/Nm^3
Plant power consumption, at catalyst reactivation:	5.0	kWh/Nm^3
Average Plant power consumption:	4.85	kWh/Nm^3

Systems Heat Integration Data

Assumptions:

- The heat demand of the CO_2 absorption process is assumed to be 2 MJ/kgCO_2 captured[36].
- Due to the phenomenon of metal dusting, explained in Section 4.3.2.2, the hot gas product from the reformers can only be used to produce steam through the temperature range of 750 – 400 °C [50].
- The flue gas is only cooled down to 100°C due to the risk of acid formation[36].

The Heat integration data is for all the reforming processes presented in

Table 44 to

Table 48. As seen from all the tables, the total heat production in the production plant is greater than the plant heat demand. The heat available in all systems consists of enough high-temperature gas streams to supply the demanding heat in the production plant.

---

[36] Information provided by David Berstad, SINTEF Energy Research

SMR:

Table 44 - Heat demand and heat available in SMR

	Value	Unit
Heat Demands:		
Preheating Water (350°C):	487.3	GJ/h
Preheating Gas input in GHR and SMR (400 and 700°C):	172.7	GJ/h
GHR (700°C):	130.3	GJ/h
SMR (950°C):	714.9	GJ/h
CO_2 Absorption (115°C)[36]:	253.9	GJ/h
Preheating Furnace inputs (335 and 500°C):	137.9	GJ/h
TOTAL:	**1897.0**	GJ/h
Heat Available:		
Cooling the reforming product (950 - 320°C):	389.6	GJ/h
WGS (320 - 25°C):	380.7	GJ/h
Furnace (1000°C):	714.9	GJ/h
Cooling the Flue Gas (1000 - 100°C):	412.4	GJ/h
TOTAL:	**1897.6**	GJ/h
Difference:	**0.6**	GJ/h

SMR+:

Table 45 - Heat demand and sources in SMR+

	Value	Unit
Heat Demands:		
Preheating Water (350°C):	625.9	GJ/h
Preheating Gas input in GHR and SMR (400 and 650°C):	184.1	GJ/h
GHR (700°C):	167.3	GJ/h
SMR (950°C):	955.9	GJ/h
CO_2 Absorption (115°C)[37]:	326.1	GJ/h
Preheating Furnace inputs (335 and 500°C):	186.0	GJ/h
TOTAL:	**2445.3**	GJ/h
Heat Available:		
Cooling the reforming product (950 - 320°C):	500.4	GJ/h
WGS (320 - 25°C):	489.0	GJ/h
Furnace (1000°C):	955.9	GJ/h
Cooling the Flue Gas (1000 - 100°C):	501.9	GJ/h
TOTAL:	**2447.3**	GJ/h
Difference:	**2.0**	GJ/h

---

[37] Information provided by David Berstad, SINTEF Energy Research

POX:

Table 46 - Heat demand and heat available in POX

	Value	Unit
Heat Demands:		
Preheating Water (320°C):	314.1	GJ/h
Preheating NG input in POX (400°C):	93.0	GJ/h
CO_2 Absorption (115°C)[37]:	327.6	GJ/h
Preheating Air and Tail Gas (350 and 500°C):	19.9	
TOTAL:	**754.7**	GJ/h
Heat Available:		
Intercooling in the two-stage oxygen compression (277-25°C):	17.1	GJ/h
Cooling the reforming product (1300 - 320°C):	170.0	GJ/h
WGS (320 - 25°C):	422.3	GJ/h
Cooling Tail gas before PSA-2 (450 - 25°C):	14.7	
Heat from burning Tail Gas and cooling the flue gas (1000 - 100°C):	130.6	GJ/h
TOTAL:	**754.7**	GJ/h
Difference:	**0.0**	GJ/h

ATR:

Table 47 - Heat demand and heat available in ATR

	Value	Unit
Heat Demands:		
Preheating Water (320 and 350°C):	327.1	GJ/h
Preheating gas input in GHR (400°C):	69.5	GJ/h
Preheating oxygen (250°C):	1.8	GJ/h
GHR (700°C):	155.5	GJ/h
CO_2 Absorption (115°C)[38]:	318.0	GJ/h
Preheating Air and Tail Gas (350 and 500°C):	15.9	GJ/h
TOTAL:	**887.7**	GJ/h
Heat Available:		
Intercooling in the two-stage oxygen compression (277-25°C):	15.5	GJ/h
Cooling the reforming product (1000 - 320°C):	408.2	GJ/h
WGS (320 - 25°C):	378.4	GJ/h
Cooling Tail gas before PSA-2 (340 - 25°C):	14.3	
Burning Tail Gas and cooling the flue gas (1000 - 100°C):	98.1	GJ/h
TOTAL:	**914.4**	GJ/h
Difference:	**26.7**	GJ/h

---

[38] Information provided by David Berstad, SINTEF Energy Research

CRE:

Table 48 - Heat demand and heat available in CRE

	Value	Unit
Heat Demands:		
Preheating Water (320 and 350°C):	237.4	GJ/h
Preheating gas input in GHR (400°C):	50.3	GJ/h
Preheating oxygen (250°C):	1.2	GJ/h
GHR (700°C):	112.4	GJ/h
CO_2 Absorption (115°C)[38]:	229.3	GJ/h
Preheating Air and Tail Gas (350 and 500°C):	12.9	GJ/h
TOTAL:	**643.5**	GJ/h
Heat Available:		
Intercooling in the two-stage oxygen compression (277-25°C):	11.0	GJ/h
Cooling the reforming product (1000 - 320°C):	288.4	GJ/h
WGS (320 - 25°C):	272.7	GJ/h
Cooling Tail gas before PSA-2 (340 - 25°C):	10.5	
Burning Tail Gas and cooling the flue gas (1000 - 100°C):	82.8	GJ/h
TOTAL:	**665.5**	GJ/h
Difference:	**22.0**	GJ/h

Component Modelling HYSYS

The values are based on input from the thesis supervisors, as well as Jostein Sogge at Statoil and the paper of Mari Voldsund [8]. All pressures listed in the report are absolute pressures.

Inputs:

Natural Gas

Table 49 - Natural Gas composition and properties. Mean Values from Heidrun gas field [51]

	Value	Unit
Pressure:	50	Bar
Temperature:	50	°C
Composition, Mole fraction:		
CH_4	0.8532	
CO_2	0.0221	
C_2H_6	0.0705	
C_3H_8	0.0273	
i-Butane	0.0055	
n-Butane	0.0094	
i-Pentan	0.0027	
n-Pentan	0.0027	
n-Hexane	0.0018	
n-Heptane	0.0013	
n-Octane	0.0004	

N_2	0.0033	

Air

Table 50 - Air design parameters

	Value	Unit
Pressure:	1.013	Bar
Temperature:	25	°C
Composition, Mole fraction: N_2 O_2	 0.79 0.21	

Water

Table 51 - Water design parameters

	Value	Unit
Pressure:	1.013	Bar
Temperature:	25	°C
Composition, Mole fraction: H_2O	 1.0	

Oxygen

Table 52 - Oxygen design parameters

	Value	Unit
Pressure:	1.013	Bar
Temperature:	25	°C
Composition, Mole fraction: O_2	 1.0	

Heaters and Coolers

Table 53 - Heaters and Coolers modelling parameters

	Value	Unit
Pressure drop:	25	kPa
Nozzle Parameters: Diameter: Elevation (Base): Elevation (Ground):	 0.05 0 0	 m m m
Heat loss:	None	

Compressors, Expanders and Pumps

Compressors

Table 54 - Compressors modelling parameters

	Value	Unit
Adiabatic efficiency:	75	
Polytropic Method:	Schultz	
Operating mode:	Centrifugal	

Curve Input Option:	Single-MW	
Nozzle Parameters:		
Diameter:	0.05	m
Elevation (Base):	0	m
Elevation (Ground):	0	m
Friction Loss Factor:	0.006	kg-m^2/s
Inertia Modeling Parameters:		
Rotational Inertia:	6.0	kg-m^2
Radius of Gyration:	0.2	m
Mass:	150.0	kg

Expanders

Table 55 - Expanders modelling parameters

	Value	**Unit**
Adiabatic efficiency:	75	
Curve Input Option:	Single Curve	
Nozzle Parameters:		
Diameter:	0.05	m
Elevation (Base):	0	m
Elevation (Ground):	0	m
Friction Loss Factor:	0.006	kg-m^2/s
Inertia Modeling Parameters:		
Rotational Inertia:	6.0	kg-m^2
Radius of Gyration:	0.2	m
Mass:	150.0	kg

Pumps

Table 56 - Pumps modelling parameters

	Value	**Unit**
Adiabatic efficiency:	75	
Nozzle Parameters:		
Diameter:	0.05	m
Elevation (Base):	0	m
Elevation (Ground):	0	m
Friction Loss Factor:	0.05	kg-m^2/s
Inertia Modeling Parameters:		
Rotational Inertia:	0.5	kg-m2
Radius of Gyration:	0.1	m
Mass:	50.0	kg

Reactors

GHR

Table 57 - GHR modelling parameters

	Value	**Unit**
Type of Reactor:	Gibbs Reactor	
Pressure Drop:	50	kPa

Reactor Type:	Specify Equilibrium Reactions	
Equilibrium Reactions:	$CO + H_2O \rightarrow CO_2 + H_2$ $CH_4 + H_2O \rightarrow CO + 3H_2$ $C_2H_6 + 2H_2O \rightarrow 2CO + 5H_2$ $C_3H_8 + 3H_2O \rightarrow 3CO + 7H_2$ $iC_4H_{10} + 4H_2O \rightarrow 4CO + 9H_2$ $nC_4H_{10} + 4H_2O \rightarrow 4CO + 9H_2$ $iC_5H_{12} + 5H_2O \rightarrow 5CO + 11H_2$ $nC_5H_{12} + 5H_2O \rightarrow 5CO + 11H_2$ $nC_6H_{14} + 6H_2O \rightarrow 6CO + 13H_2$ $nC_7H_{16} + 7H_2O \rightarrow 7CO + 15H_2$ $nC_8H_{18} + 8H_2O \rightarrow 8CO + 17H_2$	
Solving Options: Maximum Number of Iterations: Tolerance:	 100 1.0e-007	
Nozzle Parameters: Diameter: Elevation (Base): Elevation (Ground):	 0.05 0 0	 m m m
Heat loss:	None	

SMR

Table 58 - SMR modelling parameters

	Value	Unit
Type of Reactor:	Gibbs Reactor	
Pressure Drop:	50	kPa
Reactor Type:	Specify Equilibrium Reactions	
Equilibrium Reactions:	$CO + H_2O \rightarrow CO_2 + H_2$ $CH_4 + H_2O \rightarrow CO + 3H_2$ $C_2H_6 + 2H_2O \rightarrow 2CO + 5H_2$ $C_3H_8 + 3H_2O \rightarrow 3CO + 7H_2$ $iC_4H_{10} + 4H_2O \rightarrow 4CO + 9H_2$ $nC_4H_{10} + 4H_2O \rightarrow 4CO + 9H_2$ $iC_5H_{12} + 5H_2O \rightarrow 5CO + 11H_2$ $nC_5H_{12} + 5H_2O \rightarrow 5CO + 11H_2$ $nC_6H_{14} + 6H_2O \rightarrow 6CO + 13H_2$ $nC_7H_{16} + 7H_2O \rightarrow 7CO + 15H_2$ $nC_8H_{18} + 8H_2O \rightarrow 8CO + 17H_2$	
Solving Options: Maximum Number of Iterations: Tolerance:	 100 1.0e-007	
Nozzle Parameters: Diameter: Elevation (Base): Elevation (Ground):	 0.05 0 0	 m m m
Heat loss:	None	

Furnace

Table 59 - Furnace modelling parameters

	Value	Unit
Type of Reactor:	Gibbs Reactor	
Pressure Flue Gas:	1	atm
Reactor Type:	Specify Equilibrium Reactions	
Equilibrium Reactions:	$\mathrm{CO} + 0.50_2 \rightarrow CO_2$ $H_2 + 0.50_2 \rightarrow H_2O$ $CH_4 + 20_2 \rightarrow CO_2 + 2H_2O$ $C_2H_6 + 3.50_2 \rightarrow 2CO_2 + 3H_2O$ $C_3H_8 + 50_2 \rightarrow 3CO_2 + 4H_2O$ $iC_4H_{10} + 6.50_2 \rightarrow 4CO_2 + 5H_2O$ $nC_4H_{10} + 6.50_2 \rightarrow 4CO_2 + 5H_2O$ $iC_5H_{12} + 80_2 \rightarrow 5CO_2 + 6H_2O$ $nC_5H_{12} + 80_2 \rightarrow 5CO_2 + 6H_2O$ $nC_6H_{14} + 9.50_2 \rightarrow 6CO_2 + 7H_2O$ $nC_7H_{16} + 110_2 \rightarrow 7CO_2 + 8H_2O$ $nC_8H_{18} + 12.50_2 \rightarrow 8CO_2 + 9H_2O$	
Solving Options: Maximum Number of Iterations: Tolerance:	 100 1.0e-007	
Nozzle Parameters: Diameter: Elevation (Base): Elevation (Ground):	 0.05 0 0	 m m m
Heat loss:	None	

POX

Table 60 - POX modelling parameters

	Value	Unit
Type of Reactors:	Conversion Reactor and Equilibrium Reactor	
Pressure Drop: Conversion Reactor: Equilibrium Reactor:	 25 25	 kPa kPa
Reactions:	**Conversion Reactions:** $CH_4 + 1.50_2 \rightarrow CO + 2H_2O$ $C_2H_6 + 2.50_2 \rightarrow 2CO + 3H_2O$ $C_3H_8 + 3.50_2 \rightarrow 3CO + 4H_2O$ $iC_4H_{10} + 4.50_2 \rightarrow 4CO + 5H_2O$ $nC_4H_{10} + 4.50_2 \rightarrow 4CO + 5H_2O$ $iC_5H_{12} + 5.50_2 \rightarrow 5CO + 6H_2O$ $nC_5H_{12} + 5.50_2 \rightarrow 5CO + 6H_2O$ $nC_6H_{14} + 6.50_2 \rightarrow 6CO + 7H_2O$ $nC_7H_{16} + 8.50_2 \rightarrow 7CO + 8H_2O$ $nC_8H_{18} + 9.50_2 \rightarrow 8CO + 9H_2O$ **Equilibrium Reactions:** $CO + H_2O \rightarrow CO_2 + H_2$	

	$CH_4 + H_2O \rightarrow CO + 3H_2$ $C_2H_6 + 2H_2O \rightarrow 2CO + 5H_2$ $C_3H_8 + 3H_2O \rightarrow 3CO + 7H_2$ $iC_4H_{10} + 4H_2O \rightarrow 4CO + 9H_2$ $nC_4H_{10} + 4H_2O \rightarrow 4CO + 9H_2$ $iC_5H_{12} + 5H_2O \rightarrow 5CO + 11H_2$ $nC_5H_{12} + 5H_2O \rightarrow 5CO + 11H_2$ $nC_6H_{14} + 6H_2O \rightarrow 6CO + 13H_2$ $nC_7H_{16} + 7H_2O \rightarrow 7CO + 15H_2$ $nC_8H_{18} + 8H_2O \rightarrow 8CO + 17H_2$	
Nozzle Parameters: Diameter: Elevation (Base): Elevation (Ground):	 0.05 0 0	 m m m
Heat loss:	None	

ATR

Table 61 - ATR modelling parameters

	Value	Unit
Type of Reactor:	Gibbs Reactor	
Pressure Drop:	50	kPa
Reactor Type:	Specify Equilibrium Reactions	
Equilibrium Reactions:	$CO + H_2O \rightarrow CO_2 + H_2$ $CH_4 + 0.5O_2 \rightarrow CO + 2H_2$ $CH_4 + H_2O \rightarrow CO + 3H_2$ $C_2H_6 + 2H_2O \rightarrow 2CO + 5H_2$ $C_3H_8 + 3H_2O \rightarrow 3CO + 7H_2$ $iC_4H_{10} + 4H_2O \rightarrow 4CO + 9H_2$ $nC_4H_{10} + 4H_2O \rightarrow 4CO + 9H_2$ $iC_5H_{12} + 5H_2O \rightarrow 5CO + 11H_2$ $nC_5H_{12} + 5H_2O \rightarrow 5CO + 11H_2$ $nC_6H_{14} + 6H_2O \rightarrow 6CO + 13H_2$ $nC_7H_{16} + 7H_2O \rightarrow 7CO + 15H_2$ $nC_8H_{18} + 8H_2O \rightarrow 8CO + 17H_2$ $2CO \rightarrow CO_2 + \mathrm{C}$	
Solving Options: Maximum Number of Iterations: Tolerance:	 100 1.0e-007	
Nozzle Parameters: Diameter: Elevation (Base): Elevation (Ground):	 0.05 0 0	 m m m
Heat loss:	None	

WGS

Table 62 - WGS modelling parameters

	Value	Unit
Type of Reactor:	Equilibrium Reactors	
Pressure Drop:	25	kPa

Equilibrium Reactions:	$CO + H_2O \rightarrow CO_2 + H_2$	
Nozzle Parameters:		
Diameter:	0.05	m
Elevation (Base):	0	m
Elevation (Ground):	0	m
Heat loss:	None	

Separators and Purification

Separators

Table 63 - Separator modelling parameters

	Value	Unit
HYSYS Separator Type:	Separator	
Pressure Drop:	0	kPa
Geometry:	Vertical Flat Cylinder	
Nozzle Parameters:		
Diameter:	0.05	m
Elevation (Base):	0	m
Elevation (Ground):	0	m
Heat loss:	None	

CO_2 Absorption

Table 64 - CO_2 Absorption modelling parameters

	Value		Unit
HYSYS Component:	Component Splitter		
Pressure Drop:	50		kPa
Recovery rate:	95		% mole-basis
CO_2 Pressure:			kPa
Splits:	**CO_2 Absorbed:**	**PSA feed:**	Mole basis
CH_4	0	1	
H_2	0	1	
CO	0	1	
CO_2	0.95	0.05	
H_2O	0	1	
C	0	1	
C_2H_6	0	1	
C_3H_8	0	1	
i-Butane	0	1	
n-Butane	0	1	
i-Pentan	0	1	
n-Pentan	0	1	
n-Hexane	0	1	
n-Heptane	0	1	
n-Octane	0	1	
N_2	0	1	
O_2	0	1	

PSA

Table 65 - PSA modelling parameters

	Value		Unit
HYSYS Component:	Component Splitter		
Pressure Drop hydrogen:	200		kPa
Recovery rate:	90		%
Pressure tail gas:	250		kPa
Splits:	**H_2 Adsorbed:**	**Tail Gas:**	
CH_4	0	1	
H_2	0.9	0.1	
CO	0	1	
CO_2	0	1	
H_2O	0	1	
C	0	1	
C_2H_6	0	1	
C_3H_8	0	1	
i-Butane	0	1	
n-Butane	0	1	
i-Pentan	0	1	
n-Pentan	0	1	
n-Hexane	0	1	
n-Heptane	0	1	
n-Octane	0	1	
N_2	0	1	
O_2	0	1	

HYSYS Models:

SMR:

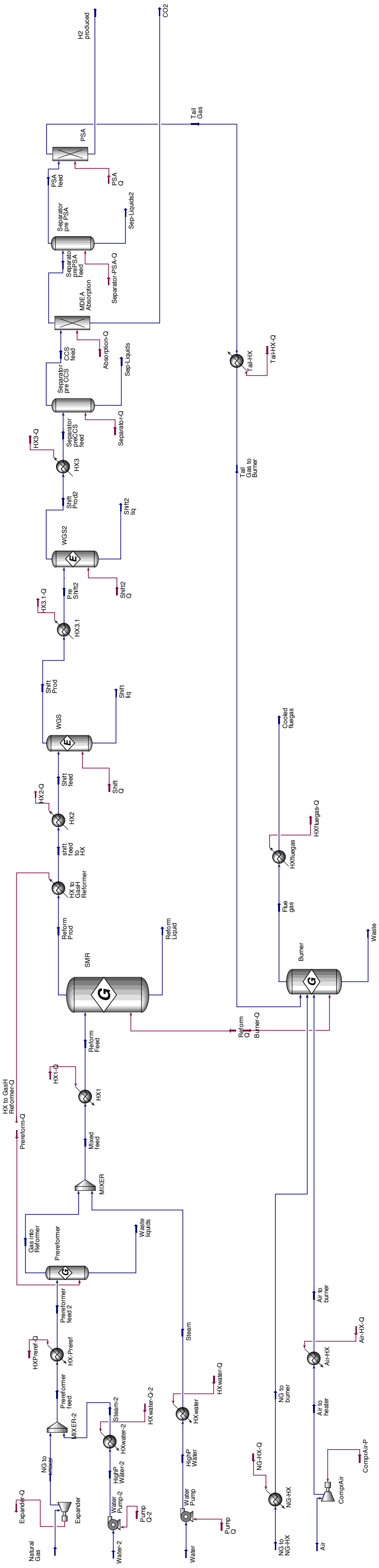

SMR+:

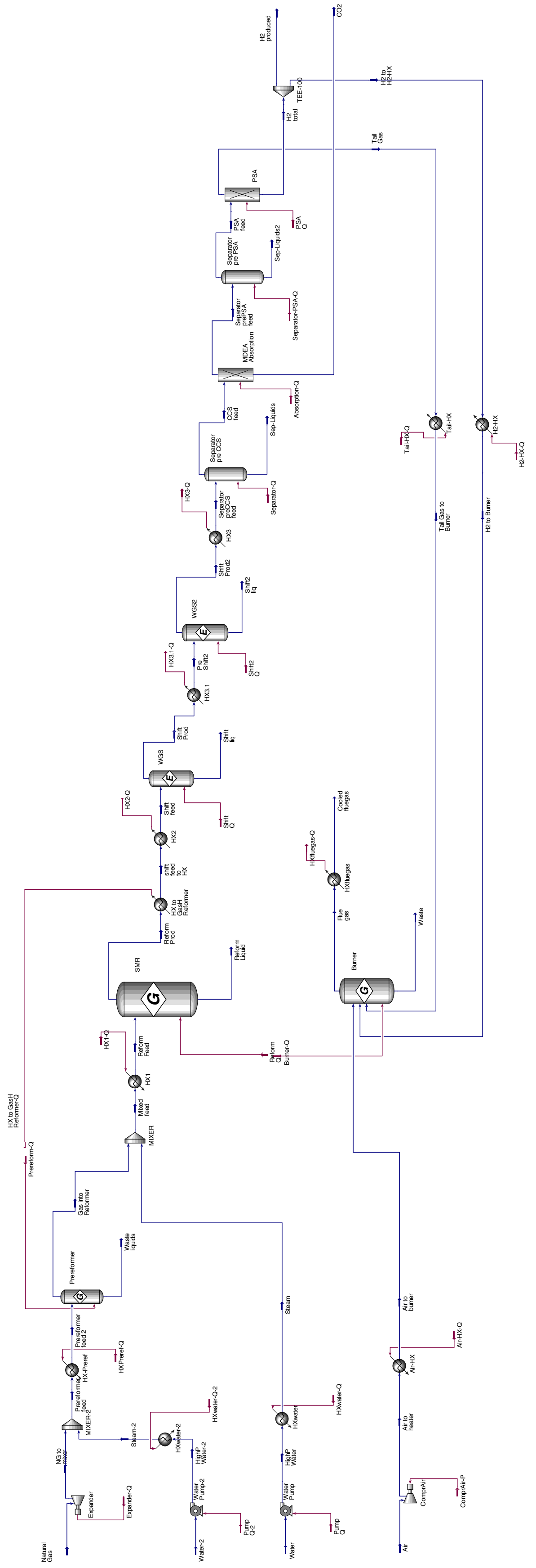

Natural Gas
Expander
Expander-Q
NG to mixer
MIXER-2
Prereformer feed
HX-Preref
HXPreref-Q
Prereformer feed 2
Prereformer
Waste liquids
Gas into Reformer
Prereform-Q
HX to GasH Reformer-Q
MIXER
Mixed feed
HX1
HX1-Q
Reform Feed
SMR
Reform Liquid
Reform Prod
HX to GasH Reformer
shift feed to HX
HX2
HX2-Q
Shift feed
WGS
Shift Q
Shift liq
Shift Prod
HX3.1
HX3.1-Q
Pre Shift2
WGS2
Shift2 Q
Shift2 liq
Shift Prod2
HX3
HX3-Q
Separator preCCS feed
Separator pre CCS
Separator-Q
Sep-Liquids
CCS feed
MDEA Absorption
Absorption-Q
Separator prePSA feed
Separator pre PSA
Separator-PSA-Q
Sep-Liquids2
PSA feed
PSA
PSA Q
H2 total
TEE-100
H2 produced
CO2
H2 to H2-HX
Tail Gas
Tail-HX
Tail-HX-Q
H2-HX
H2-HX-Q
Tail Gas to Burner
H2 to Burner
Burner
Waste
Flue gas
HXfluegas
HXfluegas-Q
Cooled fluegas
Reform Q
Burner-Q
Water-2
Water Pump-2
Pump Q-2
HighP Water-2
HXwater-2
HXwater-Q-2
Steam-2
Water
Water Pump
Pump Q
HighP Water
HXwater
HXwater-Q
Steam
Air
CompAir
CompAir-P
Air to heater
Air-HX
Air-HX-Q
Air to burner

POX:

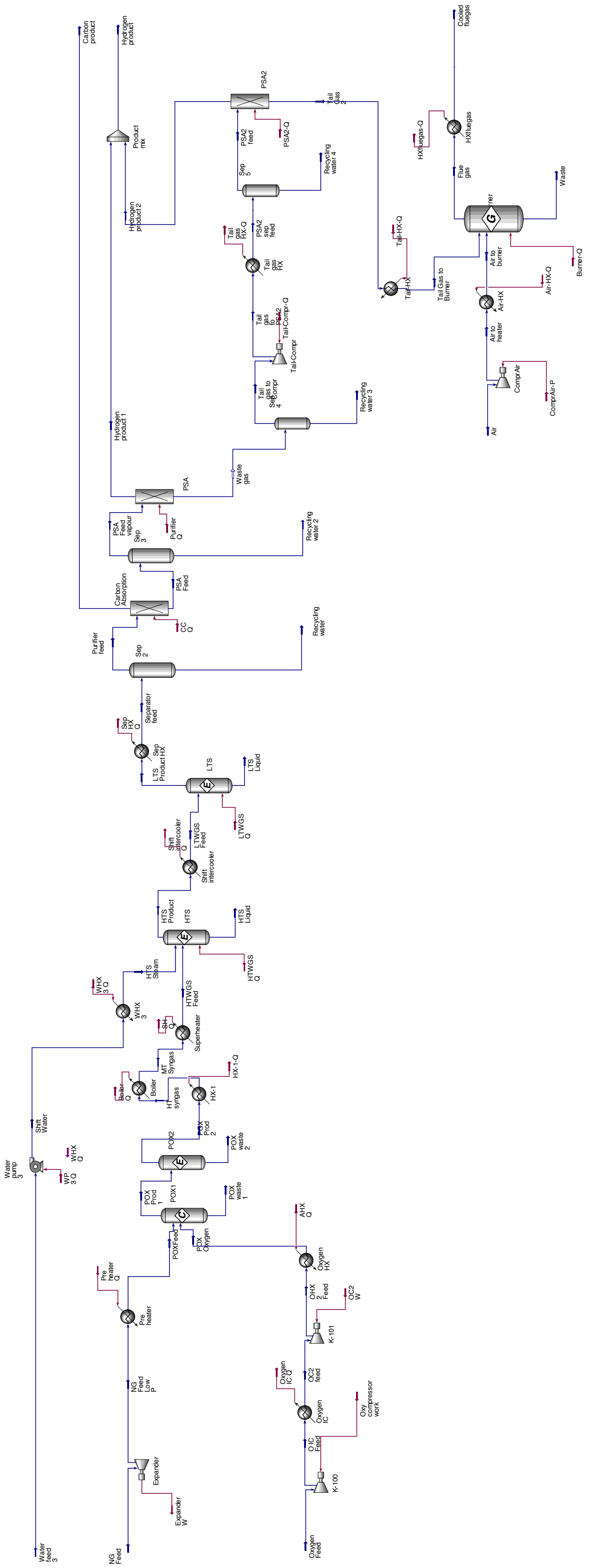

Water feed 3
NG Feed
Oxygen Feed
Expander
Expander W
K-100
Oxy compressor work
O IC Feed
Oxygen IC
Oxygen IC Q
OC2 feed
K-101
OC2 W
OHX 2 Feed
Oxygen HX
AHX Q
NG Feed Low P
Pre heater
Pre heater Q
POXFeed
POX Oxygen
POX1
POX Prod 1
POX waste 1
POX2
POX Prod 2
POX waste 2
Water pump 3
WP 3 Q
WHX Q
Shift Water
HX-1
HX-1-Q
HT syngas
Boiler
Boiler Q
MT Syngas
Superheater
SH Q
HTWGS Feed
WHX 3
WHX 3 Q
HTS Steam
HTS
HTS Product
HTS Liquid
HTWGS Q
Shift intercooler
Shift intercooler Q
LTWGS Feed
LTS
LTS Product
LTS Liquid
LTWGS Q
Sep HX
Sep Product HX
Sep HX Q
Separator feed
Sep 2
Recycling water
Purifier feed
Carbon Absorption
CC Q
PSA Feed
Sep 3
PSA Feed vapour
Recycling water 2
Purifier Q
PSA
Hydrogen product 1
Waste gas
Recycling water 3
Tail gas to Sep 4
Tail-Compr
Tail-Compr-Q
Tail gas to PSA2
Tail gas HX
Tail gas HX-Q
PSA2 sep feed
Sep 5
Recycling water 4
PSA2 feed
PSA2-Q
PSA2
Tail Gas 2
Hydrogen product2
Product mix
Hydrogen product
Carbon product
Tail-HX
Tail-HX-Q
Tail Gas to Burner
Air
ComprAir
ComprAir-P
Air to heater
Air-HX
Air-HX-Q
Air to burner
Burner
Burner-Q
Waste
Flue gas
HXfluegas
HXfluegas-Q
Cooled fluegas

ATR:

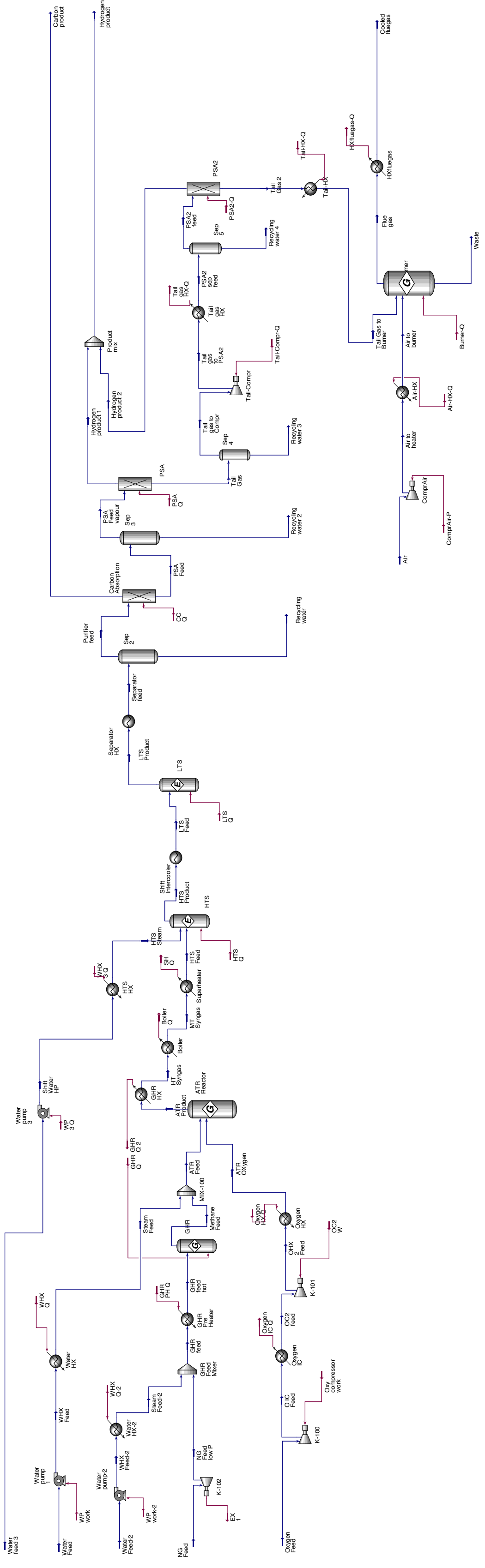
Carbon product
Hydrogen product
Cooled fluegas
HXfluegas-Q
HXfluegas
Tail-HX-Q
Tail-HX
Tail Gas 2
PSA2
PSA2-Q
PSA2 feed
Sep 5
Recycling water 4
Flue gas
Waste
Burner
Burner-Q
Tail gas to Burner
Air to burner
Air-HX
Air-HX-Q
Air to heater
CompAir
CompAir-P
Air
PSA2 sep feed
Tail gas HX-Q
Tail gas HX
Product mix
Tail gas to PSA2
Tail-Compr-Q
Tail-Compr
Hydrogen product 1
Hydrogen product 2
Tail gas to Compr
Sep 4
Recycling water 3
PSA
PSA Q
Tail Gas
PSA Feed vapour
Sep 3
Recycling water 2
Carbon Absorption
PSA Feed
CC Q
Purifier feed
Sep 2
Recycling water
Separator feed
Separator HX
LTS Product
LTS
LTS Q
LTS Feed
Shift Intercooler
HTS Product
HTS
HTS Steam
HTS Feed
HTS Q
WHX 3 Q
HTS HX
SH Q
Superheater
Boiler Q
Boiler
MT Syngas
HT Syngas
GHR HX
ATR Product
ATR Reactor
Shift Water HP
Water pump 3
WP 3 Q
GHR Q 2
GHR Q
ATR Feed
ATR Oxygen
MIX-100
Steam Feed
GHR
Methane Feed
Oxygen HX Q
Oxygen HX
OC2 W
OHX 2 Feed
K-101
GHR PH Q
GHR feed hot
GHR Pre Heater
WHX Q
Oxygen IC Q
OC2 feed
Water HX
GHR feed
GHR Feed Mixer
Oxygen IC
Oxy compressor work
WHX Q-2
Steam Feed-2
OIC Feed
WHX Feed
Water HX-2
K-100
NG Feed low P
Water pump 1
WHX Feed-2
Water pump-2
K-102
WP work
WP work-2
EX 1
Water feed 3
Water Feed
Water Feed-2
NG Feed
Oxygen Feed

CRE:

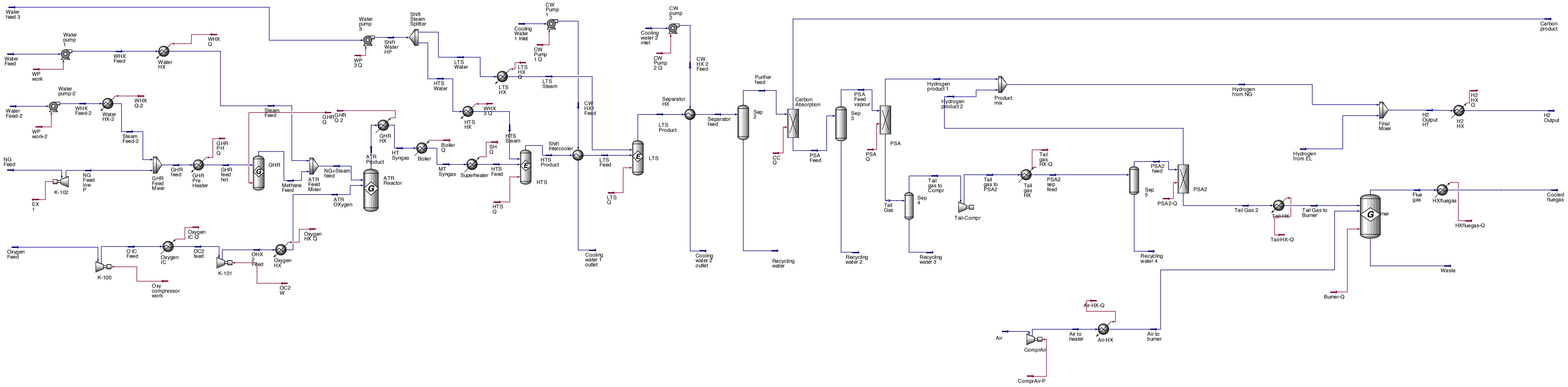
Water feed 3
Water Feed
Water pump 1
WP work
WHX Feed
Water HX
WHX Q
Water Feed-2
Water pump-2
WP work-2
WHX Feed-2
Water HX-2
WHX Q-2
Steam Feed-2
NG Feed
K-102
EX 1
NG Feed low P
GHR Feed Mixer
GHR feed
GHR Pre Heater
GHR PH Q
GHR feed hot
GHR
Steam Feed
GHR Q
GHR Q 2
Methane Feed
ATR Feed Mixer
NG+Steam feed
ATR OXygen
ATR Reactor
ATR Product
GHR HX
HT Syngas
Boiler
Boiler Q
MT Syngas
Superheater
SH Q
HTS Feed
HTS Q
HTS
HTS Steam
HTS Product
Oxygen Feed
K-100
Oxy compressor work
O IC Feed
Oxygen IC
Oxygen IC Q
OC2 feed
K-101
OHX 2 Feed
Oxygen HX
Oxygen HX Q
OC2 W
Water pump 3
WP 3 Q
Shift Water HP
Shift Steam Splitter
LTS Water
HTS Water
HTS HX
WHX 3 Q
LTS HX
LTS HX Q
LTS Steam
Cooling Water 1 Inlet
CW Pump 1
CW Pump 1 Q
CW HX1 Feed
Shift Intercooler
Cooling water 1 outlet
LTS Feed
LTS
LTS Q
LTS Product
Cooling water 2 inlet
CW pump 2
CW Pump 2 Q
CW HX 2 Feed
Separator HX
Cooling water 2 outlet
Separator feed
Sep 2
Recycling water
Purifier feed
Carbon Absorption
CC Q
PSA Feed
Sep 3
Recycling water 2
PSA Feed vapour
PSA
PSA Q
Tail Gas
Sep 4
Recycling water 3
Tail gas to Compr
Tail-Compr
Tail gas to PSA2
Tail gas HX
Tail gas HX-Q
PSA2 sep feed
Sep 5
Recycling water 4
PSA2 feed
PSA2
PSA2-Q
Hydrogen product 1
Hydrogen product 2
Product mix
Hydrogen from NG
Carbon product
Hydrogen from EL
Final Mixer
H2 Output HT
H2 HX
H2 HX Q
H2 Output
Tail Gas 2
Tail-HX
Tail-HX-Q
Tail Gas to Burner
rner
Burner-Q
Waste
Flue gas
HXfluegas
HXfluegas-Q
Cooled fluegas
Air
ComprAir
ComprAir-P
Air to heater
Air-HX
Air-HX-Q
Air to burner

C. Wind Data[39]

When calculating the wind power supply factor[40] in Section 6.3, these wind data and this Matlab script was used.

Wind Data text file (mnwind.txt):

Only the first 30 of 8058 entries total is showed in Table 66. It is inconvenient to attach the wind data in the report due to the length of the text file. The text file (mnwind.txt) can be sent on request.

Table 66 - Wind data text file used in the Matlab script. Only the first 30 of 8058 entries is showed in the table. The wind data is captured over a year at 3 different locations in Mid-Norway.

Data number	Wind data location 1 [m/s]	Wind data location 2 [m/s]	Wind data location 3 [m/s]
1:	1.0500000e+001	1.2100000e+001	6.8000000e+000
2:	1.5900000e+001	1.4600000e+001	5.4000000e+000
3:	1.5500000e+001	1.4700000e+001	8.6000000e+000
4:	1.5600000e+001	1.4500000e+001	7.1000000e+000
5:	1.3600000e+001	1.6300000e+001	8.0000000e+000
6:	1.5700000e+001	1.5100000e+001	6.1000000e+000
7:	1.7700000e+001	1.7900000e+001	6.5000000e+000
8:	1.5400000e+001	1.5200000e+001	7.2000000e+000
9:	1.5900000e+001	1.5500000e+001	6.6000000e+000
10:	1.6000000e+001	1.4800000e+001	6.5000000e+000
11:	1.5400000e+001	1.4100000e+001	6.6000000e+000
12:	1.6300000e+001	1.3000000e+001	8.0000000e+000
13:	1.5400000e+001	1.3900000e+001	7.4000000e+000
14:	1.5800000e+001	1.3800000e+001	6.8000000e+000
15:	1.6000000e+001	1.3600000e+001	7.4000000e+000
16:	1.3400000e+001	8.6000000e+000	6.0000000e+000
17:	1.2400000e+001	1.3000000e+001	6.7000000e+000
18:	1.3500000e+001	1.3300000e+001	7.7000000e+000
19:	1.3200000e+001	1.2600000e+001	7.3000000e+000
20:	1.3600000e+001	1.3200000e+001	7.8000000e+000
21:	1.3500000e+001	1.2400000e+001	7.4000000e+000
22:	1.3600000e+001	1.2700000e+001	7.8000000e+000
23:	1.4700000e+001	1.4900000e+001	7.7000000e+000
24:	1.4600000e+001	1.3900000e+001	8.6000000e+000
25:	1.4900000e+001	1.2900000e+001	1.0000000e-001
26:	1.4200000e+001	1.4400000e+001	0.0000000e+000
27:	1.4400000e+001	1.2700000e+001	8.3000000e+000
28:	1.4800000e+001	1.1800000e+001	0.0000000e+000
29:	1.3600000e+001	1.1200000e+001	0.0000000e+000
30:	1.3700000e+001	1.0200000e+001	0.0000000e+000

---

[39] Wind data provided by Professor Magnus Korpås

[40] The wind power supply factor is the power directly supplied by the wind farm, divided by the total power demand of the electrolysis plant.

Matlab Script (windproduction.m):

```
%Script for generating wind power production time series

wspeed = load('mnwind.txt'); %Wind speed time series for three locations
[Nsteps, Nsites] = size(wspeed);

Pw_rat = [1 1 1]; %Installed wind power capacity
wspeed_factor = [1 1 1]; %Multiplication factor for adjusting wind speed

%Enercon E70 with storm control
Power_Curve = [0 0;1 0;2 2;3 18;4 56;5 127;6 240;7 400;8 626;9 892; 10
1223;11 1590;12 1900;13 2080;14 2230;15 2300;25 2300;30 0;100 0];
Power_Curve(:,2)=Power_Curve(:,2)./max(Power_Curve(:,2)); % Normalised
power curve



%% Create wind power output for each time step for each wind site
Pw = zeros(size(wspeed));
for i=1:Nsites
    Pw(:,i) =
interp1(Power_Curve(:,1),Power_Curve(:,2),wspeed_factor(i)*wspeed(:,i)).*Pw
_rat(i);
end
Pw(Pw<0)=0;

WPSF = (1-sum(Pw(:,1)>0)/length(Pw(:,1))+1-sum(Pw(:,2)>0)/length(Pw(:,2))+1
sum(Pw(:,3)>0)/length(Pw(:,3)))/3;
```